ABSTRACT

Title of Document: CELLULAR AND MOLECULAR MECHANISMS UNDERLYING HOMEOSTATIC SYNAPTIC PLASTICITY

Anubhuti Goel, PhD, 2008

Directed By: Professor, Hey-Kyoung Lee, NACS

It is well established that modification of sensory cortices of animals is integral to many functions of the brain. While input-specific synaptic plasticity mechanisms are thought to underlie developmental refinement of synaptic connectivity with sensory experience, theoretical analyses suggest that slower global homeostatic mechanisms are required to stabilize dynamic neural networks. One of the homeostatic mechanisms that have been proposed is synaptic scaling, where a prolonged increase in neural activity globally scales down excitatory synaptic responses, while a chronic decrease in activity scales them up. This phenomenon has been demonstrated by pharmacological manipulations in cultured neurons, as well as in vivo visual cortex by several days of visual deprivation. However, whether restoring vision could reverse these changes and the molecular mechanisms of visual experience-induced homeostatic synaptic plasticity were not known. Moreover, whether there are more global regulations beyond one sensory modality was unknown.

Several human studies demonstrated that loss of vision is usually accompanied by increased functionality of other sensory modalities. We found that visual deprivation produces synaptic changes in primary somatosensory and auditory cortices, opposite to that seen in the visual cortex. The reversible homeostatic synaptic modification in primary sensory cortices by visual experience correlated with changes in alpha-amino-3-hydroxy-5-methyl-4-isoxazolepropionic acid (AMPA) receptor phosphorylation and subunit composition, which could underlie changes in AMPA receptor function. Interestingly, the reversible homeostatic modification occurred in juveniles and also in adults well beyond the closure of the "classical" critical period in the superficial layers of the visual cortex. This correlates with the persistence of synapse-specific plasticity in this cortical layer, supporting the need for homeostatic synaptic plasticity in stabilizing dynamic circuits. Our investigation of the molecular mechanisms of synaptic scaling in juvenile visual cortex suggest that multiplicative scaling up of excitatory synapses by dark rearing may occur in two steps, requiring phosphorylation of the GluR1-S845 residue and anchoring of GluR1 to the postsynaptic density. Our data also suggests that GluR2-mediated mechanisms may interact with the GluR1-dependent processes to enable synaptic scaling following visual deprivation. Collectively, this study shows that the AMPA receptor regulation is a common downstream mechanism shared between Hebbian and homeostatic plasticity.

CELLULAR AND MOLECULAR MECHANISMS UNDERLYING HOMEOSTATIC SYNAPTIC PLASTICITY

By

Anubhuti Goel

Dissertation submitted to the Faculty of the Graduate School of the
University of Maryland, College Park, in partial fulfillment
of the requirements for the degree of
Doctor of Philosophy
2008

Advisory Committee:
Dr Hey-Kyoung Lee, Chair
Dr Catherine Carr
Dr Cynthia Moss
Dr John Isaac
Dr Amanda Woodward

Dedication

“To Ajji and Vyola”.

Acknowledgements

I would like to thank:

My advisor Dr Hey-Kyoung Lee, whose ideas and constant motivation fuelled this study. She is a very thorough and well accomplished scientist and also a great mentor. Her guidance and teaching was highly instrumental in shaping my career as a scientist. I am extremely grateful to her and really enjoyed working with her.

Apart from Dr Hey-Kyoung Lee, the other NACS faculty, with whom I interacted and took courses with were also incredible teachers. The input and constructive criticism I received from them was very helpful.

My parents, brother and fiancé were an immense source of moral sustenance; their love and support helped me through all the ups and downs.

Importantly all of this would have been impossible without my friends, especially Saranga, Mathangi, Amrit, Vinit, who were my family here. I am also indebted to colleagues and friends in the lab and department who made the work environment very positive and working with them was not only fun but also a learning experience.

Table of Contents

List of Tables

List of Figures

Chapter 1: Introduction

Section 1: Requirement for a homeostatic mechanism

Many functions of the brain depend on alterations and modifications that occur to a large extent at specialized points of communication between neuronal cells called synapses. Long after Cajal had established that neurons communicated with each other at specialized junctions called synapses, Hebb and Konerski's ideas laid the ground for how synapses might be modified in response to experience-dependent changes (Hebb, 1949; Konorski et al., 1952; Konorski and Szwejkowska, 1953). Hebb's ideas revolved around the concept of coincidence-detection wherein, "cells that fire together wire together". Therefore if 2 cells connected together by a synapse were active at the same time then that synaptic connection would be strengthened. This was experimentally proven in 1973 by Bliss and Collingridge who showed this strengthening at hippocampal synapses, and called the effect Long-Term Potentiation (LTP) (Bliss and Gardner-Medwin, 1973; Bliss and Collingridge, 1993). Later on Stent proposed that anticorrelated activity leads to synaptic weakening, wherein if 2 connected cells were not active at the same time that connection would be weakened. The phenomenon of synapse weakening was termed Long-Term Depression (LTD) and almost 2 decades later LTD was experimentally shown in the CA1 region of the hippocampus (Dudek and Bear, 1992).

Synaptic modifications are imperative since the innumerable synapses in the network must have the appropriate synaptic strengths in order to respond to changes in stimuli and also enable efficient information storage. While the flexibility of synapses is an

integral part of a neuronal network, it is critical that the neuronal firing remains within a stable dynamic range. It was soon realized by various groups that if synaptic modifications were solely Hebbian, and only LTP and LTD operated in neuronal networks then that would ultimately lead to "runaway potentiation" or "runaway depression" causing the networks to become chaotic (Bienenstock et al., 1982; Miller, 1996). This would lead to instability and ultimately result in faulty information processing (Turrigiano and Nelson, 2000, 2004). Therefore to counterbalance this imbalance, Hebbian mechanisms must be constrained by non-Hebbian homeostatic mechanisms like synaptic scaling and sliding threshold (Bienenstock et al., 1982; Bear et al., 1987; Abbott and Nelson, 2000; Turrigiano and Nelson, 2004). It is important to realize that while LTP and LTD are input specific synaptic modifications, homeostatic changes involve more global alterations in synaptic weights. There are several ways to counterbalance prolonged increases or decreases in activity in neuronal networks to provide homeostatic stability: synaptic scaling, sliding threshold, changes in excitation and inhibition balance, changes in neuronal intrinsic excitability, spike timing-dependent plasticity and synaptic redistribution. In the following sections I will describe the details of each of these homeostasis mechanisms.

Section 2: Mechanisms of maintaining homeostasis

Initial reports of homeostasis showed that this phenomenon occurs at the neuromuscular junction, as a result of denervation. Due to a lack of input to the skeletal muscle there was a decrease in synaptic drive and this was compensated for

by an increase in excitability and contractions of the skeletal muscle. Various studies showed that increase in excitability can be attributed to changes in the muscle fiber wherein there was an increase in input resistance and an up-regulation of extrajunctional acetylcholine receptors (Axelsson and Thesleff, 1959; Berg and Hall, 1975). At the *Drosophila* neuromuscular junction, it was shown that a reduction in number of synapses was accompanied by an increase in quantal amplitude while a reduction in quantal amplitude was followed by an elevation of presynaptic transmitter release (Davis and Goodman, 1998). These results show that there are several homeostatic mechanisms that ensure that the synaptic transmission at the neuromuscular junction is stable.

While these studies looked at the compensatory mechanisms at the neuromuscular junction, several other investigations sought to examine how hippocampal and cortical neuronal networks maintain constancy in the face of changing input. The following sections discuss the various proposed mechanisms and experimental work supporting them.

Subsection 1: Changes in excitation: Sliding Threshold mechanism

The sliding threshold model was originally proposed to explain the synaptic modifications in the visual cortex in response to dark rearing (Bear et al., 1987). According to this model a "modification threshold (θ_M)" decides whether synaptic weights will be increased or decreased in response to changes in input activity. If postsynaptic activity falls above this threshold, then LTP is induced at those synapses and if the postsynaptic activity falls below the modification threshold then LTD is induced. This θ_M is not a constant value and varies according to the average

postsynaptic activity which is integrated at a relatively long time scale (range of hours to days) (Bienenstock et al., 1982; Bear et al., 1987). In the event of a chronic increase in average postsynaptic activity, θ_M slides to larger values, such that LTD is preferred. With a prolonged decrease in average postsynaptic activity, θ_M slides to smaller values, such that LTP is preferred. This sliding threshold has been demonstrated in rats, where prolonged periods of dark rearing, which in principle should decrease the average postsynaptic activity, caused LTP to be preferably induced at layer 2/3 visual cortical synapses. This effect of dark rearing was reversed by re-exposure to light, such that now it was easier to induce LTD at these synapses. (Kirkwood et al., 1996; Sermasi et al., 1999). NMDA receptors have been attributed to be the key regulators in the "sliding threshold" mechanism since the calcium that enters through these receptors determines whether LTP or LTD will be induced (Artola and Singer, 1993; Cummings et al., 1996; Cho et al., 2001).

NMDARs are heteromers composed of NR1, NR2 and NR3 subunits. There are 4 different NR2 subunits (a-d), which determine the functional properties of NR2-containing NMDARs changes (Monyer et al., 1994; Flint et al., 1997; Vicini et al., 1998; Quinlan et al., 1999b). NR2a containing NMDARs have faster kinetics (Carmignoto and Vicini, 1992; Monyer et al., 1994) and mediate shorter excitatory postsynaptic currents than those containing NR2b. There is evidence showing that dark rearing prevents a developmental change in NMDAR subunit composition (Fox et al., 1991; Carmignoto and Vicini, 1992; Quinlan et al., 1999a; Quinlan et al., 1999b). It is shown that the NR2a/b ratio increases over development (Quinlan et al., 1999a) which leads to a shortening of NMDAR mediated currents. This change in

kinetics may then influence the modification threshold θ_M by sliding it to the left and thus favoring induction of LTD over LTP.

Subsection 2: Changes in excitation: Synaptic scaling

According to the synaptic scaling model a chronic decrease in activity leads to an increase in the strength of all the excitatory synapses while a prolonged increase in activity is compensated for by a decrease in the strength of all the synapses. This change in synaptic strength is executed by alterations in AMPA receptor-mediated synaptic gain (Turrigiano and Nelson, 2000).

Initially, this model of maintaining homeostasis was shown experimentally *in vitro* where a chronic decrease in activity, by pharmacological manipulations, leads to an increase in the size of AMPA receptor-mediated miniature excitatory postsynaptic currents (mEPSCs) (Lissin et al., 1998; O'Brien et al., 1998; Turrigiano et al., 1998). mEPSCs are synaptic currents that occur due to the spontaneous release of a synaptic vesicle in a random manner following action potential blockade (Bekkers and Stevens, 1994). Two important parameters that are measured from mEPSC recordings are mEPSC amplitude and frequency, both of which reflect different aspects of synaptic transmission. Changes in mEPSC amplitude indicate postsynaptic modifications, such as regulation of receptor number or conductance. On the other hand, alterations in mEPSC frequency are interpreted as either changes in presynaptic release probability, vesicle recycling, un-silencing of silent synapses, or number of synapses. Importantly, sampling many mEPSCs allows estimation of an average synaptic strength across a large number of synapses.

Recently, in vivo manipulations like monocular inactivation involving 2 days of intraocular TTX injections in P21 rats have been shown to cause an increase in amplitude of AMPAR-mediated mEPSCs in layer 2/3 visual cortical neurons (Desai et al., 2002; Maffei et al., 2004). Another in vivo manipulation that has been used to chronically reduce visual activity is dark rearing, which I have used to investigate the effects of visual deprivation on excitatory synaptic transmission in primary sensory cortices in mice and rats (details in chapter 2 and chapter 3). Chronic dark rearing is known to decrease the excitatory drive to the visual cortex causing an overall decrease in activity (Czepita et al., 1994) while the spontaneous activity is shown to be either the same (Czepita et al., 1994) or increased (Benevento et al., 1992). It is important to realize that while monocular inactivation eliminates all neural activity at the retina, dark rearing does not prevent spontaneous activity in the retina.

Unlike the sliding threshold model, the mechanisms of synaptic scaling involve changes in synaptic strength mediated by AMPARs. In vitro studies of synaptic scaling showed that rat visual cortical cultures grown in the presence of an NMDA receptor antagonist, AP5, do not express changes in the mEPSC amplitude while 48 hours of blockade with CNQX leads to a significant increase in mEPSC amplitude (O'Brien et al., 1998; Turrigiano et al., 1998). These studies indicated that blocking NMDAR mediated Ca^{2+} signaling alone neither induces nor prevents synaptic scaling (Watt et al., 2000; Leslie et al., 2001). This conclusion does not hold true for all studies, since work by other groups suggests that NMDAR mediated signaling does play a role in synaptic scaling. One study found that in hippocampal neurons blocking NMDA receptor mediated mEPSCs along with TTX application caused a significant

increase in AMPAR-mediated mEPSC amplitude within 1 hour (Sutton et al., 2006). Their work suggests that NMDAR blockade along with action potential elimination may actually accelerate synaptic scaling. In another study, contrary to Turrigiano et al. (1998), chronic NMDAR blockade by AP5 causes an increase in AMPAR-mediated mEPSCs in hippocampal cultured neurons (Kato et al., 2007). It is possible that this discrepancy in the data is due to differences in brain region from which the neuronal cultures are derived. Nevertheless, the controversy regarding the involvement of NMDAR mediated signaling in synaptic scaling is unresolved, and this is also evident in the experiments involving in vivo manipulations. One particular investigation showed that reducing the Ca^{2+} permeability of NMDARs in hippocampal neurons influences the AMPA responses by decreasing the current amplitude and the frequency, both in adult and juvenile animals (Pawlak et al., 2005). In summary, the involvement of NMDAR mediated Ca^{2+} signaling in synaptic scaling remains undetermined.

i) What are the induction mechanisms of synaptic scaling?

An important and not thoroughly investigated aspect of synaptic scaling is the nature of the induction signals or triggers that allow homeostatic alterations in synaptic strength. There could be a combination of pre- and post-synaptic signals that might contribute to the activity dependent change or it could be a cell autonomous phenomenon. One important question that I have addressed in my work is the role of intracellular signaling events and machinery in translating changes in activity to global homeostatic alterations in synaptic strength.

Two recent studies have investigated the possible signals involved in homeostatic increase in synaptic strength. Leslie et al. (2001) showed that chronic depolarization of neuronal cultures using increased external K^+ leads to a scaling down of synaptic strength indicated by a decrease in quantal amplitude without a change in mEPSC frequency. This decrease in mEPSC amplitude occurred in the presence of NMDAR, AMPAR and $GABA_AR$ blockade implying that the activation of ionotropic receptors are not required, and depolarization alone is sufficient to scale down synapses. In addition, action potentials accompanying depolarization were not required for synaptic scaling, because blocking spiking did not affect the decrease in synaptic strength. Similarly one particular study (Burrone et al., 2002) showed that a chronic hyperpolarization of individual hippocampal neurons scales up excitatory synaptic strength, though in this case the increase in mEPSC amplitude was accompanied by an increase in mEPSC frequency. This study also showed that the adjustment of synaptic strength can be cell autonomous since hyperpolarizing a single cell leads to a homeostatic increase in mEPSC frequency.

While the above studies emphasize the importance of postsynaptic depolarization in triggering synaptic scaling, very recent work in hippocampal cultured neurons shows that presynaptic input activity to a given neuron is an important signal for adjusting synaptic strength (Hou et al., 2008). However, in this case the changes were homosynaptic in nature, hence they do not fit the global cell-wide synaptic scaling as suggested initially by Turrigiano et al. (1998).

ii) Possible molecular candidates involved in synaptic scaling

Brain derived neurotrophic factor (BDNF) is known to homeostatically modify excitatory synapses made onto interneurons (Rutherford et al., 1998). BDNF expression increases during seizures (Isackson et al., 1991), and has been reported to prevent scaling up of synapses (Rutherford et al., 1998). On the other hand, a chronic decrease in activity is associated with a reduction in BDNF release, and a corresponding scaling up of mEPSC amplitude (Rutherford et al., 1998). Importantly, while BDNF prevents TTX-induced increase in mEPSC amplitude, exogenous BDNF application does not cause a reduction in mEPSC amplitude by itself. This suggests that neural activity releases endogenous BDNF that prevents scaling up of synapses, and this effect is probably saturating, therefore exogenous BDNF does not cause any further decrease. In addition, since BDNF can diffuse and act on a number of synapses including those between pyramidal neurons and between pyramidal neurons and interneurons, it is an attractive candidate for maintaining homeostasis in a chronically active network (Rutherford et al., 1998; Turrigiano et al., 1998). Indeed, there is evidence that when neural activity is high the elevation in BDNF release preferentially increases synaptic strength at inhibitory synapses (Rutherford et al., 1998). Collectively, these results imply that when activity is chronically increased BDNF release is elevated and this adjusts the synaptic strengths such that there is a reduction in excitation and an enhancement of inhibition. Therefore BDNF appears to alter the excitation–inhibition balance in response to changes in activity.

Another exogenously acting molecule is Tumor necrosis factor (TNF-α), which is released from glia and is demonstrated to be involved in synaptic scaling up of excitatory synaptic transmission by chronic inactivity (Beattie et al., 2002;

Stellwagen and Malenka, 2006). Interestingly, TNF-α is not involved in scaling down synapses by enhanced activity in hippocampal cultures (Stellwagen and Malenka, 2006).

iii) Intracellular signaling molecules

CAMKII: Bidirectional regulation of CAMKII is an important mechanism by which neurons respond to changes in activity. CAMKII is one of the enzymes that phosphorylates GluR1. α-CAMKII is activated by higher levels of intracellular Ca^{2+} concentration compared to β- CAMKII (Brocke et al., 1999). When the 2 isoforms are combined in a heteromer the response to Ca^{2+} signals depends on the α/β ratio. Ca^{2+} mediated intracellular signaling is an important mechanism that is integral to many signal transduction pathways. Therefore, CAMKII can be a Ca^{2+} sensor linking changes in activity of various intracellular signaling events that eventually modify synaptic strength. Thiagarajan et al. (2002) showed that a chronic increase in activity in hippocampal cultures caused an up-regulation in α/β ratio while application of TTX was accompanied by a decrease in α/β ratio. Therefore, the level of α-CAMKII and β-CAMKII can be an important mechanism for regulating synaptic strength in response to changes in activity.

β-Catenin: In an effort to study the structural changes that accompany chronic changes in activity, recent work has identified β-Catenin as a probable candidate. Several cell adhesion molecules have been implicated in morphological changes that occur at synaptic junctions (Scheiffele, 2003). These adhesion molecules, particularly, cadherins, are connected to the extracellular cytoskeleton through β- and

α-catenins. One study shows that ablation of β-Catenin prevents TTX-induced scaling of synaptic strength (Okuda et al., 2007). Hence β-Catenin is an important link between synapse function and spine morphology.

Phosphoinositide-3 kinase : Phosphoinositide-3 kinase (PI3K) has been implicated in increasing AMPAR surface expression (Man et al., 2003);(Passafaro et al., 2001). A recent paper addressed the role of PI3K in homeostatic up-regulation of AMPAR at the surface in response to chronic activity deprivation. Suppression of single neuronal activity with transfection of inwardly rectifying potassium channel Kir2.1 caused an increase in AMPAR accumulation at the synaptic surface and this effect was PI3K dependent (Hou et al., 2008).

iv) Is the expression locus of synaptic scaling presynaptic or postsynaptic? The effects of global activity blockade by TTX in neuronal cultures are manifest as pre- and postsynaptic changes ultimately leading to stronger synapses. Neuronal cultures subjected to chronic activity blockade show an increase in AMPAR quantal amplitude (Turrigiano et al., 1998) and accumulation of postsynaptic AMPA receptors (Lissin et al., 1998; O'Brien et al., 1998; Wierenga et al., 2005) implying a postsynaptic locus of expression. In particular Turrigiano et al. (1998) and O'Brien et al. (1998) showed that there is an increase in postsynaptic response amplitude to glutamate application in chronically deprived cultures. These observations provide compelling evidence for chronic activity-induced postsynaptic changes. Furthermore, evidence so far indicates that synaptic scaling *in vivo* is mainly mediated by postsynaptic changes. For example, chronic visual deprivation causes an increase in mEPSC amplitude without a change in mEPSC frequency in visual cortical neurons

(Desai et al., 2002; Maffei et al., 2004; Goel et al., 2006; Goel and Lee, 2007), and also produces an increase in spine head size (Wallace and Bear, 2004).

While numerous studies implicate postsynaptic expression of synaptic scaling, there is a large volume of work supporting presynaptic involvement as well. Several studies demonstrated that neuronal cultures deprived of activity show an increase in mEPSC frequency (Burrone et al., 2002; Thiagarajan et al., 2002), presynaptic release probability (Murthy et al., 2001) and an elevation in spontaneous release (Bacci et al., 2001). Variability in the amount of neurotransmitter loaded into vesicles may also contribute to variations in quantal release (Liu et al., 1999). If altering the number of transporters on vesicles can lead to differences in quantal size then regulation of these transporters can provide another mechanism for changing synaptic strength in response to activity. A study showed that a chronic TTX application in neuronal cultures is associated with an increase in vesicular excitatory transporter (VGLUT1) mRNA and a decrease in vesicular inhibitory transporter (VIAAT) mRNA. Conversely a prolonged increase in activity leads to an up-regulation of VIAAT and a down-regulation of VGLUT1 mRNA (De Gois et al., 2005).

Differences between Synaptic scaling and Sliding threshold mechanism

Sliding threshold mechanism	Synaptic scaling mechanism
•Changes in synaptic strength are not global.	•Global changes in synaptic strength
•Dependent on NMDARs	•Independent of NMDARs, dependent on AMPARs
•Induced by changes in timed average postsynaptic activity; change in postsynaptic firing rate is a potentially important readout	•Induced by changes in average postsynaptic depolarization ; action potentials not required
•Absolute LTP/LTD range will remain the same	•Absolute LTP/LTD range will change
•Changes the ratio of NR2A/NR2B	•Changes the ratio of GluR1/2

Subsection 3: Spike timing-dependent plasticity (STDP)

As suggested by Larry Abbot, a delicate balance between LTP and LTD in neuronal networks can also be used to constrain instability by regulating the total level of synaptic drive. Spike timing-dependent plasticity (STDP) refers to synaptic modifications that are based on temporal correlations between pre- and postsynaptic activity. This implies that if postsynaptic neuronal firing is followed by presynaptic neuronal firing then that synapse will be strengthened. On the other hand, if postsynaptic activity precedes presynaptic firing then that synapse will be weakened. Presynaptic spikes can occur randomly in time with respect to postsynaptic firing and

hence depending on the temporal order, at any given moment, either LTP or LTD could be induced at these synapses (Abbott and Nelson, 2000). A few studies have examined the various criteria that determine whether LTP or LTD is induced at synapses. One particular study that looks at inputs to layer2/3 in the barrel cortex shows that stochastic correlations in pre- and post synaptic activity lead to an overall reduction in synaptic strength (Feldman, 2000). Therefore it appears that overall, in the cortex, LTD dominates over LTP. Now, if a neuron is chronically receiving high input, its firing rate will increase initially but over a prolonged period of time there will be a net decrease in synaptic efficacy due to the preponderance of LTD over LTP. This will subsequently lead to a weakening of the synaptic drive and hence a decrease in the firing rate of the neuron at this longer time scale. Therefore the temporal asymmetry underlying STDP can impose a fine balance and thus have a stabilizing influence in a neuronal network.

However it is important to know that work in hippocampus has shown that STDP induction is also governed by the initial strength of synapses and target cell specific mechanisms (Bi and Poo, 1998). Hence it is not clear if the temporal asymmetry underlying STDP is a ubiquitous mechanism.

Subsection 4: Changes in Inhibition

Maintaining a balance between excitation and inhibition is critical for efficient functioning of neuronal networks. Even minute changes in this balance can lead to runaway excitability (Kriegstein, 1987). In addition, disruption of the excitation to inhibition balance can affect the output of visual cortical neurons and therefore bring

about significant modifications in experience-dependent synaptic plasticity (Kirkwood and Bear, 1994; Kirkwood et al., 1995; Hensch et al., 1998). One recent study addressed the effect of chronic changes in sensory experience on the excitation-inhibition balance of cortical neurons. Depriving the visual cortex of input by intraocular TTX injections brought about an adjustment in the excitation-inhibition balance by increasing the strength of excitatory connections and decreasing the synaptic gain at inhibitory connections (Maffei et al., 2004).

Subsection 5: Changes in Intrinsic excitability

Recent investigations revealed that modulations in neuronal intrinsic excitability occur as a result of changes in activity in neuronal networks (Turrigiano et al., 1994; Turrigiano et al., 1995; Magee, 2003). In an effort to determine if a chronic decrease in activity brought about changes in neuronal intrinsic excitability, Desai et al. (Desai et al., 1999) deprived cortical cultures of activity for 2 days by TTX application and then investigated alterations, if any, in intrinsic excitability. They found that there was an increase in firing frequency and also the threshold to spike was lowered. In addition, activity deprivation led to a regulation of ionic conductances leading to an increase in Na+ current (also shown in Wierenga, 2005).

A recent study in Xenopus demonstrated that changes in intrinsic properties play a critical role in ensuring that developing visual circuits remain within a stable dynamic firing range (Pratt and Aizenmann , 2007).

The above description shows that there are several mechanisms that can be involved in homeostatic plasticity. Homeostasis can be mediated either by one

mechanism alone or a combination. In addition it is possible that these agents of homeostatic plasticity might be specific to brain regions or age and might operate depending on the computational requirements of that circuit. One advantage of having so many potential strategies of stabilizing neural networks is that in the absence or failure of one mechanism the neuronal system can rely on another method of homeostatic plasticity.

Visual deprivation- induced plasticity

Subsection 1: Critical period and Ocular dominance (OD) plasticity

In an attempt to understand the functional architecture of the visual cortex and how it is affected by experience, the classical work of Wiesel and Hubel spearheaded an era of 'visual experience-induced plasticity' research. Their studies of the cat visual cortex gave birth to the idea of the "critical period" which is a distinct period early in cortical development, when synaptic connections can be transformed easily by experience (Wiesel and Hubel, 1963; LeVay et al., 1980; Hubel, 1982; Gordon and Stryker, 1996). To investigate differences in visual experience-dependent modifications within and outside the critical period, monocular deprivation paradigm was, and is still currently being used. This procedure involves temporarily suturing the eyelid of the eye that sends its input to the contralateral hemisphere in the visual cortex. Hubel and Wiesel categorized visual cortical cells into different ocular dominance classes depending on the responsiveness of the neurons to either eye (Hubel and Wiesel, 1970). Following monocular deprivation, Hubel and Wiesel observed that there is a shift in ocular dominance of neurons, such that the majority

responded preferentially to the open eye stimulation. This type of plasticity was termed Ocular Dominance plasticity (OD plasticity), and was found to be prominent early in development (Hubel and Wiesel, 1970; Gordon and Stryker, 1996). Later, studies found that monocular deprivation in juveniles produces 2 important effects: rapid deprivation induced depression (LTD) of the deprived eye responses occurring over the first 3 days and a delayed potentiation (LTP) of the ipsilateral eye responses occurring after 5 days (Frenkel and Bear, 2004). A recent investigation shows that the critical period for Long Term Potentiation (LTP) and Long Term Depression (LTD) in layer 4 of the visual cortex ends soon after eye opening (Jiang et al., 2007). Also there is a developmental decrease that correlates with the closure of OD plasticity (around P35) induced by MD (Gordon and Stryker, 1996). However, the ability to induce LTP and LTD persists past the critical period in layer 2/3 (Kirkwood et al., 1993; Kirkwood and Bear, 1994; Jiang et al., 2007). These studies demonstrate there are layer specific differences in maturation of visual cortex and layer 2/3 remains plastic throughout adulthood.

Subsection 2: Adult visual cortical plasticity

What is so critical about age that diminishes plasticity in the adult visual cortex? The current understanding is that inhibition/excitation (I/E) ratio is an important determinant of the critical period closure; the I/E ratio increases as the animal matures and that is thought to prevent further plasticity. The idea that maturation of inhibitory circuit restricts cortical plasticity in the adult has been shaped by the work of several groups in the visual cortex (Kirkwood and Bear, 1994; Hensch et al., 1998; Huang et

al., 1999). Other reports emphasize that the organization of chondroitin sulphate proteoglycans (CSPGs) into perineuronal nets coincides with the closure of the critical period (Pizzorusso et al., 2002).

However, recent reports suggest that OD plasticity can be induced in adults under certain circumstances. Sawtell et al. (2003) showed that lengthening the period of monocular deprivation (from 3 days to 5 days) elicits ocular dominance plasticity well beyond the closure of classical "critical period" (Sawtell et al., 2003). Unlike in juveniles, the adult OD plasticity was only associated with potentiation of open eye inputs, and no change in response to the closed eye inputs (Frenkel and Bear, 2004). However, a "juvenile-like" OD plasticity can be restored in adults when a brief MD is preceded with a prolonged binocular deprivation in adult rats (He et al., 2006) or by disrupting perineuronal nets (Pizzorusso et al., 2002).

A number of studies also indicate that different cortical layers exhibit varying ability to undergo OD plasticity in adults. Most studies demonstrate that layer 4 matures earlier than extragranular layers, and hence display a short and well-defined critical period for sensory plasticity. In cats, the critical period for layer 4 in the visual cortex ends around 8 months of age (Daw et al., 1992). In contrast, superficial layers seem to have an extended critical period for OD plasticity that lasts longer than layer 4. In cat visual cortex, extragranular layers remain plastic up to 1 year (Daw et al., 1992). This corresponds nicely with the observations that LTP and LTD in layer 4 has a short distinct critical period, while layer 2/3 remain plastic through adulthood (Kirkwood et al., 1993; Kirkwood and Bear, 1994; Jiang et al., 2007). Similarly, homeostatic synaptic scaling also exhibits layer specific critical periods. In rodents, layer 4

exhibits synaptic scaling by visual deprivation only between P14 and P16, while layer 2/3 starts undergoing this type of scaling from P21 (Desai et al., 2002). I have extended the latter observation to show that layer 2/3 neurons can undergo synaptic scaling through adulthood (details in Chapter 3).

Evidence of adult plasticity in primary visual cortex have also been shown in human studies where training over days to weeks can cause robust and lasting improvement in various aspects of visual perception (Karni and Sagi, 1991). Other human studies show that contrary to conventional dogma blind people who have had no visual stimulation in childhood can learn to see. Whether adult plasticity in humans is also associated with similar neural mechanisms, such as Hebbian synaptic modification, uncovered from animal studies is unknown.

Subsection 3: Cross-modal plasticity

Loss of vision not only alters visual cortex function, but is also known to accompany increased functionality of other sensory modalities (Lessard et al., 1998; Goldreich and Kanics, 2003). Systems level analyses of cross-modal plasticity have revealed anatomical and functional rewiring of cortical circuits (Bavelier and Neville, 2002). A few animal and human studies demonstrate cross modal changes where lack of input to one modality is compensated by alterations in functionality of other sensory systems. Cats and mice that are deprived of vision from birth show supernormal growth of facial vibrissae and whisker representation in the somatosensory cortical barrel field shows enlargement (Rauschecker et al., 1992). Human studies report that Braille reading in blind subjects activates the primary visual cortex (Buchel, 1998).

However, little is known about the cellular and molecular mechanisms underlying this type of plasticity.

It would be interesting to see if these compensations involved mechanisms that were similar to homeostatic changes in synaptic strength, which occurs in the event of chronic increases or decreases in activity. During the course of this study, I found a possible cellular correlate for cross-modal plasticity, which will be discussed in Chapter 2. Briefly, the cross-modal changes in excitatory synaptic transmission following visual deprivation observe the rules of synaptic scaling and are accompanied by alterations in postsynaptic AMPA receptors.

Section 5: Alpha-amino-3-hydroxyl-5-methyl-4-isoxazolepropionic acid (AMPA) receptor regulation

Subsection 1: Regulation of AMPAR function by subunit composition

Glutamate is the predominant neurotransmitter that acts at a majority of excitatory synapses in the central nervous system. The action of glutamate is mediated by three types of ionotropic glutamate receptors: AMPA, NMDA and Kainate receptors. Though both types of receptors respond to glutamate and mediate excitatory synaptic transmission, the roles played by both the receptors are distinct. A large portion of the fast basal excitatory synaptic transmission is mediated by AMPA receptors, because NMDA receptors are normally blocked by magnesium at resting membrane potentials.

AMPA receptors are tetrameric channels composed of combinations of glutamate receptor (GluR) subunits 1-4 (Dingledine et al., 1999). In the adult forebrain, AMPA receptor population consists of primarily GluR1/GluR2 and GluR2/GluR3 heteromers with the predominant population being that of GluR1/GluR2 heteromers (Wenthold et al., 1996). Each subunit has a N-terminal domain that binds to glutamate and 4 transmembrane domains (Mayer and Armstrong, 2004). Among the transmembrane domains the second one (M2) forms the pore of the receptor channel and specifies ion selectivity. The majority of the GluR2 subunit undergoes RNA editing within the M2 region wherein, a critical glutamine 607 residue (Q607) is converted to Arginine (R607). This RNA editing, called "Q/R editing", confers distinct physiological properties to AMPA receptors containing the GluR2 subunit, namely impermeability to calcium and resistance to polyamine block (Verdoorn et al., 1991; Washburn et al., 1997). The lack of block by endogenous intracellular polyamine imparts an electrophysiological signature of GluR2-containing AMPA receptors, which display linear I/V curves (Rozov et al., 1998). On the other hand, GluR2-lacking AMPA receptors are blocked by polyamines at positive potentials, and hence display inward rectifying currents. Another biophysical property of AMPARs that is affected by the inclusion of the GluR2 subunit in an AMPAR complex is the channel conductance. GluR2-lacking receptors have a higher single channel conductance (Swanson et al., 1997).

The subunit composition of AMPA receptors also determines the kinetic properties of the AMPA receptor mediated current, wherein GluR1 containing homomeric AMPA receptors have smaller decay time constant (τ) than heteromeric AMPA receptors

(Mosbacher et al., 1994). In cells where GluR2 is one of the predominantly expressed subunit, the preferred and most stable stoichiometry of AMPA receptors are complexes containing 2 GluR1 and 2 GluR2 subunits (Mansour et al., 2001; Brorson et al., 2004). Even though most AMPA receptors exist as heteromers rather than homomers, certain types of neural activity can allow GluR2-lacking AMPARs to express at synapses (Pellegrini-Giampietro et al., 1997; Liu and Cull-Candy, 2000; Liu and Cull-Candy, 2002; Ju et al., 2004; Thiagarajan et al., 2005; Clem and Barth, 2006; Goel et al., 2006).

Each AMPAR subunit also contains a cytoplasmic tail (C-terminal tail), which is distinct, and some subunits have PDZ binding domains which enables these subunits to interact with PDZ domain containing proteins. Depending on the c-tail, different AMPARs are trafficked to synapses via distinct mechanisms. For example, AMPAR subunits with a short c-tail, such as GluR2 and GluR3, can be incorporated to synapses constitutively, while ones with a long c-tail, like GluR1 and GluR4, require synaptic activity (Shi et al., 2001). Originally it was shown that, GluR1 deficient mice lack LTP in the hippocampus (Zamanillo et al., 1999), though a later study shows that modification in the induction protocol can produce LTP in these knockout mice (Hoffman et al., 2002). In addition, it has been demonstrated that GluR1 synaptic delivery is imperative for establishing LTP (Hayashi et al., 2000). These results suggest that for activity-dependent synaptic plasticity, like LTP, insertion of GluR1 containing receptors is important.

Subsection 1: Regulation of AMPAR function by phosphorylation

Phosphorylation, a form of post-translational modification, can occur at certain residues on the C-terminal tail of AMPA receptor subunits to modify receptor function. There are two well characterized phosphorylation sites on the GluR1 subunit, serine-831 (S831) and serine-845 (S845) (Roche, 1994), both of which when phosphorylated by CAMKII and PKA, respectively, can increase AMPA receptor mediated current (Derkach et al., 1999; Banke et al., 2000). Phosphorylation at S831 is known to increase the channel conductance (Derkach et al., 1999; Esteban et al., 2003; Oh and Derkach, 2005) ,while phosphorylation at S845 is implicated in trafficking AMPA receptors to the synaptic surface (Esteban et al., 2003). Studies have shown that regulation of phosphorylation at S831 and S845 is important for LTP and LTD (Lee et al., 2000) as well as for learning and memory (Lee et al., 2003). In addition, recent studies have implicated the regulation of GluR1-containing AMPA receptors as part of an expression mechanism of homeostatic synaptic plasticity (O'Brien et al., 1998; Ju et al., 2004; Thiagarajan et al., 2005; Sutton et al., 2006). To investigate whether the homeostatic regulation of GluR1 is dependent on its phosphorylation, I used transgenic mice, GluR1-S831A and GluR1-S845A, which were generated in Dr. Richard Huganir's lab at John Hopkins. In GluR1-S831A mice, the serine residue at 831 site was mutated to an alanine and therefore prevented phosphorylation by PKC and CAMKII. Likewise in the GluR1-S845A mice, the serine residue at the 845 site was mutated to an alanine and thus eliminated PKA-dependent phosphorylation. I will describe the effects of these mutations on visual experience-induced homeostatic synaptic plasticity in chapter 4.

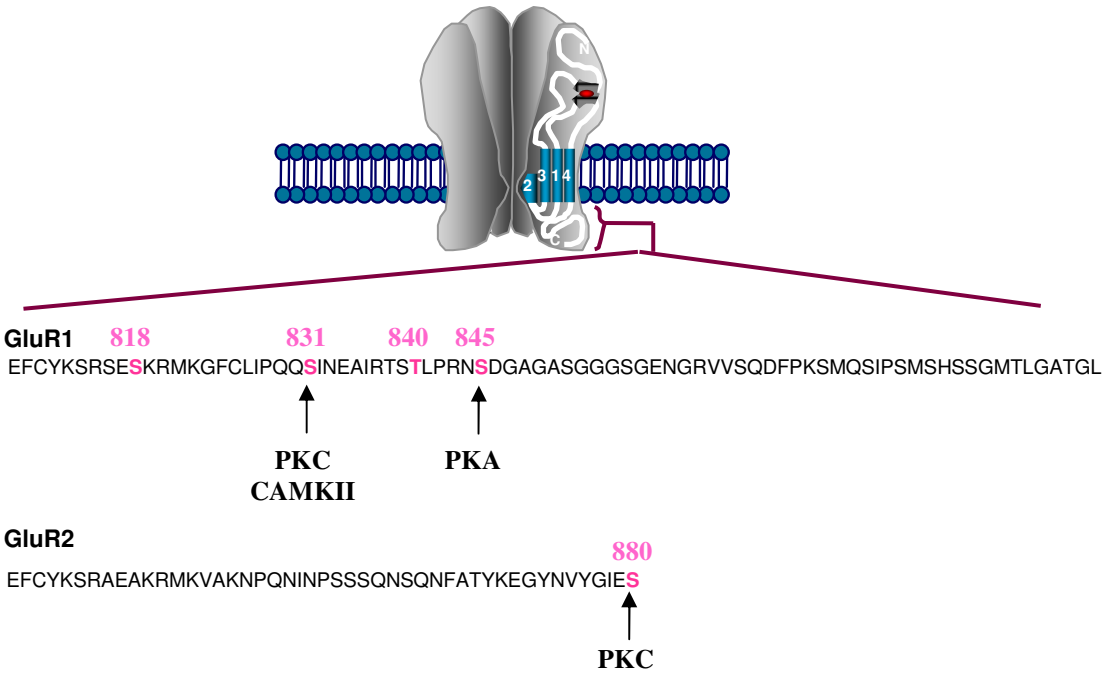

Figure 1.1: Illustration showing the various phosphorylation sites on GluR1 and GluR2 subunits

Subsection 3: Regulation of AMPAR function by intracellular binding partners

GluR2 subunit has 2 important sites on the C terminal tail that mediate direct interactions with several proteins with important functional consequences. One site, which is proximal to the fourth transmembrane domain (M4) binds N-ethylmaleimide-sensitive factor (NSF) and Adaptor protein-2 (AP2). In hippocampal neurons NSF-GluR2 interaction is essential for regulating the surface expression of AMPA receptors (Nishimune et al., 1998; Luthi et al., 1999; Noel et al., 1999). In particular studies using peptides that out-compete biding of NSF to GluR2 reported a rapid decrease in AMPAR-mediated EPSC amplitude (Nishimune et al., 1998) and an almost complete loss of AMPA receptor expression on the plasma membrane (Noel et

al., 1999). These studies indicate that NSF–GluR2 interaction is important for maintaining cell surface and synaptic AMPA receptor expression. In addition, further investigations showed that LTD involves the removal of GluR2 containing AMPARs that interact with NSF (Luthi et al., 1999). However, the latter effect may be due to disrupting binding of AP2, which binds to GluR2 at the NSF binding site (Lee et al, 2002). AP2 is involved in clathrin dependent endocytosis (Sorkin, 2004), hence may aid clathrin-mediated endocytosis required for AMPAR internalization during LTD (Carroll et al., 1999; Carroll et al., 2001).

The GluR2 subunit also has a PDZ ligand region, which interacts with PDZ domain containing proteins such as Glutamate receptor interacting protein (GRIP) (Dong et al., 1997), AMPAR binding protein (ABP or also known as GRIP2) (Srivastava et al., 1998) and protein interacting with C-kinase- 1 (PICK1) (Dev et al., 1999; Xia et al., 1999; Daw et al., 2000). Interestingly, within the PDZ ligand region is a serine residue, S880, which is phosphorylated by PKC (Chung et al., 2000). Phosphorylation of S880 allows GluR2 to preferentially interact with PICK1, and not GRIP (Matsuda et al., 1999; Chung et al., 2000; Matsuda et al., 2000). There is some discrepancy in attributing a role to GluR2/3 interaction with GRIP/ABP and PICK1, since some studies show that GluR2/3 interaction with GRIP/ABP is important for expression of hippocampal LTD (Li et al., 1999; Daw et al., 2000), while others show that it is the PICK1-GluR2 interaction that is critical (Kim et al., 2001; Seidenman et al., 2003). Despite these differences, it is clear that GluR2 associates with several proteins and these interactions play a role in regulating endocytosis of AMPA receptor.

While there is little evidence suggesting a role of GluR2 regulation in homeostatic plasticity, I wanted to examine whether GluR2 interaction with PDZ domain proteins may play a role. In order to test this, I used transgenic mice generated in Dr Richard Huganir's lab at John Hopkins, which lack the last 7 amino acids on the C terminal region of GluR2 and therefore prevent phosphorylation of S880 as well as binding to GRIP/ABP and PICK1 (GluR2 Δ 7 mice) (Gardner et al., 2005). I will describe my results on the dark rearing induced effects in these GluR2 Δ 7 mice in chapter 5.

Chapter 2: Cross- modal regulation of AMPA receptors in primary sensory cortices by visual experience

Published in Nature Neuroscience:
Goel A, Jiang B, Xu L, Song L, Kirkwood A, and Lee, HK, Nature Neuroscience 2006; 9:1001-1003

My contribution: Measurement of mEPSCs.

Section 1: Introduction

Lack of a sensory input not only alters cortical circuitry subserving the deprived sense, but also produces compensatory changes in the functionality of other sensory modalities. Several studies show that loss of vision is usually accompanied by increased functionality of other sensory modalities (Lessard et al., 1998; Goldreich and Kanics, 2003). Systems level analyses of cross-modal plasticity have revealed anatomical and functional rewiring of cortical circuits (Bavelier and Neville, 2002). However, little is known about the cellular and molecular mechanisms underlying this type of plasticity. Here we examined whether manipulation of visual experience can induce bidirectional cross-modal plasticity of synaptic function in primary sensory cortices, and investigated the molecular mechanisms underlying this form of plasticity.

In this chapter, we report that visual deprivation produces opposite changes in synaptic function at primary visual and somatosensory cortices, which are rapidly reversed by visual experience. This type of bidirectional cross-modal plasticity is associated with changes in synaptic AMPA receptor subunit composition.

Section 2: Materials and Methods

Subsection 1: Dark rearing animals

Long-Evans rats (Charles River) were raised under normal lighted environment (12 hr light/12 hr dark cycle) until 4 weeks of age. Dark-rearing was initiated either at birth for 5 weeks or at 4 weeks of age for a duration of 1 week, while control (normal-reared) animals were continuously raised in the normal lighted condition for the same duration. The animals in the dark were cared for using infrared vision goggles under dim infrared light. After 1 week of dark-rearing, some of the rats were taken out to the lighted environment for 2 days to study the effect of re-exposure to light.

Subsection 2: Whole cell recording of AMPA receptor mediated EPSCs

The cortical slices were moved to a submersion recording chamber mounted on a stage of an upright microscope (E600 FN, Nikon) equipped with infrared differential interference contrast (IR-DIC). Layer 2/3 pyramidal cells were visually identified and patched using a whole-cell patch pipette (tip resistance: 3-5 MΩ) filled with intracellular solution (130 mM Cs-gluconate, 8 mM KCl, 1 mM EGTA, 10 mM HEPES, 4 mM ATP and 5 mM QX-314; pH 7.4; 285-295 mOsm).

To isolate AMPA receptor-mediated mEPSCs, 1 µM TTX, 20 µM bicuculline, and 100 µM D,L-APV were added to the ACSF (2 ml/min, 30 ± 1˚C), which was continually bubbled with 95% O_2/5% CO_2. mEPSCs were recorded at a holding potential (Vh) of –80 mV using Axopatch-clamp amplifier (Axon Instruments), digitized at 2 kHz by a data acquisition board (National Instruments), and acquired using the Igor Pro™ software (Wave Metrics). Acquired mEPSCs were analyzed

using the Mini Analysis Program (Synaptosoft). The threshold for detecting mEPSCs was set at 3 times the Root Mean Square (RMS) noise. There was no significant difference in RMS noise between the experimental groups (Vctx: NR: 1.6 ± 0.04, n = 8; 1 wk DR: 1.9 ± 0.07, n = 16; D+L: 1.7± 0.09, n = 13, ANOVA: F (2,34) = 3.086, p > 0.05; Vctx: NR: 1.5 ± 0.1, n = 12; 5 wk DR: 1.8 ± 0.15, n = 9; t-test: p > 0.1; Sctx: NR: 1.8 ± 0.06, n = 12; 1 wk DR: 1.9 ± 0.08, n = 16; D+L: 1.7 ± 0.07, n = 15, ANOVA: F(2,40) = 0.825, p > 0.4; Sctx: NR: 2.0 ± 0.09, n = 15; 5 wk DR: 1.9 ± 0.07, n = 19; t-test: p > 0.08; Actx: NR: 1.9 ± 0.03, n = 17; DR: 1.8 ± 0.05, n = 18; t-test: p > 0.1; Fctx: NR: 1.9 ± 0.06, n = 11; DR: 2.0 ± 0.09, n = 9; t-test: p > 0.3). A possibility of dendritic filtering was assessed by plotting mEPSC amplitude against mEPSC rise time. Cells showing a negative correlation between mEPSC amplitude and rise time (i.e. dendritic filtering present) were excluded from analysis (~ 5% of cells) as well as mEPSCs with greater than 3 msec rise time (measured between 10-90% of amplitude). Average mEPSC amplitude and frequency were calculated and compared across different experimental groups using one-factor ANOVA or unpaired Student's t-test. Only the cells and recording conditions that meet the following criteria were studied: Vm ≤ –65 mV, input R ≥ 200 MΩ, series R ≤ 25 MΩ. For older mice (P 97), we only included cells that had a series R ≤ 20 MΩ. Cells were discarded if input R or series R changed more than 15%. Junction potentials were typically less than 5 mV, and were left uncompensated.

Evoked AMPA receptor-mediated synaptic currents (EPSCs) were measured from layer 2/3 pyramidal cells of either visual or somatosensory cortices in response to stimulation through an electrode (concentric bipolar, FHC) placed in layer 4. To

isolate the AMPA receptor component, 100 µM D, L-APV and 100 µM bicuculline were added to the bath solution. The concentration of $CaCl_2$ and $MgCl_2$ in the ACSF were changed to 4 mM and 2 mM, respectively, to prevent polysynaptic responses upon stimulation in the presence of bicuculline. Intracellular recording solution containing 200 µM spermine (in 90 mM $CsMeSO_3H$, 5 mM $MgCl_2$, 8 mM NaCl, 10 mM EGTA, 20 mM HEPES, 1 mM QX-314, 0.5 mM Na_3GTP, and 2 mM Mg•ATP, pH 7.2, 250-270 mOsm) was used. For generating I-V curves for rectification measurements, cells were held at –60, –40, –20, 0, +20 and +40 mV. Inward Rectification (IR) was calculated by dividing the absolute amplitude of average EPSC measured at –60 mV by that at +40 mV. There were no significant differences in calculated reversal potentials between groups (Vctx: NR = 2 ± 3.0 mV, n = 6; DR = 1 ± 1.1 mV, n = 9; D+L = 4 ± 1.4 mV, n = 5; ANOVA: $F(2,17) = 0.457$, $p > 0.6$; Sctx: NR = 4 ± 2.2 mV, n = 6; DR = 4 ± 0.9 mV, n = 9; D+L = 2 ± 1.1 mV, n = 5; ANOVA: $F(2,17) = 0.785$, $p > 0.4$). Reversal potentials were calculated using equations generated by fitting a linear regression curve to the current values collected at negative holding potentials. Only the cells and recording conditions that meet the following criteria were studied: $Vm \leq -65$ mV, input $R \geq 100$ MΩ, series $R \leq 20$ MΩ. Cells were discarded if input R or series R changed more than 15%. Junction potentials were typically less than 5 mV, and were left uncompensated.

Subsection 3: Post synaptic density (PSD) preparation

Visual and somatosensory cortices from normal-reared and dark-reared rats were gently homogenized on ice in HEPES-buffered sucrose (0.32 M sucrose, 4 mM HEPES, pH 7.4) containing 2 mM EGTA, 50 mM NaF, 10 mM sodium

pyrophosphate, 1 mM sodium orthovanadate, 1 μM okadaic acid, and protease inhibitors (Protease Inhibitor Cocktail, Pierce). Primary visual or somatosencory cortices from two animals were pooled together for one data point. The homogenates (H) were centrifuged at 800 x g for 10 min (4˚C) to remove pelleted nuclear fraction (P1), and the resulting supernatants (S1) were centrifuged at 10,000 x g for 15 min (4˚C) to yield the crude membrane pellets (P2). P2 fractions were resuspended in HEPES-buffered sucrose with inhibitors and respun at 10,000 x g for 15 min (4˚C) to yield the washed crude membrane fractions (P2'). P2' fractions were lysed by hypo-osmotic shock in ice-cold 4 mM HEPES (pH 7.4, with inhibitors), and centrifuged at 25,000 x g for 20 min to generate lysed synaptosomal membrane fractions (P3). P3 was subsequently resuspended in HEPES-buffered sucrose with inhibitors, and run on a discontinuous sucrose gradient (1.2 M, 1.0 M, and 0.8 M sucrose with inhibitors) at 150,000x g for 2 hours (4˚C). Synaptic plasma membrane (SPM) fractions were collected between 1.0 M and 1.2 M sucrose and diluted with 2.5 volumes of 4 mM HEPES with inhibitors. SP M was pelleted by centrifugation at 150,000 x g for 30 min (4˚C), resuspended in 0.5% Triton X-100, HEPES-EDTA solution (50 mM HEPES, 2 mM EDTA, pH 7.4) with inhibitors, and rotated for 15 min at 4˚C. Solubilized SPM was then centrifuged at 32,000 x g for 20 min to pellet the postsynaptic density fraction (PSD). PSD fractions were resuspended in gel sample buffer and processed for SDS-PAGE (4 μg of PSD proteins were loaded per lane) and immunoblot analysis.

Subsection 4: Immunoblot analysis

SDS-PAGE gels were transferred to polyvinyl difluoride (PVDF) membranes (Immobilon^{TM}, Millipore). The PVDF membrane blots were blocked for ~1 hr in blocking buffer (1% bovine serum albumin and 0.1% Tween-20 in phosphate buffered saline (PBS), pH 7.4), and subsequently incubated for 1-2 hrs in primary antibodies (Ab's) diluted in blocking buffer to yield the effective concentration as tested prior to the experiments. After 5 times 5 min washes in blocking buffer, the blots were incubated for 1 hr in 2nd Ab linked to alkaline phosphatase (AP) diluted 1:10,000 in blocking buffer. The blots were washed 5 times 5 min, and developed using enhanced chemifluorescence substrate (ECF substrate, Amersham). The ECF blots were scanned and quantified using a Versa Doc 3000^{TM} gel imaging system (Bio Rad). The signal of each sample on a blot was normalized to the average signal from normal-reared (NR) or dark-reared (DR) samples respectively to obtain the % of average NR or % of average DR values, which were compared across different experimental groups using one-factor ANOVA or unpaired Student's t-test.

Section 3: Results

Subsection 1: Opposite changes in mEPSC amplitude with 5 weeks of dark rearing in layer 2/3 primary sensory cortical neurons.

To study cross-modal changes in synaptic function by visual deprivation, we dark-reared Long-Evans rats from birth for a period of 5 weeks, and measured AMPA receptor (AMPAR)-mediated miniature excitatory postsynaptic currents (mEPSCs) in layer 2/3 pyramidal neurons in primary visual and somatosensory cortex slices (see

methods). In visual cortex, dark-rearing produced an increase in mESPC amplitude (5 week NR: 8.8 ± 0.6 pA, n = 12, 5 week DR: 13.7 ± 1.5 pA, n = 9; $p < 0.01$, t-test, Fig 2.1a, left panel, inset). This is evident in the cumulative probability of AMPAR-mediated mEPSC amplitudes in visual cortex neurons from normal-reared and rats dark-reared for 5 weeks. There is a shift in mEPSC amplitude from DR rats towards the right indicating an increase in mEPSC amplitude. There was a significant difference between cumulative probability of NR and DR (Kolmogorov-Smirnov test: $p < 0.001$, Fig 2.1a, left panel).

There was no significant change in mEPSC frequency between the two groups (NR: 1.6 ± 0.2 Hz, n = 12; DR: 1.5 ± 0.3 Hz, n = 9; t-test: $p > 0.7$, Fig 2.1a right panel) or kinetics (Fig 2.1a, middle panel).

To ascertain the cross modal effect of visual deprivation we assayed mEPSCs from layer 2/3 somatosensory cortex pyramidal cells. While there was a trend towards a decrease in mEPSC amplitude in somatosensory cortical neurons with dark rearing this decrease did not reach statistical significance (5 week NR: 17.1 ± 1.8 pA, n = 15; 5 week DR: 14.3 ± 1.0 pA, n = 19; t-test, $p = 0.19$, Fig 2.1b, left panel inset). While we did not detect a significant difference in mEPSC amplitude with dark rearing, there was a significant difference in the cumulative probability of mEPSC amplitude from somatosensory cortical neurons between normal reared and dark reared rats (Kolmogorov-Smirnov test between NR and DR: $p < 0.001$, Fig 2.1b, left panel). This indicates that while there was no statistically significant difference between the average amplitudes of NR and DR rats, there was a significant shift in amplitude distribution.

Also there was no change in mEPSC frequency (NR: 2.4 ± 0.4 Hz, n = 15; DR: 2.0 ± 0.4 Hz, n = 19; t-test: $p > 0.4$, Fig 2.1b, right panel) or kinetics (Fig 2.1b, middle panel)

Subsection 2: Opposite changes in GluR1/2 ratio with 5 weeks of dark rearing in layer 2/3 primary sensory cortical neurons.

The change in mEPSC amplitudes without a change in frequency implied that the locus of change was post synaptic. Hence to determine whether there was a change in post synaptic AMPA receptors that was responsible for the changes in mEPSC amplitude we biochemically isolated post synaptic density fraction and measured changes in GluR1 and GluR2. GluR1 content in PSDs from 5 weeks DR rat visual cortex was greater compared to that from NR controls (NR: 100 ± 7% of average NR, n = 9; DR: 140 ± 16% of average NR, n = 13; t-test: $p < 0.04$, Fig 2.1c, left panel), which occurred without changes in GluR2 (NR: 100 ± 4% of average NR, n = 9; DR: 111 ± 12% of average NR, n = 13; t-test: $p > 0.3$, Fig 2.1c, middle panel). This led to a significant increase in GluR1/GluR2 (R1/R2) ratio in 5 weeks DR (NR: 100 ± 6% of average NR, n = 9; DR: 137 ± 13% of average NR, n = 13; t-test: $p < 0.02$, Fig 2.1c, right panel).

In the somatosensory cortex there was a significant decrease in GluR1/GluR2 ratio in PSDs of 5 week DR compared to NR controls (NR: 100 ± 14% of average NR, n = 8; DR: 49 ± 7% of average NR, n = 9; t-test: $p < 0.01$, Fig 2.1d, right panel). This occurred without statistically significant changes in GluR1 or GluR2 content in the PSD (GluR1: NR = 100 ± 12% of average NR, DR = 74 ± 10% of average NR, t-test:

$p > 0.1$; Fig 2.1d, left panel; GluR2: NR: 100 ± 17% of average NR, DR = 141 ± 27% of average NR, t-test: $p > 0.2$; Fig 2.1d, middle panel).

We wanted to confirm these changes in GluR1/2 ratio electrophysiologically and hence we measured the inward rectification of current through synaptic AMPA receptors in normal reared and dark reared rats. Inward rectification was larger in visual cortical neurons in 5 weeks DR rats when compared to age-matched NR controls (inward rectification (I_{-60mV}/I_{+40mV}): NR = 1.63 ± 0.07, n = 11; DR = 3.25 ± 0.26, n = 14; t-test: $p < 0.0001$; Fig 2.1e). On the other hand in the somatosensory cortex, there was less inward rectification of AMPA receptor currents in neurons from 5 weeks DR rats compared to NR controls (inward rectification (I_{-60mV}/I_{+40mV}): NR = 3.65 ± 0.22, n = 14; DR = 2.20 ± 0.13, n = 18; t-test: $p < 0.0001$; Fig 2.1f).

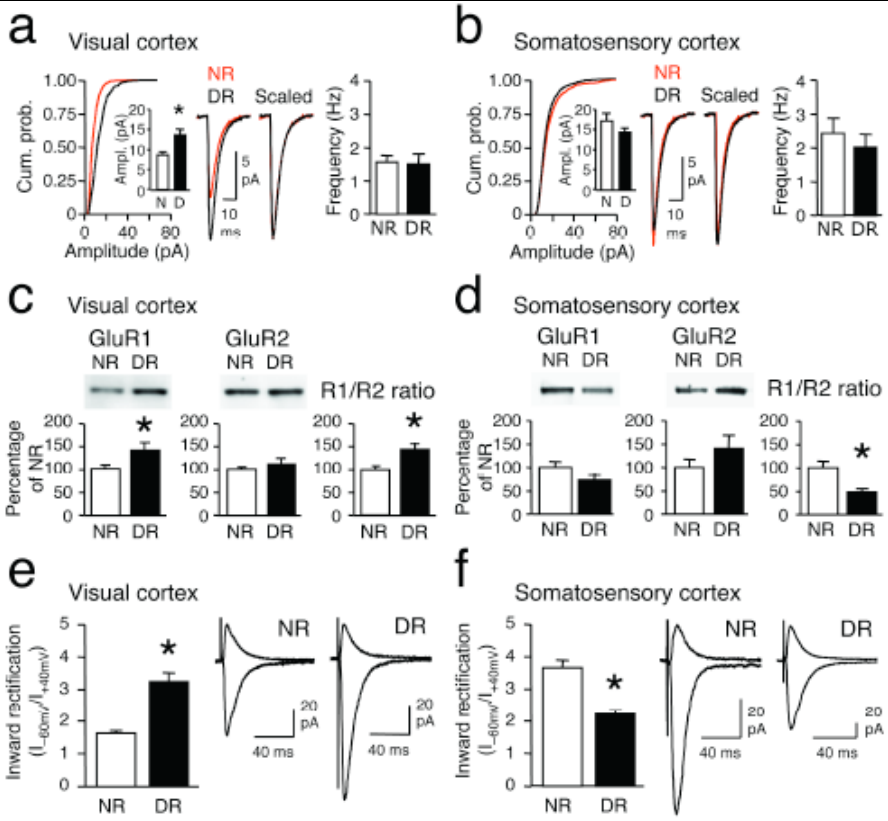

Figure 2.1. Changes in synaptic AMPA receptors in visual and somatosensory cortices by 5 weeks of dark-rearing from birth.

a. Cumulative probability of AMPAR-mediated mEPSC amplitudes in visual cortex neurons from normal-reared (NR: red line) and rats dark-reared for 5 weeks (DR: black line). Inset: comparison of average mESPC amplitude from cells of NR (N) and 5 week DR (D). Middle panel shows average mEPSC traces (NR: red, DR: black). Scaled: Average NR trace scaled (red) and superimposed on the average DR trace (black). Right panel displays a graph comparing mEPSC frequency between NR and DR in the visual cortex.
b. Cumulative probability of mEPSC amplitudes in somatosensory cortex pyramidal neurons from NR (red line) and 5 weeks DR (black line). Inset: Comparison of average mESPC amplitude from cells from NR (N) and 5 week DR (D). Middle panel shows average mEPSC traces (NR: red, DR: black). Scaled: Average DR trace was scaled (black) and superimposed on the average NR trace (red). Note no significant difference in mEPSC kinetics. Right panel: No significant change in mEPSC frequency with 5 weeks of DR in the somatosensory cortex
c. A comparison of GluR1 content in PSDs from 5 weeks DR (DR) rat visual cortex and from NR controls (NR). There was no change in GluR2 between NR and DR. There was a significant increase in GluR1/GluR2 (R1/R2) ratio in 5 weeks
d. A significant decrease in GluR1/GluR2 ratio in PSDs from somatosensory cortex of 5 week DR compared to NR controls. There was no statistically significant change in GluR1 or GluR2 content in the PSD .
e. Inward rectification of current through synaptic AMPA receptors was larger in visual cortical neurons in 5 weeks DR rats when compared to age-matched NR controls
f. In the somatosensory cortex, there was less inward rectification of AMPA receptor currents in neurons from 5 weeks DR rats compared to NR controls .

Subsection 3: Opposite changes in mEPSC amplitude with 1 week of dark rearing in layer 2/3 primary sensory cortical neurons.

Investigating cross modal effects of visual deprivation from birth has one important confounding factor and that is dark rearing right after the animal is born might be hindering the normal visual development of these rats. Hence it is possible that the effects of dark rearing that we see in the primary sensory cortices may be an artifact of this developmental hindrance. Hence to avoid this confounding factor we reared the rats in a normal 12 hour light and 12 hours dark cycle till 4 weeks of age. Then one group of rats was dark reared for a week. To study cross-modal changes in synaptic function by visual deprivation, we measured AMPA receptor (AMPAR)-mediated miniature excitatory postsynaptic currents (mEPSCs) in layer 2/3 pyramidal neurons in primary visual, somatosensory, and auditory cortex slices (see methods). In visual cortex, dark-rearing produced an increase in mEPSC amplitude that was reversed by re-exposing the animals to lighted conditions for 2 days (NR: 10.7 ± 0.6 pA, n = 8; DR: 12.4 ± 0.4 pA, n = 16; D+L: 10.7 ± 0.4 pA, n = 13; ANOVA: $F(2,34) = 5.968$, $p < 0.01$; Fig. 2.2a, left panel inset). This is evident in the cumulative probability comparison between NR, DR and D+L, wherein the mEPSC amplitude from DR group shift towards the right (larger amplitudes) (Fig 2.2a, left panel). DR was significantly different from NR and D+L (Kolmogorov-Smirnov test: $p < 0.001$). Interestingly, opposite changes were observed in somatosensory cortex, where one week of dark-rearing decreased the amplitude of mEPSCs, and 2 days of light exposure reversed this effect (NR: 13.8 ± 0.8 pA, n = 12; DR: 11.3 ± 0.7 pA, n = 16; D+L: 14.1 ± 0.9 pA, n = 16; ANOVA: $F(2,40) = 3.830$, $p < 0.04$; Fig. 2.2 b, left panel

inset). This is obvious in the cumulative probability comparison between NR, DR and D+L, wherein the mEPSC amplitude from DR group shift towards the left (smaller amplitudes) (Fig 2.2a, left panel). DR was significantly different from NR and D+L (Kolmogorov-Smirnov test: $p < 0.001$). The effects of dark rearing on synaptic transmission appear to be similar across the primary sensory cortices, since it also reduced mEPSC amplitudes in auditory cortex (NR: 13.0 ± 0.9 pA, n = 17; DR: 10.7 ± 0.5 pA, n = 18; t-test: $p < 0.04$; Fig. 2c, left panel inset), but not in frontal cortex (NR: 13.0 ± 1.2 pA, n = 11; DR: 11.7 ± 1.2 pA, n = 9; t-test: $p > 0.3$; Fig. 2.2d, left panel inset). Again the cumulative probability plots reflect the dark rearing induced decrease in mEPSC amplitude which occurs in the auditory cortex but not in the frontal cortex (Fig 2.2c,d, left panel)

There was no significant change in mEPSC frequency (Visual cortex: NR = 1.4 ± 0.2 Hz, DR = 1.5 ± 0.2 Hz, D+L = 2.0 ± 0.3 Hz, ANOVA: $F(2,34) = 1.222$, $p > 0.3$; Somatosensory cortex: NR = 2.9 ± 0.5 Hz, DR = 1.6 ± 0.1 Hz, D+L = 2.3 ± 0.6 Hz, ANOVA: $F(2,40) = 1.755$, $p > 0.1$; Auditory cortex: NR = 3.8 ± 0.5 Hz, DR = 2.8 ± 0.3 Hz, t-test: $p > 0.1$; Frontal cortex: NR = 3.1 ± 0.5 Hz, DR = 2.8 ± 0.6 Hz, t-test: $p > 0.6$; Fig. 2.2 a,b,c,d, right panel) across groups in all cortical areas.

There was no change in the mEPSC kinetics in visual and somatosensory cortex (Fig 2.2a,b, middle panel). In the auditory cortex along with changes in mEPSC amplitude, dark rearing caused a increase in mEPSC decay time constant (τ) (NR: 4.0 ± 0.25 msec, n = 17; DR: 4.9 ± 0.36 msec, n =18; t-test: $p < 0.04$, Fig 2.2c, middle panel).

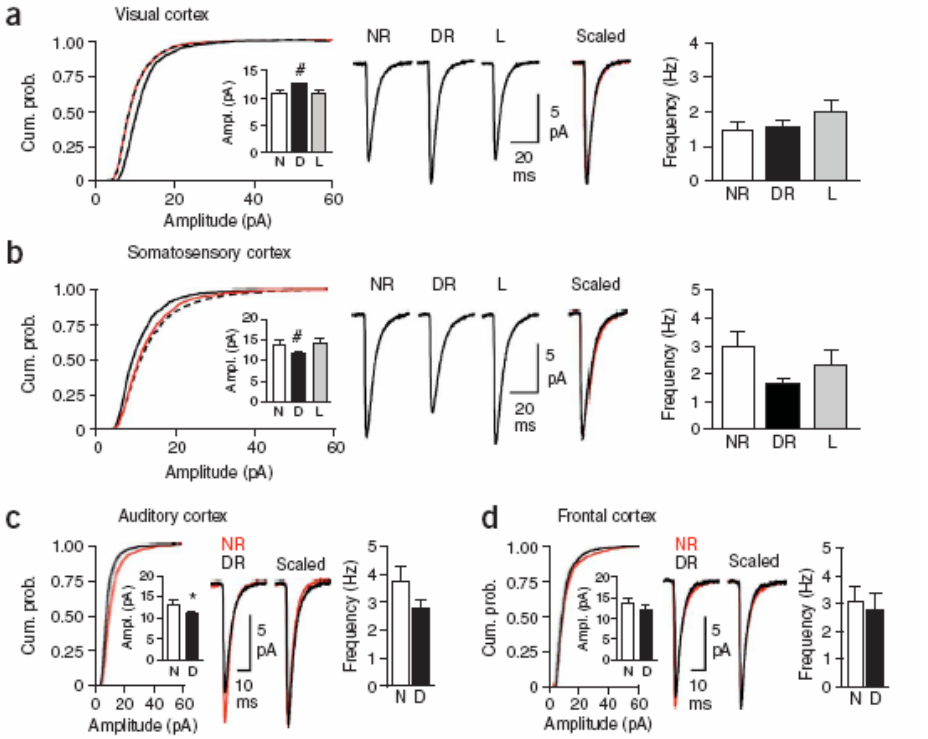

Figure 2.2: Visual experience leads to opposite changes in Visual cortex compared to other primary sensory cortices.

a. Left panel: Cumulative probability of mEPSC amplitudes in visual cortex neurons from normal-reared (NR: red solid line) shifts to the right with 1 week of dark-rearing (DR: black solid line), and reverses after 2 days of re-exposure to light (D+L: black dotted line). Inset: Average mESPC amplitude from NR (N), DR (D), and D+L (L).
Right panel: No change in mEPSC frequency with visual experience
b. Left panel: Cumulative probability of mEPSC amplitudes in somatosensory cortex neurons from normal-reared (NR: red solid line) shifts to the left with 1 week of dark-rearing (DR: black solid line), and reverses after 2 days of re-exposure to light (D+L: black dotted line). Inset: Average mESPC amplitude from NR (N), DR (D), and D+L (L).
Right panel: No change in mEPSC frequency with visual experience
c. Left panel: Cumulative probability of mEPSC amplitudes in auditory cortex neurons from normal-reared (NR: red solid line) shifts to the left with 1 week of dark-rearing (DR: black solid line) Inset: Average mESPC amplitude from NR (N) and DR (D.
Right panel: No change in mEPSC frequency with visual experience
d. Cumulative probability of mEPSC amplitudes in frontal cortex cells (NR: red solid line, 1 week DR: black solid line). Inset: Comparison of average mEPSC amplitudes. There was no change in mEPSC kinetics across groups. Average mEPSC traces from frontal cortex cells. Right: Comparison of mEPSC frequency of NR and DR frontal cortex neurons.

The observed increase in mEPSC amplitude in visual cortex of dark-reared animals was multiplicative which is consistent with homeostatic plasticity reported previously (Turrigiano et al., 1998; Desai et al., 2002). This is evident in the cumulative probability plots of mEPSC amplitudes in visual cortical neurons from normal-reared rats and rats dark reared for one week (Fig. 2.3a). Cumulative probability of mEPSC amplitudes in visual cortex neurons from 1 week dark reared rats shifted to the right towards larger amplitudes when compared with normal reared rats. Superimposed on the graph is a cumulative probability of mEPSC amplitudes from NR that are multiplied by a factor (1.2) to match the average mEPSC amplitude to that from DR (NR_{scaled}: red dotted line). There was no statistically significant difference between cumulative probability of DR and that of NR_{scaled} (Kolmogorov-Smirnov test: $p > 0.1$; Fig 2.3a).

Similarly, cumulative probability of mEPSC amplitudes in somatosensory cortex neurons from 1 week dark reared rats shifted to the left towards smaller amplitudes when compared with normal reared rats. Superimposed on the graph is a cumulative probability of mEPSC amplitudes from NR that are multiplied by a factor (0.8) to match the average mEPSC amplitude to that from DR (NR_{scaled}: red dotted line). There was no statistically significant difference between cumulative probability of DR and that of NR_{scaled} (Kolmogorov-Smirnov test: $p > 0.1$; Fig 2.3b).

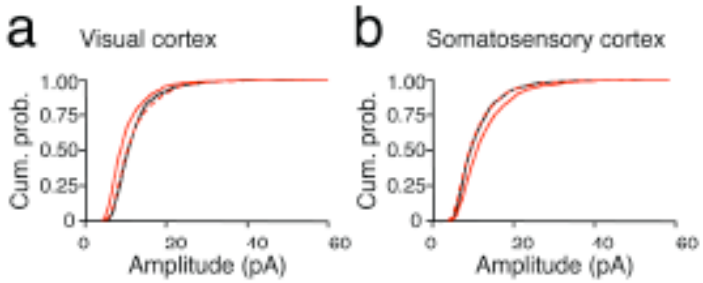

Figure 2.3. Changes in mEPSC amplitude by visual experience follow the rules of multiplicative changes in synaptic strength.

a. Normalized cumulative probability of mEPSC amplitudes in visual cortex neurons from normal-reared (NR: red solid line) and rats dark-reared for 1 week (DR: black solid line). Superimposed on the graph is a cumulative probability of mEPSC amplitudes from NR that are multiplied by a factor (1.2) to match the average mEPSC amplitude to that from DR (NR_{scaled}: red dotted line).
b. Normalized cumulative probability of mEPSC amplitudes in somatosensory cortex neurons from NR (red solid line) and 1 week DR (black solid line). Superimposed on the graph is a cumulative probability of mEPSC amplitudes from NR that are multiplied by a factor (0.8) to match the average mEPSC amplitude to that from DR (NR_{scaled}: red dotted line).

Our results demonstrate that visual deprivation decreased mEPSC amplitude in both primary somatosensory and auditory cortices while the synaptic transmission in the frontal cortex was unaltered suggesting that the effect of visual deprivation was restricted to the primary sensory cortices. In addition, our results suggest that visual experience can bidirectionally modify synapses in the visual cortex, and produce opposite changes in somatosensory cortex. Also, since dark rearing caused a change in mEPSC amplitude without any change in mEPSC frequency, it implies that the locus of change is postsynaptic.

Subsection 4: Effects of visual experience are accompanied by changes in AMPAR subunit composition

Our results implied that the expression locus of dark rearing was post synaptic and hence likely to be manifested by changes in postsynaptic AMPARs. Therefore, to examine whether the bidirectional changes in mEPSC amplitude by visual experience are due to regulating postsynaptic AMPARs, we biochemically isolated postsynaptic density (PSD) fractions from both visual and somatosensory cortices (see methods, Fig. 2.4).

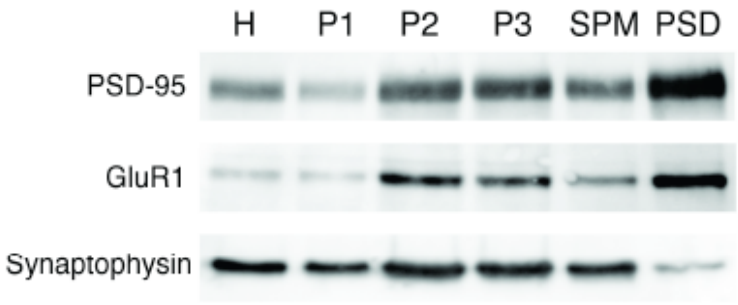

Figure 2.4 Biochemical isolation of postsynaptic density (PSD) fractions.

Equal amount of protein samples taken from each preparation step (H: homogenate, P1: pellet 1, P2: pellet 2, P3: pellet 3, SPM: synaptic plasma membrane, PSD: postsynaptic density: see Supplementary Methods for detail) were loaded on each lane and probed with PSD-95 antibody, GluR1-C terminal antibody, and synaptophysin antibody. Note an enrichment of postsynaptic proteins PSD-95 and GluR1 in the PSD fraction, while a loss of a presynaptic marker synaptophysin.

In visual cortex, one week of dark-rearing increased GluR1 (NR: 100 ± 12% of average NR, n = 9; DR: 190 ± 34% of NR, n = 9; t-test: $p < 0.04$), but not GluR2 (NR: 100 ± 21% of NR, n = 9; DR: 92 ± 11% of NR, n = 9; t-test: $p > 0.7$) (Fig. 2.5a), resulting in a significant increase in the ratio of GluR1 to GluR2 (GluR1/GluR2 ratio) (NR: 100 ± 10% of NR, n = 9; DR: 180 ± 29% of NR, n = 9; t-test: $p < 0.03$). Re-exposing dark-reared animals to light for 2 days reversed the increase in

GluR1/GluR2 ratio (DR: 100 ± 11% of average DR, n = 14; D+L: 69 ± 14% of DR, n = 14; t-test: $p < 0.05$; Fig. 2.5b). In contrast, in somatosensory cortex dark-rearing decreased GluR1 (NR: 100 ± 11% of NR, n = 12; DR: 51 ± 11% of NR, n = 12; t-test: $p < 0.005$) without changing GluR2 (NR: 100 ± 23% of NR, n = 12; DR: 101 ± 24% of NR, n = 12; t-test: $p > 0.9$), resulting in a significant decrease in the GluR1/GluR2 ratio (NR: 100 ± 22% of NR, n = 12; DR: 41 ± 10% of NR, n = 12; t-test: $p < 0.03$; Fig. 2.5c), which was reversed by 2 days of light (DR: 100 ± 13% of DR, n = 12; D+L: 224 ± 42% of DR, n = 12; t-test: $p < 0.02$; Fig. 2.5d).

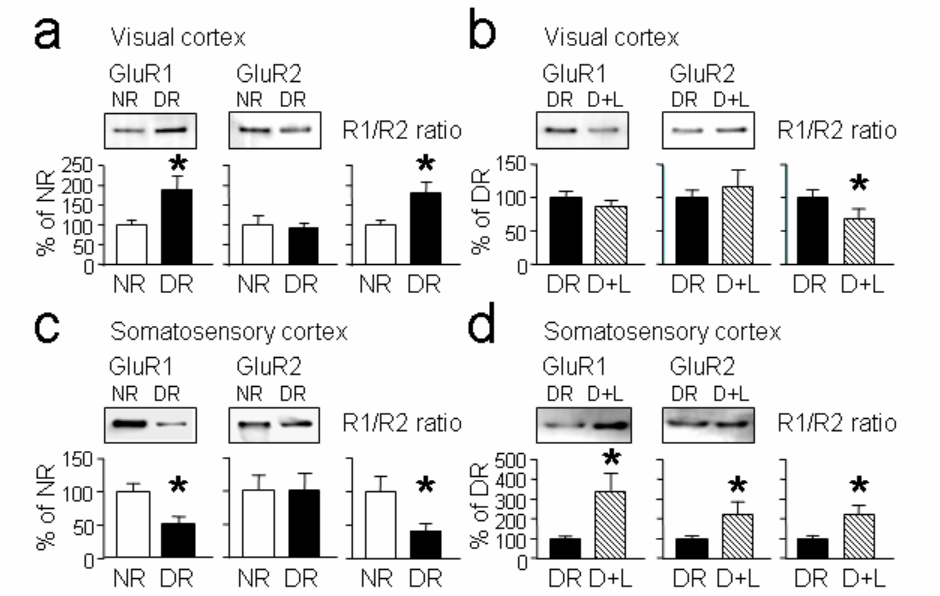

Figure 2.5. Cross-modal changes in synaptic AMPAR subunit composition by visual experience.

a. DR for 1 week increased GluR1/GluR2 (R1/R2) ratio in PSDs of visual cortex by increasing GluR1 when compared to NR.
b. Re-exposing DR rats to light for 2 days (D+L) decreased GluR1/GluR2 ratio at PSD of visual cortex.
c. DR decreased GluR1/GluR2 ratio in somatosensory cortical synapses by decreasing GluR1 content.
d. Re-exposure to light for 2 days (D+L) increased the GluR1/GluR2 ratio when compared to DR. Also there were significant increases in both GluR1 and GluR2 content

These changes at the PSD were not reflected in the total homogenate following 1 week of dark rearing (NR = 100 ± 9.3% of NR, n =8; DR = 105 ± 12.5% of NR, n = 9; t-test: $p > 0.7$), GluR2 (NR = 100 ± 10.5% of NR, n =8; DR = 84 ± 6.2% of NR, n = 9; t-test: $p > 0.2$), or GluR1/GluR2 ratio (NR = 100 ± 12.4% of NR, n = 8; DR = 132 ± 22.6% of NR, n = 9; t-test: $p > 0.2$) (Fig 2.6a). Re-exposing 1 week dark-reared (DR) animals to 2 days of light (D+L) produced no statistical changes in both GluR1 (DR = 100 ± 7.2% of DR, n = 15; D+L = 178 ± 42.4% of DR, n = 14; t-test: $p > 0.09$) and GluR2 (DR = 100 ± 14.2%, n = 15; D+L = 151 ± 41.2%, n = 14; t-test: $p > 0.2$) in visual cortex homogenate (Fig 2.6b). There was no significant change in R1/R2 ratio in the homogenate of visual cortex (DR = 100 ± 16.9%, n = 15; D+L = 125 ± 25.9%, n = 14; t-test: $p > 0.4$). Similarly in the somatosensory cortex dark-rearing for 1 week did not significantly alter GluR1 (NR: 100 ± 6.8%, n = 9; DR: 103 ± 7.4%, n = 8; t-test: $p >0.9$), GluR2 (NR: 100 ± 6.7%, n = 9; DR: 138 ± 14.2%, n = 8; t-test: $p > 0.2$), or R1/R2 ratio (NR: 100 ± 10.2%, n = 9; DR: 78 ± 10.6%, n = 8; t-test: $p > 0.4$) in the total homogenate (Fig 2.6c). Re-exposing dark-reared animals to 2 days of light did not produce statistically significant changes in GluR1 (DR: 100 ± 12.8%, n = 9; D+L: 88 ± 11.4%, n = 9; t-test: $p > 0.4$), GluR2 (DR: 100 ± 10.2%, n = 9; D+L: 143 ± 24.7%, n = 9; t-test: $p > 0.1$), or R1/R2 ratio (DR: 100 ± 14.8%, n = 9; D+L: 76 ± 15.9%, n = 9; t-test: $p > 0.2$) in the total homogenate of somatosensory cortex (Fig 2.6d). Therefore these results indicate that changes in GluR1/2 ratios occur despite lack of changes in total GluR1 or GluR2 indicating that there might be an increase in trafficking of AMPA receptors to the PSD.

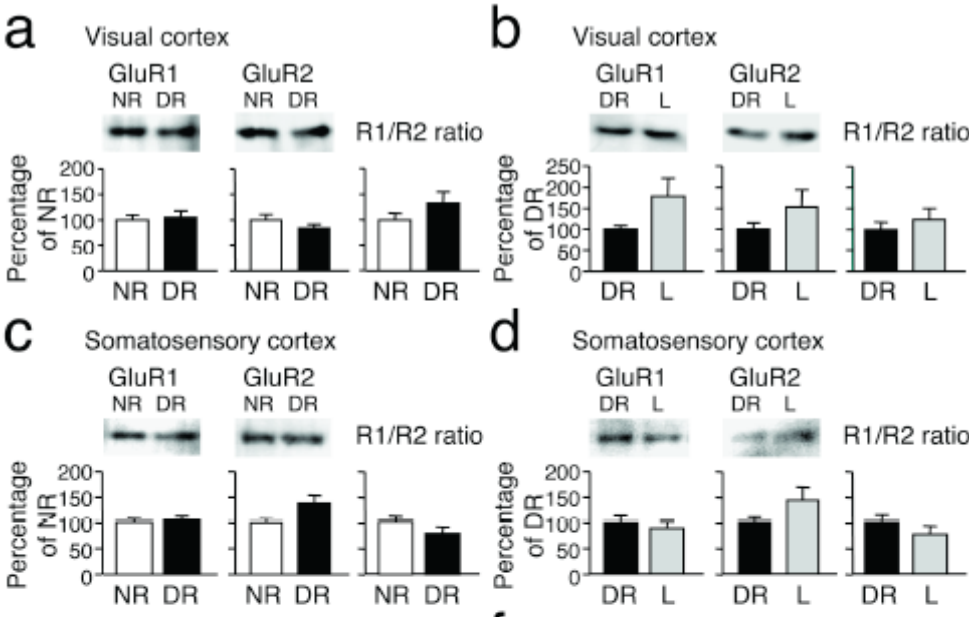

Figure 2.6. Comparison of GluR1/GluR2 ratio in total brain homogenate and alterations in GluR1 phosphorylation sites by visual experience.

a. No significant changes in GluR1, GluR2, or GluR1/GluR2 ratio in total homogenate of visual cortex following 1 week of dark-rearing.
b. Re-exposing 1 week dark-reared (DR) animals to 2 days of light (D+L) produced increases in both GluR1 and GluR2 in visual cortex homogenate, which did not reach statistical significance. There was no significant change in R1/R2 ratio in the homogenate of visual cortex.
c. Dark-rearing for 1 week did not significantly alter GluR1, GluR2, or R1/R2 ratio in total homogenate of somatosensory cortex.
d. Re-exposing dark-reared animals to 2 days of light did not produce statistically significant changes in GluR1, GluR2, or R1/R2 ratio in the total homogenate of somatosensory cortex.

Subsection 5: Visual deprivation is associated with changes in GluR1 phosphorylation.

While, there was no change in total amount of GluR1 or GluR2 indicating that visual deprivation did not affect the total protein turnover, dark rearing did affect GluR1 phosphorylation measured in the total brain homogenate.

Dark-rearing for 1 week decreased GluR1 phosphorylation on serine 831 (S831) in visual cortex (NR = 100 ± 3.9% of NR, n = 9; DR = 73 ± 9.3% of NR, n = 9; t-test: $p < 0.02$, Fig 2.7a, Left panel), which was not reversed by 2 days of re-exposure to light (DR = 100 ± 4.6% of DR, n = 9; D+L = 120 ± 10.3% of DR, n = 9; t-test: $p > 0.1$, Fig 2.7a, right panel). Dark-rearing for 1 week increased GluR1 phosphorylation on serine 845 (S845) in visual cortex (NR = 100 ± 9.1% of NR, n = 8; DR = 174 ± 30.5% of NR n = 9; t-test: $p < 0.05$, Fig 2.7b, left panel). Re-exposing DR animals to light for 2 days did not produce significant changes in GluR1 S845 phosphorylation (DR = 100 ± 8.1% of DR, n = 9; D+L = 112 ± 12.8% of DR, n = 9; t-test: $p > 0.6$, Fig 2.7b, right panel).

GluR1 S831 phosphorylation in somatosensory cortex did not change significantly following 1 week of dark-rearing (NR = 100 ± 9.0% of NR, n = 9; DR = 88 ± 23.0% of NR, n = 8; t-test: $p > 0.6$, Fig 2.7c, left panel) or re-exposing dark-rearing animals to 2 days of light (DR = 100 ± 21.5% of DR, n = 8; D+L = 67 ± 11.4% of DR, n = 9; t-test: $p > 0.1$, Fig 2.7c right panel:).

GluR1 S845 phosphorylation in somatosensory cortex did not change with 1 week of dark-rearing (NR = 100 ± 10.1%, n = 9; DR = 90 ± 36.9%, n = 6; t-test: $p > 0.8$, Fig 2.7d, left panel:), but significantly increased when DR animals were re-exposed to

light for 2 days (DR = 100 ± 24.8%, n = 6; D+L = 203 ± 36.5%, n = 9; t-test: $p < 0.04$, Fig 2.7d, right panel).

These results suggest that post-translational mechanisms may be involved in the increase in synaptic strength seen after visual deprivation. Interestingly, GluR1 serine 845 phosphorylation correlated with increase in mEPSC amplitude in both visual and somatosensory cortex (Fig 2.7 b, d).

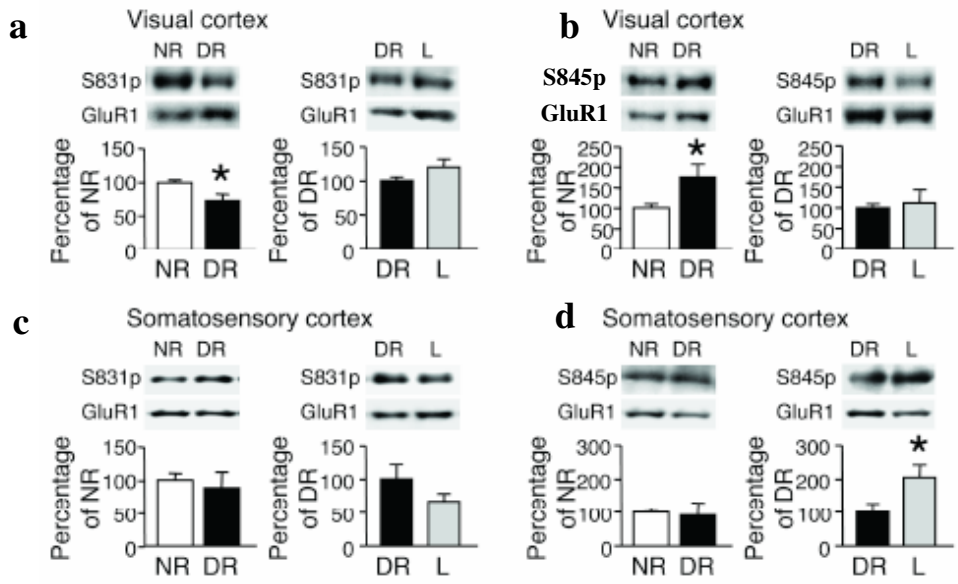

Figure 2.7. Visual deprivation is accompanied by changes in GluR1 phosphorylation.

a. Dark-rearing for 1 week decreased GluR1 phosphorylation on serine 831 (S831) in visual cortex (Left panel), which was not reversed by 2 days of re-exposure to light (Right panel)
b. Dark-rearing for 1 week increased GluR1 phosphorylation on serine 845 (S845) in visual cortex (Left panel). Re-exposing DR animals to light for 2 days did not produce significant changes in GluR1 S845 phosphorylation (Right panel)
c. GluR1 S831 phosphorylation in somatosensory cortex did not change significantly following 1 week of dark-rearing (Left panel) or re-exposing dark-rearing animals to 2 days of light (Right panel)
d. GluR1 S845 phosphorylation in somatosensory cortex did not change with 1 week of dark-rearing (Left panel), but significantly increased when DR animals were re-exposed to light for 2 days (Right panel).

Subsection 6: Bidirectional changes in AMPAR current property with visual experience.

AMPARs lacking or having reduced copies of GluR2 display inward rectification of current (Verdoorn et al., 1991; Washburn et al., 1997). Therefore, we assessed the GluR1/GluR2 ratio electrophysiologically by determining an inward rectification index (IR: I_{60mV}/I_{+40mV}) of AMPAR synaptic responses evoked by layer 4 stimulation. Consistent with our biochemical data, in visual cortex dark-rearing produced an increase in inward rectification that was reversed by re-exposure to light (NR = 1.88 ± 0.15, n = 10; DR = 3.42 ± 0.20, n = 22; D+L = 1.68 ± 0.14, n = 11; ANOVA: $F(2,40) = 25.929$, $p < 0.001$; Fig. 2.8a), whereas opposite changes were observed in somatosensory cortex (NR = 3.87 ± 0.46, n = 10; DR = 1.76 ± 0.07, n = 18; D+L = 3.07 ± 0.17, n = 9; ANOVA: $F(2,34) = 23.440$, $p < 0.001$; Fig. 2.8b). Inward rectification was specific to having intracellular spermine. When inward rectification measurements were done without spermine in the recording pipette the I/V plots were linear (Fig 2.9). Incidentally, we noticed that neurons in normal-reared somatosensory cortex show larger inward rectification and mEPSC amplitudes than visual cortical cells (Vctx: 9.5 ± 0.5 pA, n = 20; Sctx: 15.6 ± 1.1 pA, n = 27; t-test: $p < 0.0001$, Fig.2.8 and Fig 2.10). Also cells from somatosensory cortex have an elevated mEPSC frequency as well (Vctx: 1.5 ± 0.1 Hz, n = 20; Sctx: 2.6 ± 0.3 Hz, n = 27; t-test: $p < 0.001$).

The changes in mEPSC amplitude and inward rectification were consistent with basal differences in AMPAR subunit composition between these two cortical areas (Fig.2. 10). Somatosensory cortex has more GluR1 (Vctx: 100 ± 13% of average Vctx, n = 7;

Sctx: 145 ± 15% of average Vctx, n = 6; t-test: $p < 0.05$, Fig 2.10 a, left panel), while less GluR2 (Vctx: 100 ± 11% of average Vctx, n = 7; Sctx: 72 ± 7% of average Vctx, n = 6; t-test: $p < 0.05$, Fig 2.10b, middle panel) in the PSD when compared to visual cortex. This resulted in a larger GluR1/GluR2 ratio in synapses of somatosensory cortex (Vctx: 100 ± 11% of average Vctx, n = 7; Sctx: 210 ± 34% of average Vctx, n = 6; t-test: $p < 0.03$, Fig 2.10b, right panel).

Collectively, our biochemical and electrophysiological data suggest that cross-modal plasticity may be mediated by changes in subunit composition of synaptic AMPARs.

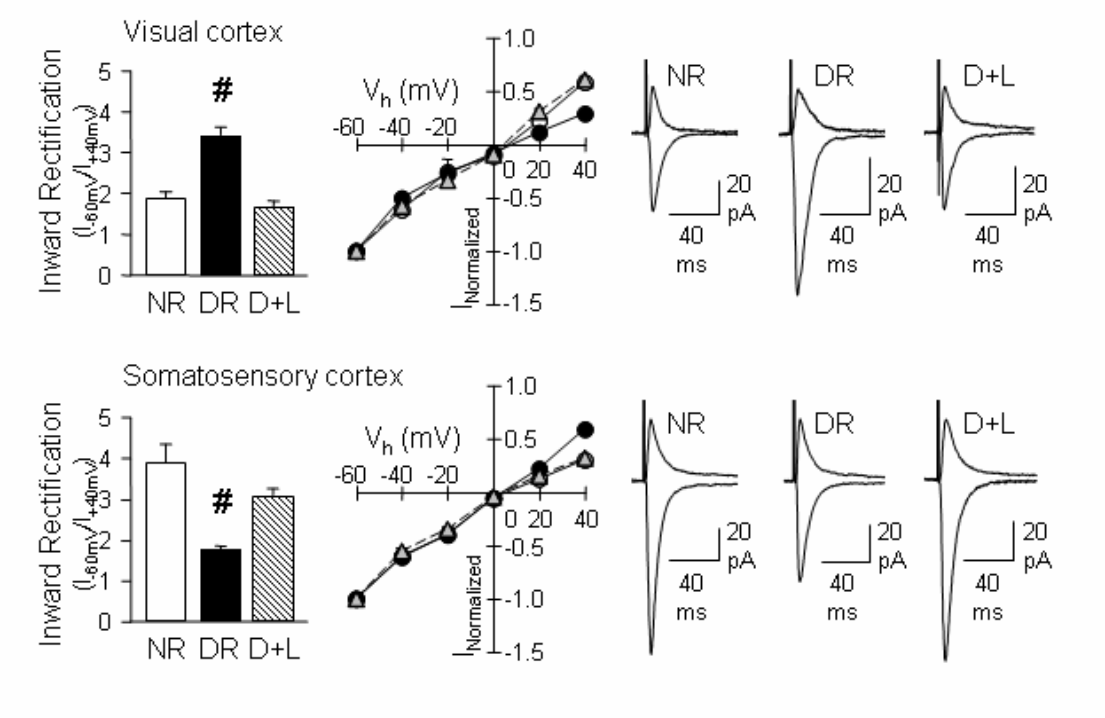

Figure 2.8. Bidirectional changes in inward rectification of AMPA current by visual deprivation

a. Larger inward rectification of current through synaptic AMPARs by 1 week of DR was reversed by 2 days of light exposure (D+L) in visual cortex. Middle panel: Comparison of I-V relationship between visual cortex neurons from NR (white circles), DR (black circles), and D+L (gray triangles). Right panel: Representative AMPAR-mediated current traces for NR, DR, and D+L in visual cortical neurons.

b. A more linear current through AMPARs in somatosensory cortex following DR was reversed by 2 days of light (D+L). Middle panel: Comparison of I-V relationship between somatosensory cortex cells from NR (white circles), DR (black circles), and D+L (gray triangles). Right panel: Representative current traces from somatosensory cortical neurons under each condition.

#: ANOVA, Fisher's PLSD post-hoc, $p < 0.01$.

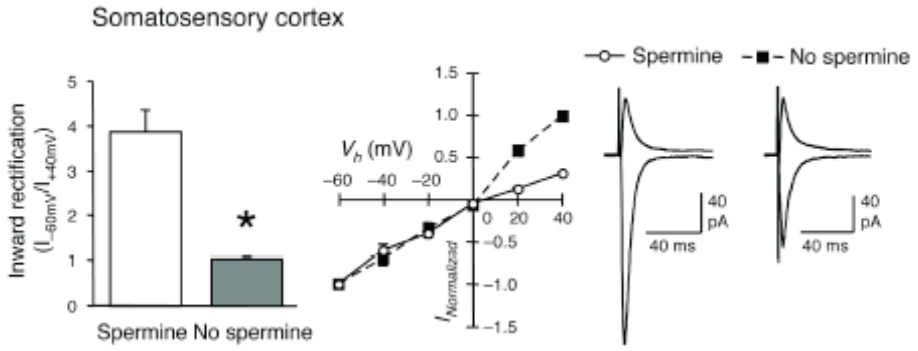

Figure 2.9. Inward rectification is dependent on intracellular spermine.

Left panel: Inward rectification (IR: I_{-60mV}/I_{+40mV}) of AMPA receptor currents observed in normal reared (NR) somatosensory cortical cells was abolished when using intracellular solution without spermine (Spermine: IR = 3.87 ± 0.46, n = 10 cells; No spermine: IR = 1.02 ± 0.04, n = 4 cells). Asterisk indicates statistically significant difference (Student's t-test: $p < 0.001$). Middle panel: Comparison of I-V relationship between NR somatosensory cortical cells recorded with (white circles) and without spermine (black squares). Right panel: Superimposed representative traces of evoked AMPA receptor-mediated currents measured at -60 mV and +40 mV from NR somatosensory cortical neurons recorded with or without spermine inside the recording pipette.

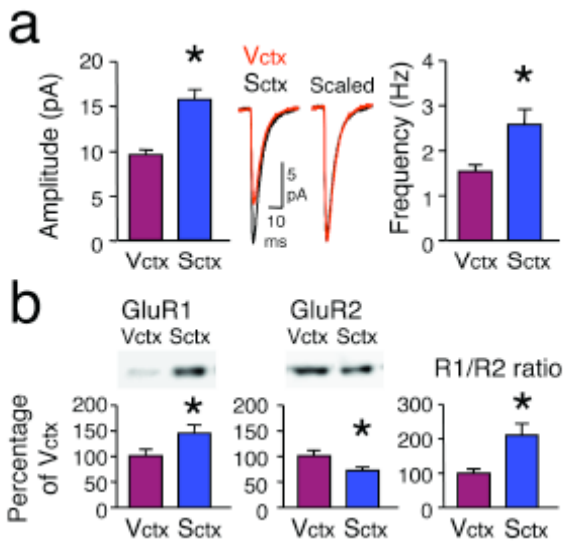

Figure 2.10. Differences in synaptic AMPA receptor function and subunit composition in visual and somatosensory cortices of normal-reared rats.

a. Left panel : In NR rats, average mEPSC amplitude in somatosensory cortex (Sctx) was greater than in visual cortex (Vctx). Middle panel shows average mEPSC traces (Vctx: red, Sctx: black). Scaled: Average mEPSC trace from visual cortex was scaled (red) and superimposed on average mEPSC trace from somatosensory cortex (black). Note no difference in mEPSC kinetics. Right panel : Comparison of mEPSC frequency of cells in visual and somatosensory cortices.
b. Somatosensory cortex has more GluR1 ,while less GluR2 in the PSD when compared to visual cortex. This resulted in a larger GluR1/GluR2 ratio in synapses of somatosensory cortex .

Section 4: Discussion

Our results demonstrate that manipulation of visual experience not only bidirectionally regulates synaptic AMPARs in visual cortex, but also produces complementary changes in the somatosensory and auditory cortex. These changes are rapid, since only one week of dark-rearing produced similar changes in AMPARs as dark-rearing from birth. It remains to be determined whether the cross-modal

plasticity induced in somatosensory cortex is due to altered cortical processing of tactile inputs (i.e. top-down) or due to differences in tactile experience (i.e. bottom-up). The former mechanism would engage intracortical inputs, while the latter involves thalamocortical inputs. In any case, similar changes in AMPA receptor function in auditory cortex suggest that these changes may occur globally across sensory cortices. Bidirectional synaptic changes we observed are consistent with a homeostatic plasticity mechanism, where chronic deprivation of inputs increases AMPAR function while a prolonged increase in activity decreases it (Turrigiano and Nelson, 2004). *In vitro* studies suggest that homeostatic synaptic plasticity is associated with changes in synaptic content(Lissin et al., 1998; O'Brien et al., 1998; Turrigiano et al., 1998) and subunit composition(Ju et al., 2004; Thiagarajan et al., 2005) of AMPARs. We not only provide evidence that these changes also occur *in vivo* by natural experience, but suggest that these mechanisms can be recruited cross-modally. Taken together with a recent study demonstrating synapse-specific regulation of AMPA receptors by sensory experience (Clem and Barth, 2006), our results suggest that AMPA receptor regulation may be a common downstream mechanism for both synapse-specific and global homeostatic plasticity *in vivo*.

Chapter 3: Persistence of experience- induced homeostatic synaptic plasticity through adulthood in superficial layers of mouse visual cortex.

Published in Journal of Neuroscience.
Goel A, Lee. HK. Journal of Neuroscience: 2007 June 20; 27(25): 6692-6700

My contribution: All the experiments.

Section 1: Introduction

Many functions of the brain depend on changes in synaptic connectivity. Research on synaptic plasticity has focused on activity-dependent changes that are rapid and occur locally at specific synapses, such as long-term potentiation (LTP) and long-term depression (LTD) (Bliss and Collingridge, 1993; Malenka and Bear, 2004). However, it was recognized early on that such synapse-specific plasticity has to be counter-balanced by a more global homeostatic mechanism to maintain stability in neural networks (Bienenstock et al., 1982; Bear et al., 1987; Abbott and Nelson, 2000; Turrigiano and Nelson, 2004). One of the homeostatic mechanisms that has been proposed is synaptic scaling (Turrigiano and Nelson, 2004), where a prolonged increase in neural activity globally scales down excitatory synaptic responses, while a chronic decrease in activity scales up the responses. Homeostatic synaptic scaling was initially demonstrated *in vitro* where excitatory synaptic strengths in cultured neurons adapt to prolonged changes in neural activity by pharmacological manipulations (Lissin et al., 1998; O'Brien et al., 1998; Turrigiano et al., 1998; Thiagarajan et al., 2002; Ju et al., 2004). These observations have been extended *in vivo* where several days of visual deprivation increases excitatory synaptic transmission in visual cortical

neurons in juvenile rats (Desai et al., 2002; Goel et al., 2006), which rapidly reverse with a few days of visual experience (Goel et al., 2006).

The majority of studies on homeostatic synaptic plasticity have been conducted in young animals within the "critical period". Therefore, it is not known whether it persists through adulthood. From the pioneering work of Wiesel and Hubel (1963), the concept of the "critical period" was proposed, which is defined as a distinct window during development when synaptic connections can be sculpted by experience. While earlier studies emphasized the enhanced plasticity during the critical period (Wiesel and Hubel, 1963; LeVay et al., 1980; Hubel, 1982; Gordon and Stryker, 1996), recent evidence showed that the critical period closure is not absolute, and may even be reversed. For example, a brief MD paradigm in rodents only produces OD plasticity within a critical period (Gordon and Stryker, 1996), but a slightly longer duration of MD (5 days) causes a robust OD shift in adults (P90) (Sawtell et al., 2003). Moreover, preceding a brief MD with a prolonged binocular deprivation in adult rats induces a "juvenile-like" OD plasticity (He et al., 2006). While these findings demonstrate that adult cortex retains the ability to undergo experience-dependent plasticity, there seem to be differences across layers, where layer 2/3 retains the ability to undergo plasticity longer than layer 4 (LeVay et al., 1980; Daw et al., 1992; Guire et al., 1999; Pham et al., 2004). Laminar differences are also reported for homeostatic synaptic scaling induced by visual deprivation in rats, where layer 4 scaling occurs only before P21, while layer 2/3 scaling is observed only after this age (Desai et al., 2002). The major focus of this study was to determine whether experience-induced homeostatic synaptic plasticity persists through

adulthood in the superficial layers of visual cortex. Here we report that experience-dependent homeostatic synaptic plasticity persists through adulthood in the superficial layers of mouse visual cortex. We found that 2 days of visual deprivation in the form of dark-rearing is necessary and sufficient to cause an increase in alpha-amino-3-hydroxy-5-methyl-4-isoxazolepropionic acid (AMPA) receptor-mediated miniature excitatory postsynaptic current (mEPSC) amplitude in layer 2/3 neurons. This increase was rapidly reversed by 1 day of light exposure. This reversible change in synaptic strength persisted in adult mice past the critical period for ocular dominance (OD) plasticity, which is reported to end around 1 month of age in rodents (Gordon and Stryker, 1996). Interestingly, the mechanism of homeostatic synaptic modifications in 3-month-old mice differed from that in young mice (3-week-old), in that the multiplicative nature of synaptic scaling is lost. Our results demonstrate that the superficial layers of adult mouse visual cortex retain the ability to undergo reversible experience-dependent homeostatic synaptic plasticity.

Section 2: Materials and methods

Subsection 1: Dark rearing animals

C57BL/6J mice (Jackson Laboratories) were raised under normal lighted environment (12 hr light/12 hr dark cycle). Dark rearing (DR) was initiated at postnatal ages 21 days (P21), 36 days (P36), or 95 days (P95) for a duration of 2 days. Control (normal-reared, NR) animals were continuously raised in the normal lighted condition for the same duration. The animals in the dark were cared for using infrared vision goggles

under dim infrared light. A group of dark-reared mice were taken out to the lighted environment for 1 day to study the effect of re-exposure to light (D+L).

Subsection 2: Whole cell recording of AMPA receptor mediated mEPSCs

The cortical slices were moved to a submersion recording chamber mounted on a stage of an upright microscope (E600 FN, Nikon) equipped with infrared differential interference contrast (IR-DIC). Layer 2/3 pyramidal cells were visually identified and patched using a whole-cell patch pipette (tip resistance: 3-5 MΩ) filled with intracellular solution (130 mM Cs-gluconate, 8 mM KCl, 1 mM EGTA, 10 mM HEPES, 4 mM ATP and 5 mM QX-314; pH 7.4; 285-295 mOsm).

To isolate AMPA receptor-mediated mEPSCs, 1 μM TTX, 20 μM bicuculline, and 100 μM D,L-APV were added to the ACSF (2 ml/min, 30 ± 1˚C), which was continually bubbled with 95% O_2/5% CO_2. mEPSCs were recorded at a holding potential (Vh) of –80 mV using Axopatch-clamp amplifier (Axon Instruments), digitized at 2 kHz by a data acquisition board (National Instruments), and acquired using the Igor Pro^{TM} software (Wave Metrics). Acquired mEPSCs were analyzed using the Mini Analysis Program (Synaptosoft). The threshold for detecting mEPSCs was set at 3 times the Root Mean Square (RMS) noise. There was no significant difference in RMS noise between the experimental groups. There was no significant difference in RMS noise between the experimental groups (P13 NR = 1.8 ± 0.09, n = 10; P13 DR = 2.0 ± 0.07, n = 10; t-test, $p > 0.1$: P22 NR = 1.8 ± 0.1, n = 9; P22 DR = 1.7 ± 0.07, n = 10; t-test, $p > 0.8$: P23 NR = 1.9 ± 0.05, n = 12; P23 DR = 1.9 ± 0.06, n = 19; P24 D+L = 1.8 ± 0.1, n = 10, ANOVA, $F(2,38) = 1.119$, $p > 0.3$: P25 NR = 1.7 ± 0.07, n = 10; P25 DR = 1.8 ± 0.05, n = 15; t-test, $p > 0.15$: P38 NR = 1.7 ± 0.1,

n = 10; P38 DR = 1.6 ± 0.1, n = 10; P39 D+L = 1.8 ± 0.1, n = 10, ANOVA, $F(2,27) = 0.684$, $p > 0.5$: P40 NR = 1.9 ± 0.1, n = 11; P40 DR = 1.8 ± 0.7, n = 10; t-test, $p > 0.5$: P97 NR = 1.9 ± 0.04, n = 11; P97 DR = 1.9 ± 0.05, n = 11; P98 D+L = 1.9± 0.06, n = 11; ANOVA, $F(2,30) = 0.546$, $p > 0.6$). A possibility of dendritic filtering was assessed by plotting mEPSC amplitude against mEPSC rise time. Cells showing a negative correlation between mEPSC amplitude and rise time (i.e. dendritic filtering present) were excluded from analysis, as well as mEPSCs with greater than 3 msec rise time (measured between 10-90% of amplitude). Average mEPSC amplitude and frequency were calculated and compared across different experimental groups using one-factor ANOVA or unpaired Student's t-test. Only the cells and recording conditions that meet the following criteria were studied: Vm ≤ –65 mV, input R ≥ 200 MΩ, series R ≤ 25 MΩ. For older mice (P 97), we only included cells that had a series R ≤ 20 MΩ. Cells were discarded if input R or series R changed more than 15%. Junction potentials were typically less than 5 mV, and were left uncompensated.

Only the cells and recording conditions that meet the following criteria were studied: Vm ≤ –65 mV, input R ≥ 200 MΩ, series R ≤ 25 MΩ. Cells were discarded if input R or series R changed more than 15%. Junction potentials were typically less than 5 mV, and were left uncompensated.

Section 3: Results

Subsection 1: Dark- rearing for 2 days is necessary and sufficient to increase AMPA receptor mediated mEPSC amplitude in layer 2/3 neurons.

To compare homeostatic plasticity across ages, we first determined the minimal duration of visual deprivation that would lead to maximal changes in AMPA receptor-mediated miniature excitatory postsynaptic currents (mEPSCs) in layer 2/3 pyramidal cells of mouse visual cortex. Studies in juvenile rats have shown that visual deprivation for 2 days by injecting TTX into one eye causes an increase in mEPSC amplitude of layer 2/3 visual cortical neurons in the contralateral monocular zone (Desai et al., 2002). Nevertheless, the question of whether 2 days of visual deprivation is necessary remained unresolved. To determine this, mice of postnatal age 21 days old (P21) were binocularly deprived of visual input by dark-rearing (DR) for 1, 2, and 4 days, and mEPSCs recorded at P22 for 1 day DR (P21- P22), P23 for 2 days DR (P21-P23), and P25 for 4 days DR (P21-P25) were compared to age matched normal-reared (NR) control mice.

We found that 1 day of dark-rearing failed to change mEPSC amplitude (P22: NR: 11.5 ± 0.9 pA, n = 9; DR: 11.7 ± 0.7 pA, n = 10; t-test: $p > 0.8$; Fig. 3.1a) or frequency (NR: 2.7 ± 0.4 Hz, n = 9; DR: 2.5 ± 0.2 Hz, n = 10; t-test: $p > 0.7$; Fig. 3.1a upper right panel) in layer 2/3 visual cortical neurons. Consistent with previous results (Desai et al., 2002), 2 days of dark rearing significantly increased the mEPSC amplitude (P23: NR: 11.02 ± 0.5 pA, n = 12; DR: 13.4 ± 0.5 pA, n = 19; t-test $p <$

0.004; Fig 3.1b), without affecting mEPSC frequency (NR: 2.3 ± 0.2 Hz, n = 12; DR: 2.5 ± 0.3 Hz, n = 19; t-test $p > 0.6$; Fig. 3.1b upper right panel) or kinetics (Table 3.1). These results suggest that dark rearing for at least 2 days is required to increase mEPSC amplitude. In addition, the increase in mEPSC amplitude without a change in frequency suggests that the locus of expression for homeostatic scaling is likely postsynaptic.

Next we examined whether 2 days of visual deprivation is sufficient to produce a maximal change in mEPSC amplitude. To do this, we increased the duration of dark rearing to 4 days (DR from P21 to P25). As expected, this also significantly increased the mEPSC amplitude (NR: 9.8 ± 0.5 pA, n = 10; DR: 14.1 ± 0.9 pA, n = 15; t-test: $p < 0.0003$; Fig. 3.1c) without changing mEPSC frequency (NR: 3.2 ± 0.6 Hz, n = 10; DR: 2.7 ± 0.4 Hz, n = 15; t-test: $p > 0.5$; Fig. 3.1c upper right panel). However, when we compared the average mEPSC amplitude following 2 and 4 days of dark rearing, there was no significant difference (t-test: $p > 0.5$). This implies that 2 days of dark rearing is sufficient to scale up neuronal responses maximally, and further deprivation of visual input does not lead to additional increases in synaptic strengths.

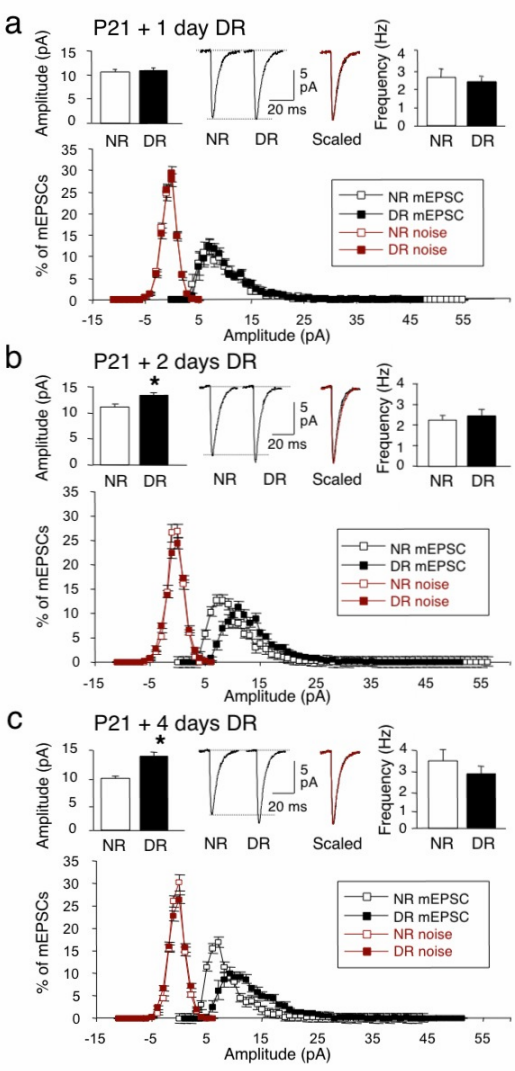

Figure 3.1. Minimum duration of dark-rearing necessary and sufficient to maximally increase AMPA receptor-mediated mEPSCs in layer

a. Top left panel: Comparison of average mEPSC amplitude of cells from P22 normal-reared (NR) and 1 day dark-reared (DR from P21 to P22) mice. Top middle panel: Average mEPSC traces from NR (left trace) and 1 day DR (right trace) mice. "Scaled" indicates the NR mEPSC average trace scaled (red trace) to match in amplitude to that of 1 day DR and superimposed on the 1 day DR average trace (black trace). Top right panel: Comparison of average mEPSC frequency from cells from NR and 1 day DR mice. Bottom panel: Distribution histogram of mEPSC amplitudes recorded from NR (open black symbols) and 1 day DR mice (closed black symbols). There was no change in the distribution of mEPSC amplitudes recorded from 1 day DR and NR mice. There is no difference in noise levels between the two groups (NR noise: open red symbols, DR noise: closed red symbols).

b. Top left panel: Comparison of average mEPSC amplitude of cells from P23 NR mice was significantly different from mice dark-reared for 2 days from P21 to P23. Top middle panel: Average mEPSC traces from NR (left trace) and 2 days DR mice (right trace). "Scaled" indicates the NR mEPSC average trace scaled (red trace) and superimposed on the DR average trace (black trace). Top right panel: Comparison of average mEPSC frequency from cells from NR and 1 day DR mice. Bottom panel: Distribution histogram of mEPSCs recorded from 2 days DR mice (closed black symbols) showed a higher percentage of mEPSCs with larger amplitudes (i.e. shift in distribution towards larger amplitudes) compared to NR (open black symbols). There was no difference between distribution of NR noise (open red symbols) and DR noise (closed red symbols).

c. Top left panel: Comparison of average mEPSC amplitude of cells from P25 NR mice to that from mice dark-reared for 4 days from P21 to P25 (DR). Top middle panel: Average mEPSC traces from NR (left trace) and 4 days DR (right trace) mice. "Scaled" indicates the NR mEPSC average trace scaled (red trace) and superimposed on the 4 days DR average trace (black trace). Top right panel: No change in average mEPSC frequency from cells from NR and 4 days DR mice. Bottom panel: Distribution histogram of mEPSC amplitudes recorded from 4 days DR mice (closed black symbols) shows a higher percentage of mEPSCs with larger amplitudes compared to NR animals (open black symbols). There was no difference between distribution of NR noise (open red symbols) and DR noise (closed red symbols).

Asterisk: $P < 0.04$ with t-test.

Subsection 2: Increase in AMPA receptor mediated mEPSC amplitude by dark-rearing is readily reversed by re-exposing the animals to light.

We have shown previously in juvenile rats that 2 days of re-exposure to light can reverse the increase in mEPSC amplitude caused by 1 week of dark rearing (Goel et al., 2006). Hence, we wanted to investigate whether reversible homeostatic synaptic changes can also be elicited in mice. To do this, mice were dark reared from P21-P23 and then exposed to light for a day. Whole cell recordings were then made from pyramidal cells in layer 2/3 of visual cortex at P24. As shown in Fig 3.2, 1 day of re-exposure to light was able to reverse the increase in mEPSC amplitude by 2 days of dark-rearing (P23: NR: 11.02 ± 0.5 pA, n = 12; DR: 13.4 ± 0.5 pA, n = 19 ; D+L: 9.2 ± 0.5 pA, n = 10; ANOVA: $F(2,38) = 15.757$, $p < 0.0001$; Fig 3.2a) without alterations in mEPSC frequency (NR: 2.3 ± 0.2 Hz, n = 12; DR: 2.5 ± 0.3 Hz, n = 19; D+L: 2.4 ± 0.3 Hz, n = 10; ANOVA: $F(2,38) = 0.134$, $p > 0.6$; Fig 3.2b) or kinetics (Table 3.1). Collectively, our results show that manipulation of visual experience can reversibly affect homeostatic synaptic plasticity in juveniles.

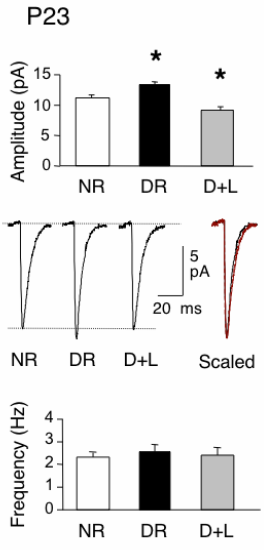

Figure 3.2. Reversible modification of AMPA receptor-mediated mEPSC amplitude in juvenile mice.

Increase in mEPSC amplitude by 2 days of DR was reversed by re-exposing the DR mice to light for 1 day (D+L). Top panel: Comparison of average mEPSC amplitudes from NR, 2 days DR, and 2 days DR followed by 1 day re-exposure to light (D+L) Middle panel: Average mEPSC traces from NR (left trace), DR (right trace) and D+L (right trace) mice. "Scaled" indicates the average mEPSC traces of NR (red solid line trace) and D+L (red dotted line trace) scaled and superimposed on the DR average trace (black trace). Note no difference in mEPSC kinetics across the three groups. Bottom panel: No change in average mEPSC frequency across NR, DR, and D+L groups.
Asterisk: $P < 0.0001$ with Fisher's PLSD post-hoc test following one-way ANOVA.

Subsection 3: Reversible homeostatic synaptic plasticity induced by visual experience persists in adults.

Experience-dependent plasticity in the sensory cortex has been shown to operate within a distinct time window during development, known as the "critical period". Though, recently, the tenet of "critical period plasticity" is rapidly being modified by the idea that synaptic reorganization does occur to some extent in the adult brain (Guire et al., 1999; Sawtell et al., 2003; Pham et al., 2004; He et al., 2006). A previous study on homeostatic synaptic scaling reported that visual deprivation induced increase in mEPSC amplitude only occurred prior to P21 in layer 4 of visual cortex, while layer 2/3 mEPSCs only scale up when visual deprivation started at P21 (Desai et al., 2002). This suggests that homeostatic synaptic scaling has distinct critical periods in different layers of the cortex. However, whether homeostatic synaptic plasticity in layer 2/3 ends at a later developmental time point or persists throughout adulthood was not determined.

We first tested whether layer 2/3 homeostatic synaptic plasticity has a defined critical period by studying the effects of dark rearing in P36 mice, which is just after the end of the critical period as defined by initial studies of ocular dominance plasticity (around P32) (Gordon and Stryker, 1996). P36 mice were dark reared for a period of 2 days and then re-exposed to light for a day. Depriving vision for 2 days in P36 mice caused a significant increase in mEPSC amplitude, which rapidly reversed by 1 day of re-exposure to light (P38: NR: 9.6 ± 0.6 pA, n = 10; DR: 14.5 ± 1.1 pA, n = 10; D+L: 9.3 ± 0.5 pA, n = 10; ANOVA: $F(2,27) = 8.472$, $p < 0.001$; Fig 3.3a) .

There was no significant change in mEPSC frequency (P38: NR: 3.1 ± 0.6 pA, n = 10; DR: 3.6 ± 0.6 pA, n = 10; D+L: 2.8 ± 0.6 pA, n = 10; ANOVA: $F(2,27) = 0.501$, $p > 0.6$; Fig 3.3b) or mEPSC rise time (Table 3.1), but was accompanied by a significant change in the decay kinetics (Table 3.1).

While an initial study of OD plasticity by brief MD reported that critical period ends at around P32 in mice (Gordon and Stryker, 1996), assessment of the effect of MD in rats using visually evoked potentials showed that OD plasticity extends to about P50 (Guire et al., 1999). Moreover, recent reports showed that a slightly longer period of MD can produce significant OD shift in rats as old as P90 (Sawtell et al., 2003; Pham et al., 2004). Therefore, we decided to investigate homeostatic synaptic plasticity at a later age (P95). Similar to what we found in younger animals, dark rearing P95 mice for 2 days also caused a significant increase in mEPSC amplitude, which was reversed by re-exposure to light for 1 day (P97: NR: 10.7 ± 0.5 pA, n = 11; DR: 13.1 ± 0.8 pA, n = 11; D+L: 9.7 ± 0.5 pA, n = 11; ANOVA: $F(2,30) = 7.871$, $p < 0.002$; Fig 3.3c). This occurred without changes in mEPSC frequency (P97: NR: 2.5 ± 0.4 pA, n = 11; DR: 2.2 ± 0.4 pA, n = 11; D+L: 2.1 ± 0.3 pA, n = 11; ANOVA: $F(2,30) = 0.36$, $p > 0.7$; Fig 3.3d) or rise time (Table 3.1), but there was a significant change in the decay kinetics (Table 3.1). These results demonstrate that layer 2/3 retains the ability to undergo reversible homeostatic plasticity through adulthood.

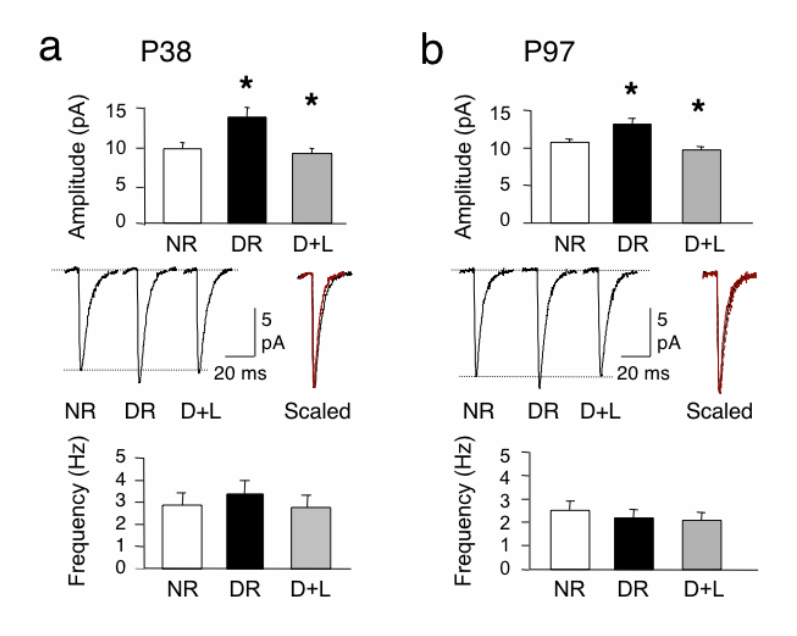

Figure 3.3. Reversible homeostatic synaptic modification in adult mice.

a. Dark-rearing P36 mice for 2 days until P38 (DR) significantly increased mEPSC amplitude compared to NR, while 1 day of re-exposure to light (D+L) reversed this increase. Top panel: Comparison of average mEPSC amplitude in NR, 2 days DR, and 2 days DR followed by 1 day re-exposure to (D+L) in P38 mice. Middle panel: Average mEPSC trace from NR (left trace), DR (middle trace) and D+L (right trace) groups. "Scaled" indicates that average mEPSC traces of NR (red solid trace) and D+L (red dotted trace) were scaled and superimposed on the average trace of DR (black trace). Bottom panel: No change in average mEPSC frequency across NR, DR, and D+L groups at P38.

b. DR for 2 days from P95 to P97 significantly increased mEPSC amplitude compared to NR, and this was reversed by 1 day of re-exposure to light (D+L). Top panel: Comparison of average mEPSC amplitude between NR, 2 days DR, and 2 days DR followed by 1 day of re-exposure to light (D+L). Middle panel: Average mEPSC trace from NR (black trace), DR (black middle trace), and D+L (black right trace) mice. "Scaled" indicates the NR mEPSC average trace (red solid trace) and D+L mEPSC average trace (red dotted trace) scaled and superimposed on the DR average trace (black trace). Bottom panel: No change in average mEPSC frequency across NR, DR, and D+L groups.

Asterisk: $P < 0.003$ with Fisher's PLSD post-hoc test following one-way ANOVA.

Subsection 4: Loss of "multiplicative synaptic scaling" in adult mice.

Initial characterization of homeostatic synaptic scaling demonstrated that prolonged changes in neural activity result in a "multiplicative scaling" of synaptic weights (Turrigiano et al., 1998). We have previously reported that visual experience driven homeostatic plasticity in juvenile rats also follows the rule of "multiplicative scaling" (Goel et al., 2006). However, there are also studies suggesting that homeostatic plasticity does not operate in a global multiplicative fashion (Thiagarajan et al., 2005). Therefore, we wanted to examine whether the homeostatic synaptic plasticity we observe in mice occurs in a multiplicative manner across ages. To determine whether scaling up of synapses by visual deprivation occurs multiplicatively, we multiplied mEPSC amplitudes recorded from normal-reared group to match the average mEPSC amplitude of DR (NR_{scaled}), and compared to mEPSC amplitudes measured from DR animals. Conversely, to test whether the decrease in synaptic weight by visual experience causes multiplicative scaling, we multiplied mEPSC amplitudes from dark-reared group to match the average mEPSC amplitude of D+L (DR_{scaled}), and compared to the mEPSC amplitudes from D+L group.

We found that reversible changes in synaptic strength by visual experience in juvenile mice followed the rules of "multiplicative scaling", but the changes in mEPSC amplitude in adults (especially in P97) did not occur in a global multiplicative manner. Comparison of the cumulative probability plots across different ages emphasizes the difference (Fig. 3.4). In P23 mice, the curve significantly shifts to the right with dark rearing (comparison of mEPSC amplitude

between NR and DR: $p < 0.0001$, Kolmogorov-Smirnov test; Fig 3.4a), and this shift is reversed with light exposure (comparison of mEPSC amplitude between DR and D+L: $p < 0.0001$, Kolmogorov-Smirnov test; Fig 3.4b). Superimposed on the graphs is a cumulative probability of mEPSC amplitudes from NR that are multiplied by a factor (1.2) to match the average mEPSC amplitude to that from DR (NR_{scaled}: red dotted line; Fig. 3.4a). There was no statistically significant difference between cumulative probability of DR and that of NR_{scaled} (Kolmogorov-Smirnov test: $p > 0.5$; Fig. 3.4a) or between D+L and DR_{scaled} (Kolmogorov-Smirnov test: $p > 0.1$; Fig.3.4b). This is consistent with a "multiplicative scaling" of synaptic strength as proposed by Turrigiano et al. (1998).

This multiplicative nature of synaptic strength modification is maintained in P38 mice for scaling up of synaptic strengths (Fig. 3.4c), but comparison of mEPSC amplitudes of DR_{scaled} and D+L group was significantly different (Kolmogorov-Smirnov test: $p < 0.01$; Fig. 3.4d) implying that scaling down at this age does not occur in a global multiplicative manner. In P97 mice, both scaling up and scaling down of mEPSC amplitude did not follow a global multiplicative mechanism as exemplified by significant differences in mEPSC amplitude cumulative probability of DR and NR_{scaled} (Kolmogorov-Smirnov Test: $p < 0.0001$; Fig 3.4e) and between NR and $D+L_{scaled}$ (Kolmogorov-Smirnov Test: $p < 0.0001$; Fig 3.4f). Our results suggest that while visual experience in juvenile mice globally changes synaptic weights in a multiplicative manner, not all synapses in adults are being modified this way.

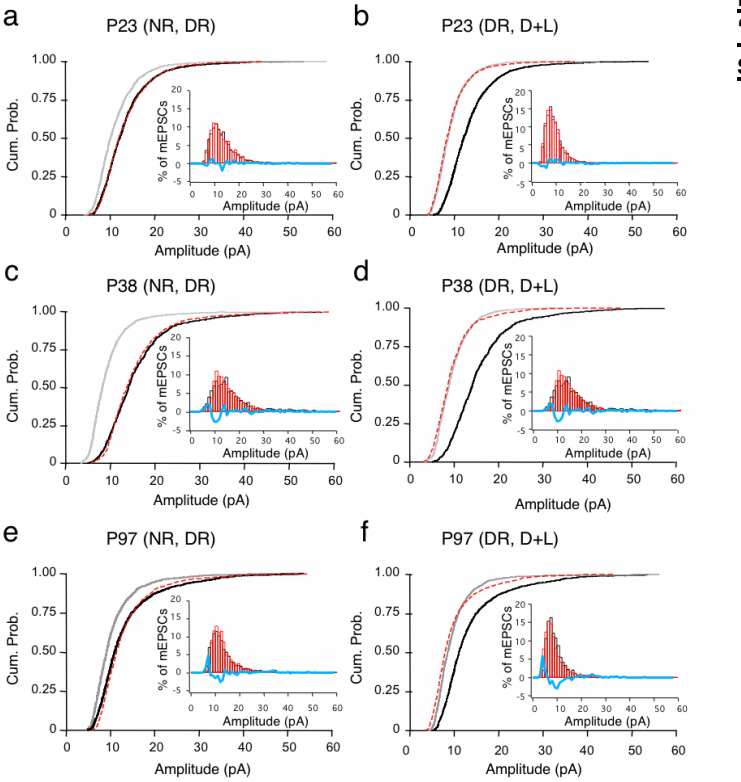

Figure 3.4. Loss of "multiplicative synaptic scaling" in adult mice

a. Cumulative probability of mEPSC amplitudes in visual cortex neurons from P23 NR (gray solid line) and 2 days DR (black solid line). Superimposed on the graph is a cumulative probability of mEPSC amplitudes from NR that are multiplied by a factor (1.2) to match the average mEPSC amplitude of that from DR (NR_{scaled}: red dotted line). Inset: Distribution histogram plotting % of mEPSCs against mEPSC amplitude of NR_{scaled} (red bars) and DR (black bars). Superimposed on the graph is a subtraction of the two distributions (blue solid line).

b. Cumulative probability of mEPSC amplitudes from 2 days dark-reared P23 mice (DR: black solid line) and 2 days of DR followed by 1 day of light exposure (D+L: gray solid line). Superimposed on the graph is a cumulative probability of mEPSC amplitudes from DR that are multiplied by a factor (0.7) to match the average mEPSC amplitude of D+L (DR_{scaled}: red dotted line). Inset: Distribution histogram plotting % of mEPSCs against mEPSC amplitude of DR_{scaled} (red bars) and D+L (black bars). Superimposed on the graph is a subtraction of the two distributions (blue solid line).

c. Cumulative probability of mEPSC amplitudes in visual cortex neurons from P38 NR (gray solid line) and 2 days DR mice (black solid line). Superimposed on the graph is a cumulative probability of mEPSC amplitudes from NR that are multiplied by a factor (1.6) to match the average mEPSC amplitude of DR (NR_{scaled}: red dotted line). Inset: Distribution histogram plotting % of mEPSCs against mEPSC amplitude of NR_{scaled} (red bars) and DR (black bars). Superimposed on the graph is a subtraction of the two distributions (blue solid line). Note that there were bit more fluctuations in the subtraction graph when comparing to that seen at P23 (inset in a).

Figure legend continued on Pg 69

d. Cumulative probability of mEPSC amplitudes in visual cortex neurons from P38 DR (black solid line) and dark-reared followed by 1 day of light re-exposure (D+L: gray solid line). Superimposed is a cumulative probability of mEPSC amplitudes from DR that are multiplied by a factor (0.6) to match the average mEPSC amplitude of D+L (DR_{scaled}: red dotted line). There was a statistically significant difference between the cumulative probability of D+L and DR_{scaled} (Kolmogorov-Smirnov test: $p < 0.01$), suggesting that the reduction in mEPSC amplitude by re-exposure to light does not follow the rules of multiplicative synaptic scaling. Inset: Distribution histogram plotting % of mEPSCs against mEPSC amplitude of DRscaled (red bars) and D+L (black bars). Superimposed on the graph is a subtraction of the two distributions (blue solid line). Note that there was a more noticeable difference in distribution as seen in the subtraction graph than in P38 NR_{scaled} to DR comparison (inset in c).

e. Cumulative probability of mEPSC amplitudes in visual cortex neurons from P97 NR (gray solid line) and 2 days DR mice (black solid line) are plotted. Superimposed on the graph is a cumulative probability of mEPSC amplitudes from NR that are multiplied by a factor (1.2) to match the average mEPSC amplitude of DR (NR_{scaled}: red dotted line). There was a statistically significant difference between cumulative probability of DR and NR_{scaled} (Kolmogorov-Smirnov test: $p < 0.001$). This suggests that global multiplicative scaling mechanism does not operate at this age. Inset: Distribution histogram plotting % of mEPSCs against mEPSC amplitude of NR_{scaled} (red bars) and DR (black bars). Note that there was an observable shift in distribution between NR_{scaled} and DR, which is shown as a large positive peak followed by a depression in the superimposed subtraction graph (blue solid line).

f. Decrease in mEPSC amplitude by re-exposing DR mice to 1 day of light (D+L) at P97 also does not occur via a global multiplicative scaling mechanism. Cumulative probability of mEPSC amplitudes in visual cortex neurons from P97 DR (black solid line) and DR followed by 1 day of light exposure (D+L: gray solid line) are shown. Superimposed on the graph is a cumulative probability of mEPSC amplitudes from DR that are multiplied by a factor (0.7) to match the average mEPSC amplitude of D+L (DR_{scaled}: red dotted line). There was a statistically significant difference between cumulative probability of DR and $D+L_{scaled}$ (Kolmogorov-Smirnov test: $p < 0.001$). Inset: Distribution histogram plotting % of mEPSCs against mEPSC amplitude of DR_{scaled} (red bars) and D+L (black bars). Note that there was an observable shift in distribution between NR_{scaled} and DR, which is shown as a large positive peak followed by a depression in the superimposed subtraction graph (blue solid line).

Subsection 5:Dark-rearing does not produce homeostatic synaptic scaling before eye opening.

Many aspects of visual cortex development are induced by experience, and hence occur after eye opening (Blue and Parnavelas, 1983; Cancedda et al., 2003; Yoshii et al., 2003). However, some aspects of visual system organization occur prior to eye opening (Katz and Shatz, 1996; Penn et al., 1998; Crowley and Katz, 2000). Therefore, to examine whether visual cortical neurons in very young animals undergo experience-dependent synaptic scaling, we measured mEPSCs from mice before eye opening. Eye opening in mice occurs around P14, hence we looked at P13 animals. Average mEPSC amplitude from layer 2/3 cells of P13 mice were larger than those recorded from P23 animals (P13: NR: 13.1 ± 0.5 pA, n = 10; P23: NR: 11.02 ± 0.5 pA, n=12; t-test: $p < 0.02$). Furthermore, dark rearing mice from P11 until P13 (2 days DR) did not alter mEPSC amplitude (P13 : NR: 13.1 ± 0.5 pA, n = 10; DR: 13.9 ± 1.1 pA, n = 12; t-test: $p > 0.5$; Fig. 3.5a) or frequency (P13 : NR: 1.9 ± 0.4 pA, n = 10; DR: 2.4 ± 0.4 pA, n = 12; t-test: $p > 0.4$; Fig. 3.5b) in layer 2/3 neurons. These results suggest that synaptic strength before eye opening may be scaled to the maximum, and dark rearing does not cause any further increase.

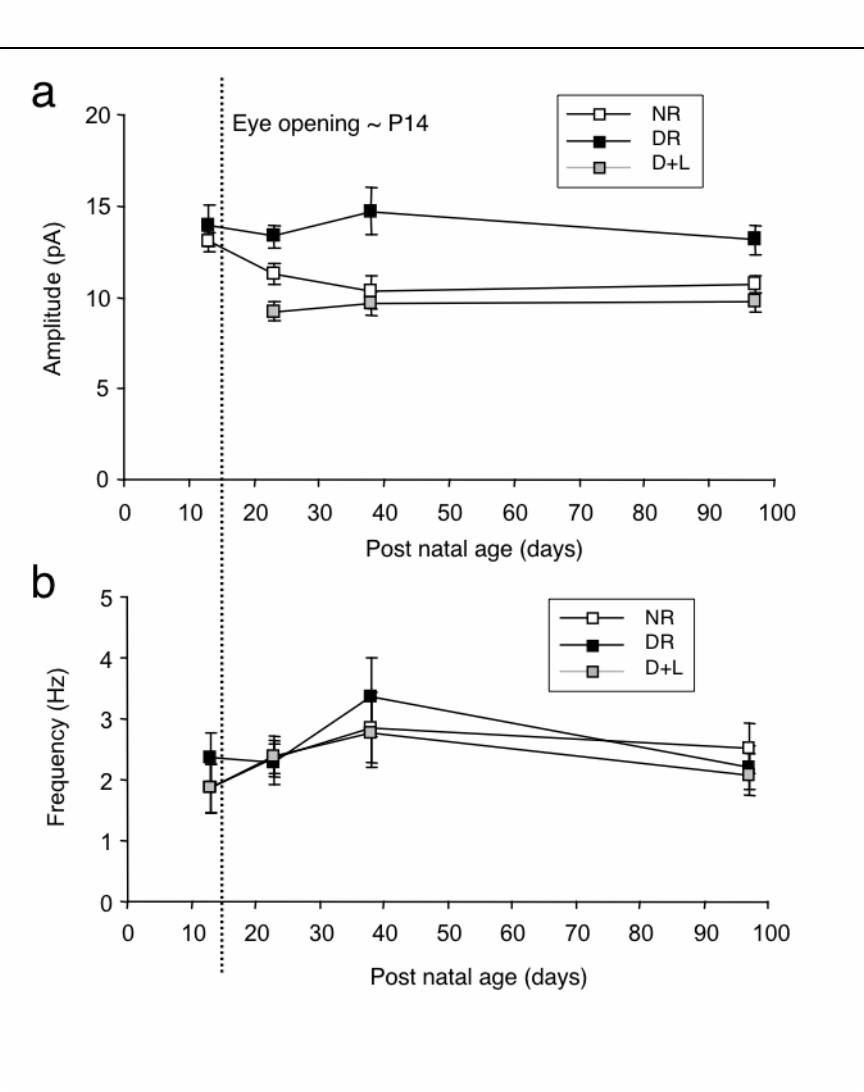

Figure 3.5. Persistence of experience-induced reversible changes in mEPSC amplitude in the superficial layers of visual cortex.

a. Comparison of average mEPSC amplitudes during development in NR (open squares), 2 days DR (black squares), and 2 days DR re-exposed to 1 day light (D+L: gray squares) mice. Black dashed line indicates eye opening, which occurs around P14 in mice. There was a developmental decrease in average mEPSC amplitude that occurred after eye opening (after P13), which plateau around P21 (one-way ANOVA: $F(3,39) = 3.249$, $p < 0.04$). There was no change in mEPSC amplitude with 2 days of DR prior to eye opening, while in all other ages recorded, we saw significant increases in mEPSC amplitude. This increase in amplitude was reversed by 1 day of light exposure.

b. Comparison of average mEPSC frequency across age in NR (open squares), 2 days DR (black squares), and DR re-exposed to 1 day light (D+L: gray squares) mice. There was no significant difference in mEPSC frequency across normal development or between NR, DR, and D+L regardless of age.

Table 3.1. Neuronal properties.

Age (days)	Conditions (n)	Rise time 10-90% (ms)	Decay time constant (τ) (ms)	R_{in} (MΩ)	R_{ser} (MΩ)
13	NR (10)	1.9 ± 0.1	5.02 ± 0.2	375 ± 39	21.6 ± 0.7
	2 d DR (10)	1.6 ± 0.8	4.4 ± 0.3	444 ± 78	20.9 ± 1.3
22	NR (9)	1.6 ± 0.1	4.02 ± 0.3	387 ± 97	20.6 ± 1.2
	1 d DR (10)	1.7 ± 0.1	4.5 ± 0.3	302 ± 35	22.2 ± 1.0
23	NR (12)	1.7 ± 0.04	4.7 ± 0.3	307 ± 36	21.7 ± 1.5
	2 d DR (19)	1.6 ± 0.1	4.04 ± 0.2	475 ± 103	21.6 ± 1.4
	2 d DR+1d LE (10)	1.7 ± 0.04	4.7 ± 0.3	283 ± 36	21.9 ± 1.5
25	NR (10)	1.8 ± 0.1	4.5 ± 0.2	490 ±126	20.4 ± 1.8
	4 d DR (15)	1.6 ± 0.1	4.3 ± 0.2	518 ± 113	21.1 ± 1.1
38	NR (10)	1.7 ± 0.1	4.5 ± 0.2	392 ± 79	18.8 ± 0.7
	2 d DR (10)	1.5 ± 0.1	3.6 ± 0.2*	492 ± 99	22.4 ± 1.1
	2 d DR+1d LE (10)	1.6 ± 0.6	4.4 ± 0.2	485 ± 126	20.3 ± 0.6
40	NR (11)	1.6 ± 0.1	4.4 ± 0.3	400 ± 38	17 ± 0.9
	4d DR (10)	1.3 ± 0.1	3.4 ± 0.3*	413 ± 88	17.4 ± 0.8
97	NR (11)	1.5 ± 0.1	3.4 ± 0.2	359 ± 55	19.7 ± 0.6
	2 d DR (11)	1.4 ± 0.1	4.1 ± 0.3*	375 ± 74	19.8 ± 0.7
	2 d DR+1d LE (11)	1.6 ± 0.1	4.4 ± 0.2*	701 ± 230	18.6 ± 0.5

* denotes statistically significant difference from NR condition at $P < 0.03$ with t-test or one-way ANOVA .

Section 5: Discussion

We found that experience-induced reversible homeostatic synaptic plasticity persists through adulthood in the superficial layers of mouse visual cortex. The minimum duration of binocular visual deprivation necessary and sufficient to induce a maximal homeostatic modification was 2 days. Visual deprivation-induced increase

in AMPA receptor function was rapidly reversed when vision was restored by re-exposing animals to 1 day of light. Our summary data shows that average mEPSC amplitude was larger in young animals before eye opening, which then decreases to plateau around the third postnatal week (Fig 3.5a). On the other hand, mEPSC frequency remained essentially the same across ages with only a trend towards an increase (Fig. 3.5b), suggesting postsynaptic loci for change. Dark rearing-induced homeostatic mechanisms were not operative before eye opening, and in essence visual deprivation at later ages seems to return mEPSC amplitude to that seen prior to eye opening (Fig. 3.5a). While reversible homeostatic synaptic changes are observed in adults, we find evidence that the mechanism of homeostatic plasticity differs from juvenile mice, in that it no longer occurs globally following a multiplicative scaling mechanism.

Our results show that in young mice (at P21) 2 days of dark rearing is necessary and sufficient for inducing homeostatic synaptic plasticity. This result is consistent with previous *in vitro* findings where 2 days of TTX application to cortical cultures maximally scales up AMPA receptor-mediated mEPSCs (Turrigiano et al., 1998). Our observation is not likely complicated by developmental issues, because 2 days of dark-rearing also maximally increased mEPSC amplitude in more mature animals (DR initiated at P36; Figure 3.6), where there is little developmental change in average mEPSC amplitude (Fig. 3.5a).

In vitro studies showed that homeostatic plasticity driven by pharmacological manipulation of neural activity is bidirectional (Lissin et al., 1998; O'Brien et al., 1998; Turrigiano et al., 1998; Thiagarajan et al., 2002). Recently, we reported that

manipulation of visual experience can also reversibly regulate synaptic scaling in juvenile rat visual cortical slices (Goel et al., 2006). The present study extends these findings to show that the reversible nature of experience-induced homeostatic regulation is operative in mice, and also elucidated the minimum duration required for producing homeostatic synaptic scaling by experience. Interestingly, while 2 days of visual deprivation was required to scale up synaptic strengths, only 1 day of visual experience was sufficient to reverse this change. This may illustrate differences in the mechanisms of synaptic scaling up versus down. While there are data supporting reversible changes in AMPA receptor subunit composition (Thiagarajan et al., 2005; Goel et al., 2006), and CaMKIIalpha/CaMKIIbeta ratio (Thiagarajan et al., 2002) during bidirectional homeostatic plasticity, recent evidence supports the notion of asymmetry in molecular mechanisms. For instance, a recent study demonstrated that tumor-necrosis factor-α (TNF-α) is only involved in synaptic scaling up of excitatory synaptic transmission by inactivity, but not for scaling down synapses by enhanced activity in hippocampal cultures (Stellwagen and Malenka, 2006). In contrast, activity-regulated cytoskeletal protein/activity-regulated gene 3.1 (Arc/Arg 3.1), which is an immediate early gene rapidly up-regulated by neural activity (Lyford et al., 1995), has been shown to be involved in scaling down synapses (Shepherd et al., 2006). Asymmetry in homeostatic plasticity mechanisms also seems to occur *in vivo*, since we reported that increase in AMPA receptor phosphorylation on GluR1-S845 by dark-rearing does not reverse with re-exposure to light (Goel et al., 2006).

One of our major findings is that reversible homeostatic plasticity induced by visual experience in the superficial layers of the visual cortex can occur through

adulthood, well beyond the "classical" critical period. Initial studies of cortical plasticity emphasized the sharp loss of plasticity around puberty, as defined as the "critical period" (reviewed in (Berardi et al., 2000)). However, recent studies demonstrate that a substantial level of visual cortex plasticity remains in adulthood (Guire et al., 1999; Sawtell et al., 2003; Pham et al., 2004), especially in the superficial layers of the cortex (Guire et al., 1999; Pham et al., 2004). Moreover, certain manipulations, such as visual deprivation (He et al., 2006) or degradation of extracellular matrix (Pizzorusso et al., 2002; Berardi et al., 2004) or knockout of Nogo signaling (McGee et al., 2005), enhance OD plasticity in adults. Adult plasticity is not restricted to the visual cortex. While initial studies on plasticity in the barrel cortex showed that there is a critical period for experience-dependent plasticity (Fox, 1992), further investigations showed that barrel cortex receptive fields can be altered by experience in adult rats (Diamond et al., 1993; Glazewski et al., 1996; Wallace et al., 2001; Fox, 2002; Polley et al., 2004). Furthermore, a recent finding showed that a brief exposure to an enriched environment can accelerate barrel cortex receptive field plasticity in adult rats (Rema et al., 2006). Interestingly, dendritic spines, which are considered to be the morphological correlates of experience-dependent synaptic plasticity, continue to turnover in both visual and somatosensory cortices even in adults (Grutzendler et al., 2002; Trachtenberg et al., 2002; Holtmaat et al., 2005; Zuo et al., 2005; Holtmaat et al., 2006), albeit to a lesser extent than in young animals (Grutzendler et al., 2002; Holtmaat et al., 2005; Zuo et al., 2005).

While adult plasticity is observed in different sensory cortices, the majority of studies indicate that different cortical layers have varying capacity to undergo

plasticity. Specifically, layer 4 is known to mature earlier than extragranular layers, and hence display a short and well-defined critical period for sensory plasticity. In cats, the critical period for layer 4 in the visual cortex ends around 8 months of age (Daw et al., 1992) while in the mouse barrel cortex layer 4 matures by P12 (Stern et al., 2001). In contrast, superficial layers seem to have an extended critical period for OD plasticity that lasts longer than layer 4. In cat visual cortex, extragranular layers remain plastic up to 1 year (Daw et al., 1992), and in the barrel cortex critical period for layer 2/3 spans between P12-P14 (Stern et al., 2001). Similarly, homeostatic synaptic scaling also exhibits layer specific critical periods. Monocular deprivation by TTX injections between P14 and P16 produced synaptic scaling in layer 4, but not in layers 2/3 of the visual cortex (Desai et al., 2002). In contrast, the same monocular deprivation paradigm performed between the ages P21 and P23 failed to produce synaptic scaling in layer 4, but caused homeostatic scaling in layer 2/3 (Desai et al., 2002). Collectively, these results suggest that layer 4 plasticity (whether it be OD plasticity or homeostatic synaptic scaling) is more limited to early development, while layer 2/3 plasticity seems to last longer. Our data extends these studies to demonstrate that experience-induced homeostatic plasticity in layer 2/3 persists through adulthood.

Even though reversible homeostatic plasticity persists in layers 2/3 of visual cortex in adults, the mechanism seems to differ from that in young animals. Initial descriptions of homeostatic synaptic scaling in cortical cultures by Turrigiano et al. (1998) demonstrated that scaling occurs via a multiplicative mechanism. Therefore, all synapses on a cell globally scale up or down with the same multiplicative factor.

We previously reported that this is also the case for visual experience-induced homeostatic plasticity in juvenile rat visual cortex (Goel et al., 2006). In contrast, work using hippocampal cultures showed that homeostatic changes differentially modify subsets of synapses, which implies that it does not follow a strict global multiplicative mechanism (Thiagarajan et al., 2005). We found that experience-induced reversible homeostatic plasticity in visual cortex occurs via a global multiplicative mechanism in young animals (P23), but not in adults (especially at P97), suggesting that age may be a determining factor. Incidentally, there were statistically significant changes in mEPSC decay kinetics with visual manipulations only in adults (Table 3.1), which further implies a potential difference with age. Similarly, a recent study demonstrated that an increase in the *in vitro* age of neuronal cultures causes the expression locus of homeostatic plasticity to shift from predominantly postsynaptic to having both pre- and postsynaptic components (Wierenga et al., 2006). Interestingly, spines turnover more slowly in the visual cortex of adult mice (Grutzendler et al., 2002; Holtmaat et al., 2005), implying that there may be a smaller proportion of dynamic synapses which undergo activity-dependent modifications. Therefore, we surmise that visual-experience may preferentially affect this dynamic population of synapses in adult cortex. Recent studies highlighted that synapses on neocortical neurons may utilize different rules for inducing synaptic plasticity depending on their dendritic location (Froemke et al., 2005; Gordon et al., 2006; Letzkus et al., 2006; Sjostrom and Hausser, 2006). Therefore, it is also plausible that there may be select dendritic compartments that undergo homeostatic plasticity in adults. In any case, the non-multiplicative scaling in

adults occurred without alterations in mEPSC frequency suggesting that a subset of pre-existing synapses likely undergo homeostatic changes. Collectively, our results suggest that there is persistent homeostatic regulation of synapses through adulthood in the superficial layers of visual cortex, but that the mechanisms change, perhaps due to different computational requirements neural networks need to fulfill as the animals mature.

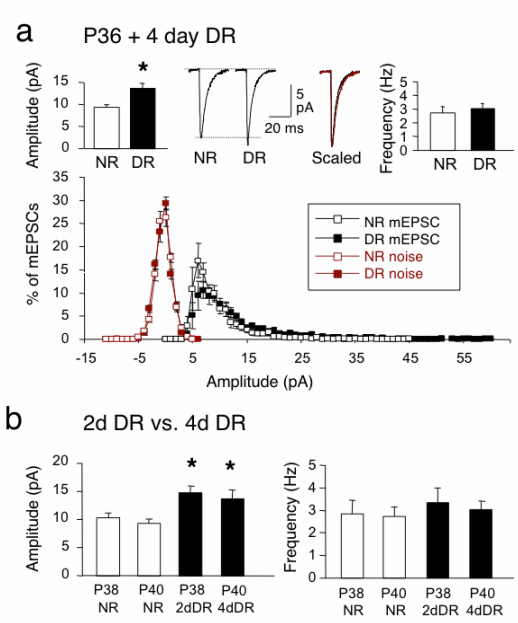

Figure 3.6. Minimum duration of dark-rearing needed to maximally increase AMPA receptor-mediated mEPSCs in layer 2/3 neurons in post-critical period mice is also 2 days.

a. Dark-rearing post-critical period (P36) mice for 4 days increased mEPSC amplitude (NR: 9.4 ± 0.7 pA, n = 11; DR: 13.6 ± 1.7 pA, n = 10; t-test: $p < 0.04$) without changes in frequency (NR: 2.7 ± 0.4 Hz, n = 11; DR: 3.0 ± 0.4 Hz, n = 10; t-test: $p > 0.6$). Top left panel: Comparison of average mEPSC amplitude of cells from P40 NR mice to that from mice dark-reared for 4 days from P36 to P40 (DR). Top middle panel: Average mEPSC traces from NR (left trace) and 4 days DR (right trace) mice. "Scaled" indicates the NR mEPSC average trace scaled (red trace) and superimposed on the 4 days DR average trace (black trace). Note a statistically significant decrease in decay time constant (τ) following 4 days of DR (t-test: $p < 0.03$). Top right panel: No change in average mEPSC frequency from cells from NR and 4 days DR mice. Bottom panel: Distribution histogram of mEPSC amplitudes recorded from 4 days DR mice (closed black symbols) shows a higher percentage of mEPSCs with larger amplitudes compared to NR animals (open black symbols). There was no difference between distribution of NR noise (open red symbols) and DR noise (closed red symbols). Asterisk: $P < 0.04$ with t-test.

b. No additional increase in mEPSC amplitude with 4 days of DR compared to 2 days of DR initiated at P36. Left panel: Comparison of average mEPSC amplitude of cells from P38 NR , P40 NR, P38 2dDR (dark reared for 2 days from P36-P38) and P40 4dDR (dark reared for 4 days from P36-P40) mice. Note that there is no significant difference between P38 NR and P40 NR groups. Right panel: No change in average mEPSC frequency from cells across the 4 groups.

Asterisk: denotes statistically significant difference from P38 NR and P40 NR at $p < 0.02$ with Fisher's PLSD post-hoc test following one-way ANOVA ($F(3,37) = 5.14$, $p < 0.005$).

Chapter 4: Experience-induced homeostatic synaptic plasticity in the visual cortex requires AMPA receptor phosphorylation

This manuscript is in preparation.
Putative authors: Anubhuthi Goel, Linda Xu, Kevin Snyder, Lihua Song, Yamila Goenaga-Vazquez and Hey-Kyoung Lee

My contribution: All the electrophysiological recordings and analyses (Measurement of AMPAR mediated mEPSCs and rectification).

Section 1: Introduction

Glutamate is the predominant neurotransmitter that acts at a majority of excitatory synapses in the central nervous system. The action of glutamate is mediated by two types of ionotropic glutamate receptors: AMPA receptors and NMDA receptors. Though both types of receptors respond to glutamate and mediate excitatory synaptic transmission, the roles played by both receptors are distinct.

AMPA receptors are tetrameric channels composed of combinations of glutamate receptor (GluR) subunits 1-4 (Dingledine et al., 1999). In the adult forebrain, AMPA receptor population consists of primarily GluR1/GluR2 and GluR2/GluR3 heteromers with the predominant population being that of GluR1/GluR2 heteromers (Wenthold et al., 1996). Each subunit has a N-terminal domain that binds to glutamate and 4 transmembrane domains (Mayer and Armstrong, 2004). Among the transmembrane domains the second one (M2) forms the pore of the receptor channel and specifies ion selectivity. The majority of the GluR2 subunit undergoes RNA editing within the M2 region wherein, a critical glutamine 607 residue (Q607) is converted to an arginine (R607). This RNA editing, called "Q/R editing", confers distinct physiological properties to AMPA receptors containing the GluR2 subunit, namely impermeability to calcium and resistance to polyamine block (Verdoorn et al., 1991; Washburn et al.,

1997). The lack of block by endogenous intracellular polyamine imparts an electrophysiological signature to GluR2-containing AMPA receptors, which display linear I/V curves (Rozov et al., 1998). On the other hand, GluR2-lacking AMPA receptors are blocked by polyamines at positive potentials, and hence display inward rectifying currents. In addition, GluR2-lacking receptors have a higher single channel conductance (Swanson et al., 1997). The subunit composition of AMPA receptors also determines the kinetic properties of the AMPA receptor mediated current, wherein GluR1 containing homomeric AMPA receptors have smaller decay time constant (τ) than heteromeric AMPA receptors (Mosbacher et al., 1994). Even though most AMPA receptors exist as heteromers rather than homomers, certain types of neural activity can allow GluR2-lacking AMPARs to express at synapses (Ju et al., 2004; Thiagarajan et al., 2005; Clem and Barth, 2006; Plant et al., 2006; Goel and Lee, 2007).

Phosphorylation, a form of post-translational modification, can occur at certain residues on the C-terminal tail of AMPA receptor subunits to modify receptor function. There are two well characterized phosphorylation sites on the GluR1 subunit, serine-831 (S831) and serine-845 (S845), both of which when phosphorylated by CAMKII and PKA, respectively, can increase AMPA receptor mediated current (Derkach et al., 1999; Banke et al., 2000). Phosphorylation at S831 is known to increase the channel conductance (Derkach et al., 1999; Esteban et al., 2003; Oh and Derkach, 2005), while phosphorylation at S845 is implicated in trafficking AMPA receptors to the synaptic surface (Esteban et al., 2003). Studies have shown that regulation of phosphorylation at S831 and S845 is important for LTP

and LTD (Lee et al., 2000), as well as for learning and memory (Lee et al., 2003). In addition, recent studies have implicated the regulation of GluR1-containing AMPA receptors as part of an expression mechanism of homeostatic synaptic plasticity (O'Brien et al., 1998; Ju et al., 2004; Thiagarajan et al., 2005; Sutton et al., 2006). To investigate whether the homeostatic regulation of GluR1 is dependent on its phosphorylation, I used transgenic mice, GluR1-S831A and GluR1-S845A, which were generated in Dr. Richard Huganir's laboratory at the John Hopkins School of Medicine. In GluR1-S831A mice, the serine residue at 831 site was mutated to an alanine and therefore prevents phosphorylation by PKC and CAMKII. Likewise in the GluR1-S845A mice, the serine residue at 845 site was mutated to an alanine and thus eliminated PKA-dependent phosphorylation.

Here we report that lacking GluR1-S831 results in an abnormal regulation of the remaining S845 phosphorylation and synaptic scaling by visual experience. On the other hand, lacking the GluR1-S845 site prevents visual experience-induced homeostatic synaptic scaling.

Section 2: Materials and methods

Subsection 1: Dark rearing animals

Wild-type (GluR1-S831WT and GluR1-S845WT) and transgenic mice (GluR1-S831A and GluR1-S845A) mice were raised under normal lighted environment (12 hr light/12 hr dark cycle). Dark rearing (DR) was initiated at postnatal ages 21 days (P21) for 2 days, while control (normal-reared) animals were continuously raised in the normal lighted condition for the same duration. The animals in the dark were

cared for using infrared vision goggles under dim infrared light. After 2 days of dark-rearing, some of the mice were taken out to the lighted environment for 1 day to study the effect of re-exposure to light.

Subsection 2: Whole cell recording of AMPA receptor mediated EPSCs

The cortical slices were moved to a submersion recording chamber mounted on a stage of an upright microscope (E600 FN, Nikon) equipped with infrared differential interference contrast (IR-DIC). Layer 2/3 pyramidal cells were visually identified and patched using a whole-cell patch pipette (tip resistance: 3-5 MΩ) filled with intracellular solution (130 mM Cs-gluconate, 8 mM KCl, 1 mM EGTA, 10 mM HEPES, 4 mM ATP and 5 mM QX-314; pH 7.4; 285-295 mOsm).

To isolate AMPA receptor-mediated mEPSCs, 1 µM TTX, 20 µM bicuculline, and 100 µM D,L-APV were added to the ACSF (2 ml/min, 30 ± 1˚C), which was continually bubbled with 95% O_2/5% CO_2. mEPSCs were recorded at a holding potential (Vh) of –80 mV using Axopatch-clamp amplifier (Axon Instruments), digitized at 2 kHz by a data acquisition board (National Instruments), and acquired using the Igor Pro™ software (Wave Metrics). Acquired mEPSCs were analyzed using the Mini Analysis Program (Synaptosoft). The threshold for detecting mEPSCs was set at 3 times the Root Mean Square (RMS) noise. There was no significant difference in RMS noise between the experimental groups. There was no significant difference in RMS noise between the experimental groups (WT NR =1.71 ±0.05; n =18; WT DR =1.8 ± 0.05, n =7; ttest, $p > 0.1$: S831 WT NR = 1.7 ± 0.06, n = 10; S831A NR = 1.8 ± 0.07, n = 11; t-test, $p > 0.8$: S845 WT NR = 1.6 ± 0.06, n = 11; S845A NR = 1.8 ± 0.04, n = 10; ttest $p > 0.1$: S831A NR = 1.8 ± 0.07, n = 11 ;

S831A DR = 1.7 ± 0.05, n = 10; S831A D+L = 1.8 ± 0.05 ,n = 9, ANOVA, $F(2,27) = 0.943$, $p > 0.9$: S845A NR = 1.8 ± 0.06, n = 10, S845A DR = 1.7 ± 0.07, n = 11; S845A D+L = 1.8 ± 0.04 ,n = 12, ANOVA, $F(2,30) = 1.933$, $p > 0.2$). A possibility of dendritic filtering was assessed by plotting mEPSC amplitude against its rise time. Cells showing a negative correlation between mEPSC amplitude and rise time (i.e. dendritic filtering present) were excluded from analysis, as well as mEPSCs with greater than 3 msec rise time (measured between 10-90% of amplitude). Average mEPSC amplitude and frequency were calculated and compared across different experimental groups using one-factor ANOVA or unpaired Student's t-test. Only the cells and recording conditions that meet the following criteria were studied: $Vm \leq -65$ mV, input $R \geq 200$ MΩ, series $R \leq 25$ MΩ. Cells were discarded if input R or series R changed more than 15%. Junction potentials were typically less than 5 mV, and were left uncompensated.

Evoked AMPA receptor-mediated synaptic currents (EPSCs) were measured from layer 2/3 pyramidal cells of either visual or somatosensory cortices in response to stimulation through an electrode (concentric bipolar, FHC) placed in layer 4. To isolate the AMPA receptor component, 100 µM D, L-APV and 100 µM bicuculline were added to the bath solution. The concentration of $CaCl_2$ and $MgCl_2$ in the ACSF were changed to 4 mM and 2 mM, respectively, to prevent polysynaptic responses upon stimulation in the presence of bicuculline. Intracellular recording solution containing 200 µM spermine (in 90 mM $CsMeSO_3H$, 5 mM $MgCl_2$, 8 mM NaCl, 10 mM EGTA, 20 mM HEPES, 1 mM QX-314, 0.5 mM Na_3GTP, and 2 mM Mg•ATP, pH 7.2, 250-270 mOsm) was used. For generating I-V curves for rectification

measurements, cells were held at –60, –40, –20, 0, +20 and +40 mV. Inward Rectification (IR) was calculated by dividing the absolute amplitude of average EPSC measured at –60 mV by that at +40 mV. There were no significant differences in calculated reversal potentials between groups (WT NR = 10 ± 1.3 mV, n = 10; WT DR = 8.8 ± 1.5 mV, n = 5; ttest, $p > 0.6$; S831 WT NR = 8.5 ± 1.3 mV, n = 5; S831A NR = 9.8 ± 1.0 mV, n = 5; S831A DR = 8.8 ± 1.3 mV, n = 5; ttest, $p > 0.5$; S845 WT NR = 11.2 ± 2.1 mV, n = 5; S845A NR = 9.6 ± 0.9 mV, n = 8; ttest, $p > 0.6$; S845A DR = 9.1 ± 1.5 mV, n = 6; ttest, $p > 0.8$; S831A washout = 11 ± 1.6 mV, n = 3; ttest, $p > 0.5$; S845A washout = 11.2 ± 1.4 mV, n = 4; ttest, $p > 0.4$). Reversal potentials were calculated using equations generated by fitting a linear regression curve to the current values collected at negative holding potentials. Only the cells and recording conditions that meet the following criteria were studied: $Vm \leq -65$ mV, input $R \geq 100$ MΩ, series $R \leq 20$ MΩ. Cells were discarded if input R or series R changed more than 15%. Junction potentials were typically less than 5 mV, and were left uncompensated.

Subsection 3: Post synaptic density (PSD) preparation

Visual cortices from normal-reared and dark-reared rats were gently homogenized on ice in HEPES-buffered sucrose (0.32 M sucrose, 4 mM HEPES, pH 7.4) containing 2 mM EGTA, 50 mM NaF, 10 mM sodium pyrophosphate, 1 mM sodium orthovanadate, 1 μM okadaic acid, and protease inhibitors (Protease Inhibitor Cocktail, Pierce). Primary visual cortices from two animals were pooled together for one data point. The homogenates (H) were centrifuged at 800 x g for 10 min (4˚C) to remove pelleted nuclear fraction (P1), and the resulting supernatants (S1) were

centrifuged at 10,000 x g for 15 min (4˚C) to yield the crude membrane pellets (P2). P2 fractions were resuspended in HEPES-buffered sucrose with inhibitors and respun at 10,000 x g for 15 min (4˚C) to yield the washed crude membrane fractions (P2'). P2' fractions were lysed by hypo-osmotic shock in ice-cold 4 mM HEPES (pH 7.4, with inhibitors), and centrifuged at 25,000 x g for 20 min to generate lysed synaptosomal membrane fractions (P3). P3 was subsequently resuspended in HEPES-buffered sucrose with inhibitors, and run on a discontinuous sucrose gradient (1.2 M, 1.0 M, and 0.8 M sucrose with inhibitors) at 150,000 x g for 2 hours (4˚C). Synaptic plasma membrane (SPM) fractions were collected between 1.0 M and 1.2 M sucrose and diluted with 2.5 volumes of 4 mM HEPES with inhibitors. SPM was pelleted by centrifugation at 150,000 x g for 30 min (4˚C), resuspended in 0.5% Triton X-100, HEPES-EDTA solution (50 mM HEPES, 2 mM EDTA, pH 7.4) with inhibitors, and rotated for 15 min at 4˚C. Solubilized SPM was then centrifuged at 32,000 x g for 20 min to pellet the postsynaptic density fraction (PSD). PSD fractions were resuspended in gel sample buffer and processed for SDS-PAGE (4 µg of PSD proteins were loaded per lane) and immunoblot analysis.

Subsection 4: Immunoblot analysis

SDS-PAGE gels were transferred to polyvinyl difluoride (PVDF) membranes (Immobilon^{TM}, Millipore). The PVDF membrane blots were blocked for ~1 hr in blocking buffer (1% bovine serum albumin and 0.1% Tween-20 in phosphate buffered saline (PBS), pH 7.4), and subsequently incubated for 1-2 hrs in primary antibodies (Ab's) diluted in blocking buffer to yield the effective concentration as tested prior to the experiments. After 5 times 5 min washes in blocking buffer, the

blots were incubated for 1 hr in 2nd Ab linked to alkaline phosphatase (AP) diluted 1:10,000 in blocking buffer. The blots were washed 5 times 5 min, and developed using enhanced chemifluorescence substrate (ECF substrate, Amersham). The ECF blots were scanned and quantified using a Versa Doc 3000™ gel imaging system (Bio Rad). The signal of each sample on a blot was normalized to the average signal from normal-reared (NR) or dark-reared (DR) samples respectively to obtain the % of average NR or % of average DR values, which were compared across different experimental groups using one-factor ANOVA or unpaired Student's t-test.

Section 3: Results

Subsection 1: Dark rearing leads to increase in mEPSC amplitude in wild-type mice.

We reported in chapter 3 that dark rearing wild type mice for 2 days is necessary and sufficient to maximally scale up the mEPSC amplitudes of pyramidal neurons in layer 2/3 of visual cortex (Goel and Lee, 2007). This effect was seen in both juveniles (P21-P23) mice as well as adult mice (P95-P97). As shown in chapter 2, 1 week of dark rearing in rats was accompanied by a increase in S845 and a decrease in S831 phosphorylation (Goel et al., 2006). Therefore to further investigate the role of S845 and S831 phosphorylation I studied the effects of dark rearing in GluR1-S831A and GluR1-S845A mutant mice. Since 2 days of dark rearing at P21 produced significant and robust homeostatic changes we restricted our experiments in GluR1-S831A and GluR1-S845A mutant mice within that age group. In order to ensure that the wild

type mice with the same genetic background as the mutant mice showed visual deprivation induced synaptic scaling we dark reared P21 GluR1-S831 WT and GluR1-S845 WT mice for 2 days. An initial investigation of normal reared GluR1-S831 WT and GluR1-S845 WT showed no significant differences between the mEPSC amplitudes (S831 WT: 10.19 ± 0.3 pA, n = 9; S845 WT: 9.22 ± 0.53 pA, n = 11; t-test $p > 0.14$), frequency (S831 WT: 3.4 ± 0.4 Hz, n = 9; S845 WT: 2.6 ± 0.2 Hz, n = 11; t-test $p > 0.1$) or kinetics. Hence we combined the data obtained from the 2 groups and compared the mEPSC changes between the combined (GluR1-S831 WT and GluR1-S845 WT) normal reared and the dark reared groups. Consistent with our previous work (Goel and Lee, 2007) visual deprivation for 2 days significantly increased the mEPSC amplitude (WT: NR: 9.66 ± 0.3 pA, n = 20; DR: 13.4 ± 0.8 pA, n = 7; t-test $p < 0.002$, Fig 4.1B , left panel) with no change in frequency (WT: NR: 3.5 ± 0.4 Hz, n = 20; DR: 3.8 ± 0.4 Hz, n = 7; t-test $p > 0.3$, Fig 4.1B , right panel) . The increase in mEPSC amplitude was reflected in a shift in amplitude distribution of mEPSCs recorded from WT DR mice towards larger values (Fig 4.1A). There was significant decrease in decay time with 2 days of dark rearing (WT: NR: 4.7 ± 0.1 ms, n = 20; DR: 3.5 ± 0.2 ms, n = 7; t-test $p < 0.001$, Table 4.1). In addition consistent with our previous results (Goel and Lee, 2007) the increase in mEPSC in amplitude was multiplicative (Fig. 4.1C).

Also, similar to our previous work in rats (Goel et al., 2006) 2 days of dark rearing led to a significant increase in the GluR1 to GluR2 (GluR1/GluR2) ratio at the PSD of wild-type mice (NR = 100 ± 12.4%, n = 11; DR = 183 ± 26.3%, n = 10; t-test: $p < 0.02$; Fig 4.1E), as well as inward rectification index of AMPA receptor-mediated

evoked synaptic currents (WT: NR: 2.09 ± 0.07, n = 9; DR = 3.9 ± 0.2, n = 5; ttest , $p < 0.002$; Fig 4.1D).

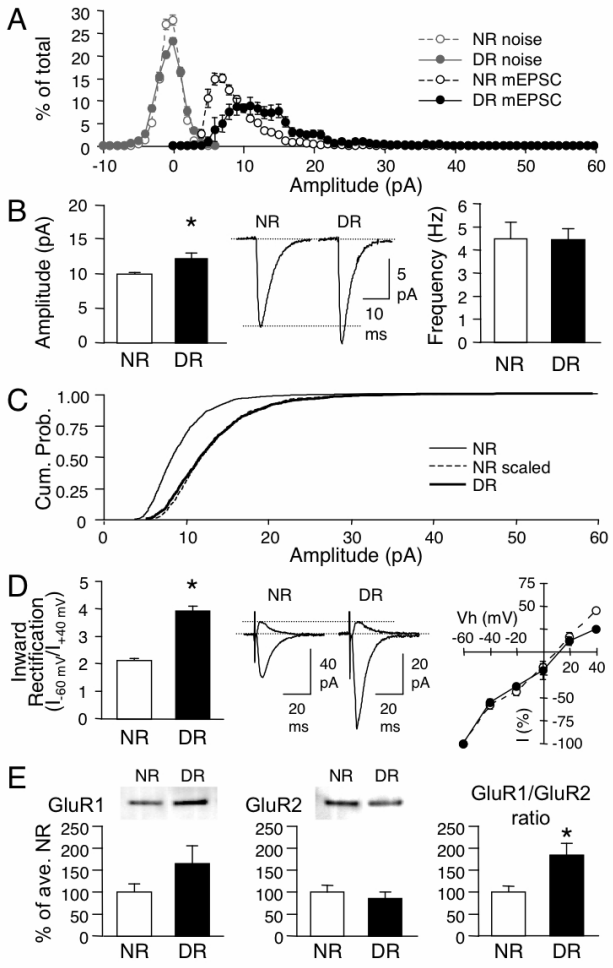

Figure 4.1. Visual deprivation leads to an increase in mEPSC amplitude in wild-type (WT) mice.

A. Wild-type (WT) mice dark reared (DR) for 2 days from P21-23 had larger mEPSC amplitudes compared to normal reared (NR). Distribution histogram of mEPSC amplitudes recorded from WT NR (open black symbols) and WT DR mice (closed black symbols). The distribution histogram in the DR mice towards larger amplitudes and also clearly shows that there was no overlap between signal and noise, and that there is no difference in noise levels between the two groups (WT NR noise: open gray symbols, WT DR noise: closed gray symbols).

B. Left panel: Average mEPSC amplitude of cells from WT DR mice was larger than the NR counterparts. Middle panel: Average mEPSC traces from WT NR (left trace) and WT DR (right trace) mice. Right panel: Comparison of average mEPSC frequency from cells from WT NR and DR mice.

C. Shift in cumulative probability towards the right in wild- type DR mice. Cumulative probability of mEPSC amplitudes in visual cortex neurons from WT NR (thin black solid line) and DR mice (thick black solid line). Superimposed on the graph is a cumulative probability of mEPSC amplitudes from NR that are multiplied by a factor (1.4) to match the average mEPSC amplitude of DR (NR_{scaled}: black dotted line). There was no difference between cumulative probability of DR and NR_{scaled} (Kolmogorov-Smirnov test: $p > 0.057$) indicative of a multiplicative increase in mEPSC amplitude.

D. Larger inward rectification of current through synaptic AMPARs in dark reared wild –type mice. Left panel: Significant increase in rectification index in WT DR mice compared to NR. Middle panel: Representative AMPAR-mediated current traces for WT NR and WT DR mice in visual cortical neurons. Right panel: Comparison of I-V relationship between neurons from WT NR (white circles) and WT DR (black circles). Note that the I/V relationship is more linear in NR mice.

E. Increase in synaptic AMPAR GluR1/2 ratio in PSDs by dark rearing. Left panel: DR for 2 days showed a trend towards an increase in GluR1 in PSDs of visual cortex when compared to NR, though this increment did not reach statistical significance. Middle panel: There was a trend towards a decrease in GluR2 in PSDs of visual cortex when compared to NR, but it was not significant. Right panel: When computed as a ratio, DR significantly increased GluR1/GluR2 ratio in the PSDs.

Asterisk: $P < 0.002$ with t-test.

Subsection 2: Higher basal S845 phosphorylation causes larger basal mEPSC amplitude in GluR1-S831A mutant mice.

In GluR1-S831A mutants, we first confirmed the mutation of the phosphorylation site by immunoblot analysis using phosphorylation site-specific antibodies. Detection of GluR1 by phosphospecific antibody to S831 was completely absent in the S831A mutant mice (Fig 4.2A, upper left panel). Surprisingly, the remaining S845 site on the GluR1 subunit was highly phosphorylated under basal conditions in the GluR1-S831A mutants (S831 WT: 100 ± 15% of S831 WT, n = 10; S831A: 265 ± 40% of S831 WT, n = 11; t-test: $p < 0.007$, Fig 4.2A, right panel).

We found that S831A mutant mice also show a significant increase in mEPSC amplitude in comparison to their WT counterparts (S831 WT: 10.19 ± 0.3 pA, n = 9; S831A: 13.8 ± 0.7 pA, n = 11; t-test $p < 0.0002$; Fig.4.2C, left panel), without affecting mEPSC frequency (S831 WT: 3.4 ± 0.4 Hz, n = 9; S831A: 3.6 ± 0.5 Hz, n = 11; t-test $p > 0.7$; Fig. 4.2C, right panel). There was a significant decrease in the decay kinetics of the mEPSCs obtained from GluR1-S831A compared to the wild type counterparts (S831 WT: 4.8 ± 0.13 ms, n = 9; S831A: 4.0 ± 0.3 ms, n = 11; t-test $p < 0.02$; Table 4.1). The increase in mEPSC amplitude without a change in frequency suggests that the locus of change in basal synaptic strength is likely postsynaptic.

The increase in mEPSC amplitude is reflected in a shift in amplitude distribution of mEPSCs recorded from S831A towards larger values (Fig.4.2B), however, this increase was not multiplicative in nature (Fig. 4.2D). This fact is emphasized in the comparison of the cumulative probability plots between the 2 groups. In S831A mice, the curve significantly shifts to the right with dark rearing (comparison of mEPSC amplitude between S831 WT and S831A: $p < 0.0001$, Kolmogorov-Smirnov test; Fig 4.2D). Superimposed on the graph is a cumulative probability of mEPSC amplitudes from S831 WT that are multiplied by a scaling factor (1.4) to match the average mEPSC amplitude to that from S831A (S831 WT_{scaled}: red dotted line). There was a statistically significant difference between cumulative probability of S831A and that of S831 WT_{scaled} (Kolmogorov-Smirnov test: $p < 0.009$) providing support for a non-multiplicative nature of the increase in mEPSC amplitude in S831A mutant mice.

The larger average basal mEPSC amplitude in S831A mutants (Fig.4.2B, C) correlated with a higher basal phosphorylation of S845 (Fig. 4.2A). GluR1 phosphorylation at S845 is known to be involved in trafficking GluR1 containing AMPA receptors to the synapses (Esteban et al., 2003; Oh and Derkach, 2005). To test this we assessed the composition of AMPA receptors at the synapse electrophysiologically by determining the inward rectification index (IR: I_{60mV}/I_{+40mV}, see methods) of AMPAR-mediated synaptic responses evoked by layer 4 stimulation. GluR1-S831A mutant mice showed larger inward rectification of AMPA receptor current compared to the wild type counterparts (S831 WT = 2.11 ± 0.11, n =

5; DR = 3.32 ± 0.12, n = 5; ttest, $p < 0.0001$; Fig 4.2E.), which was dependent on intracellular spermine (Fig. 4.6A). These results suggest that the lack of phosphorylation site S831 in these mutant mice is compensated for by an increase in phosphorylation at S845, which then causes an increase in AMPAR mediated synaptic transmission perhaps by incorporation of homomeric GluR1 to synapses. To examine whether this is the case, we measured synaptic GluR1 and GluR2 content at synaptic sites by biochemically isolating PSDs. Unexpectedly, there were no significant differences in GluR1 (WT = 100 ± 13%, n = 8; S831A = 78 ± 15%, n = 8; t-test: $p > 0.3$) or GluR2 (WT = 100 ± 20%, n = 8; S831A = 69 ± 13%, n = 8; t-test: $p > 0.2$) content at PSDs in GluR1-S831A mutants when comparing to those in wild-types (GluR1/GluR2 ratio: WT = 100 ± 17%, n = 8; S831A = 114 ± 21%, n = 8; t-test: $p > 0.6$; Fig. 4.2F). This implies that the electrophysiologically measured increase in GluR1 function at synapses in S831A mutants may be due to homomeric GluR1s that are not tightly associated to the PSDs.

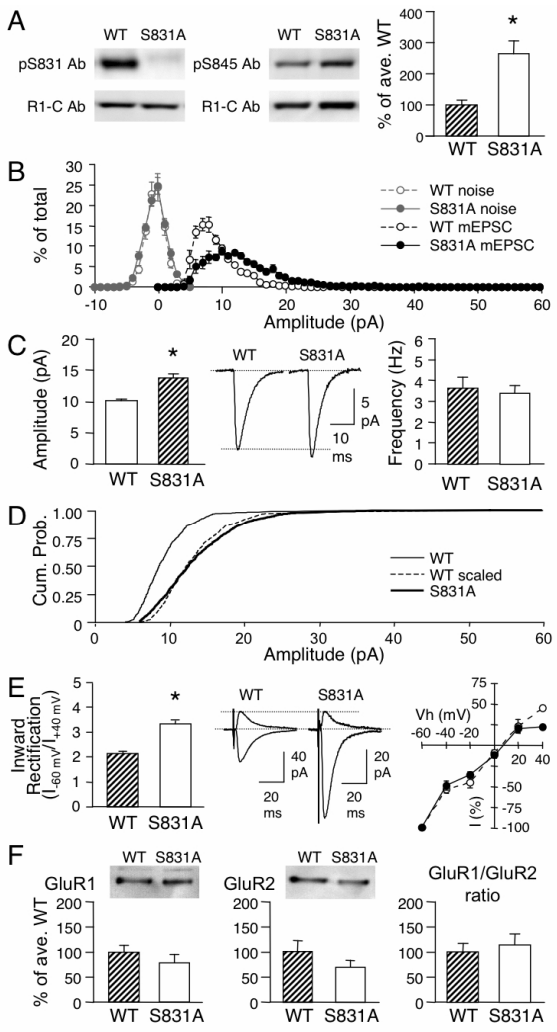

Figure 4.2. Larger basal mEPSC amplitude in GluR1-S 831A mutant mice due to higher basal S845 phosphorylation.

A. Left panel: Immunoblot analysis showing lack of signal on probing visual cortex homogenate obtained from GluR1-S831A mice with phosphospecific antibody to S831 (top lane). Note that there is no change in the total GluR1 level indicated by probing the homogenate with antibody specific to the c terminus of GluR1 (bottom lane). Middle panel: The blot shows an increase in signal when the homogenate obtained from GluR1-S831A mice is probed with phosphospecific antibody to S845A compared to GluR1-S831 WT (top lane). Right panel: Bar graph showing a quantification of the above result where there is a significant increase in S845 phosphorylation in GluR1-S831A mutant mice.

B. Distribution histogram of mEPSC amplitudes recorded from GluR1-S831 WT (open black symbols) and GluR1-S831A mutant mice (closed black symbols) shows a shift in the distribution of mEPSC amplitudes recorded from GluR1-S831A mice towards larger mEPSC amplitudes. The distribution histogram also shows that there was no overlap between signal and noise (GluR1-S831 WT noise: open gray symbols, GluR1-S831A noise: closed gray symbols).

C. Left panel: Average mEPSC amplitude of cells from GluR1-S831A mutant mice was larger compared to GluR1-S831 WT. Middle panel: Average mEPSC traces from GluR1-S831 WT (left trace) and GluR1-S831A (right trace) mice. Right panel: Comparison of average mEPSC frequency from cells from GluR1-S831 WT and GluR1-S831A mutant mice.

D. Cumulative probability of mEPSC amplitudes in visual cortex neurons from GluR1-S831A (thick black solid line) shifts towards the right compared to GluR1-S831 WT (thin black solid line) and. Superimposed on the graph is a cumulative probability of mEPSC amplitudes from GluR1-S831 WT that are multiplied by a factor (1.4) to match the average mEPSC amplitude of GluR1-S831A (WT_{scaled}: black dotted line).

E. Left panel: Significant increase in rectification index in GluR1-S831A mutant mice compared to GluR1-S831 WT. Middle panel: Representative AMPAR-mediated current traces for GluR1-S831 WT and GluR1-S831A mutant mice in visual cortical neurons. Right panel: I-V relationship of neurons from GluR1-S831 WT (white circles) is more liner than GluR1-S831A (black circles).

F. GluR1, GluR2 and GluR1/2 ratio in PSDs of visual cortex from GluR1-S831A mutant mice did not change when compared to GluR1-S831 WT.

Asterisk: P < 0.007 with t-test.

Subsection 3: Visual deprivation leads to an abnormal decrease in mEPSC amplitude in layer 2/3 neurons of GluR1-S831A mutant mice.

Next, we wanted to investigate the effect of visual manipulation in these mice lacking the phosphorylation site at S831. Previous work from our lab has shown that 2 days of dark rearing is necessary and sufficient to maximally scale up mEPSC amplitudes in layer 2/3 visual cortex and light exposure for 1 day reverses this increase (Goel and Lee, 2007). Hence we visually deprived the S831A mutant mice for 2 days from P21-P23 and then re-exposed them to light for 1 day. Unlike the effects of dark rearing in the wild type mice, in the S831A mutant mice dark rearing led to a significant decrease in mEPSC amplitude which did not show any further decrease with light exposure (S831A: NR: 13.8 ± 0.6 pA, n = 11; DR: 11.02 ± 0.7 pA, n = 10; D+L: 9.6 ± 0.6 pA, n = 9; ANOVA: $F(2,27) = 10.993$, $p < 0.0003$; Fig 4.3B, left panel). This was emphasized by the shift in amplitude distribution of S831A DR mice towards smaller values (Fig 4.3A). Again, while there were changes in mEPSC amplitude there were no changes in mEPSC frequency (S831A: NR: 3.6 ± 0.5 Hz, n = 11; DR: 2.9 ± 0.4 Hz, n = 10; D+L: 3.1 ± 0.4 Hz, n = 9; ANOVA: $F(2,27) = 0.801$, $p > 0.5$; Fig 4.3B, right panel), or kinetics (Table 4.l). While 2 days of dark rearing produced a significant decrease in mEPSC amplitude in GluR1-S831A mutants, this decrease was not multiplicative (Kolmogorov-Smirnov test: $p < 0.01$, Fig 4.3C).

To investigate if the decrease in mEPSCs was associated with a change in AMPA receptor subunit composition at the surface we compared the inward rectification index (IR: I_{-60mV}/I_{+40mV}, see methods) of AMPAR synaptic responses evoked by layer 4 stimulation. Dark rearing the S831A mutant mice caused a

significant decrease in inward rectification index (S831A: NR: 3.32 ± 0.12, n = 5; DR = 1.83 ± 0.17, n = 5; t-test, $p < 0.00007$; Fig 4.3E). This suggests that the decrease in mEPSC amplitude is accompanied by a loss of homomeric GluR1 from the synapses. However, the receptors removed are not likely tightly anchored to the PSD, because we did not find significant changes in GluR1 (WT = 100 ± 5%, n = 9; S831A = 96 ± 7%, n = 8; t-test: $p > 0.7$) or GluR2 (WT = 100 ± 11%, n = 9; S831A = 111 ± 23%, n =8; t-test: $p > 0.6$) levels in the PSD by visual deprivation in GluR1-S831A mutants (GluR1/GluR2 ratio: WT = 100 ± 10%, n = 9; S831A = 106 ± 19%, n = 8; t-test: $p >0.8$; Fig. 4.3F). Collectively, these results suggest that misregulation of S845 site in GluR1-S831A mutants may have led to abnormal basal AMPAR-mEPSCs, as well as experience-dependent changes in AMPAR-mEPSCs.

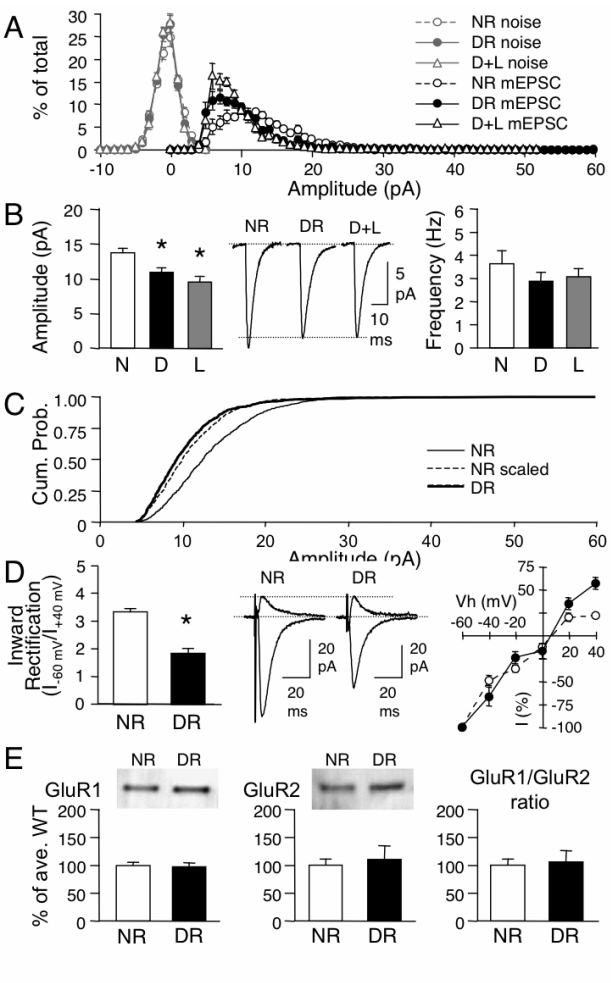

Figure 4.3. Abnormal decrease in mEPSC amplitude in GluR1-S831A mice with dark rearing.

A. GluR1-S831A normal reared (GluR1-S831A NR) mutant mice had significantly smaller mEPSC amplitudes compared to GluR1-S831 dark reared (GluR1-S831A DR) mice indicated by a shift in amplitude distribution histogram in the GluR1-S831A DR mice towards smaller amplitudes. Distribution histogram of mEPSC amplitudes recorded from GluR1-S831A NR (open black circles), GluR1-S831A DR (closed black circles) and GluR1-S831A D+L mutant mice (open black triangles). The distribution histogram also clearly shows that there was no overlap between signal and noise (GluR1-S831A NR noise: open gray circles, GluR1-S831 DR noise: closed gray circles, GluR1-S831A D+L noise: open gray triangles).

B. Left panel: Comparison of average mEPSC amplitude of cells from GluR1-S831A NR, GluR1-S831A DR and GluR1-S831A D+L mutant mice. Middle panel: Average mEPSC traces from GluR1-S831A NR (left trace), GluR1-S831A DR (middle trace) and GluR1-S831A D+L (right trace) mice. Right panel: No change in average mEPSC frequency across GluR1-S831A NR, DR, and D+L groups.

C. Shift in cumulative probability of mEPSC amplitudes towards the left in GluR1-S831A DR Superimposed on the graph is a cumulative probability of mEPSC amplitudes from GluR1-S831 NR that are multiplied by a factor (1.4) to match the average mEPSC amplitude of GluR1-S831A DR (NR_{scaled}: black dotted line).

D. Left panel: Significant increase in rectification index in GluR1-S831A NR compared to GluR1-S831A DR mutant mice. Middle panel: Representative AMPAR-mediated current traces for GluR1-S831A NR and DR mutant mice in visual cortical neurons. Right panel: I-V relationship of neurons from GluR1-S831A NR (white circles) and GluR1-S831A DR (black circles) indicates it is more linear in GluR1-S831A DR mice.

E. GluR1, GluR2 and GluR1/2 ratio in PSDs of visual cortex from GluR1-S831A NR and DR mutant mice remained unchanged.

#: ANOVA, Fisher's PLSD post-hoc: $p < 0.0003$; *: t-test: $p < 0.00007$

Subsection 4: Larger basal mEPSC amplitude in layer2/3 neurons in GluR1-S845A mutant mice.

Our data on GluR1-S831A mutants suggested that phosphorylation of GluR1-S845 may be important for proper regulation of AMPAR-mediated synaptic transmission. Therefore, we characterized the GluR1-S845A mutants, which specifically lack the S845 phosphorylation site. To begin with, we confirmed the mutation of the phosphorylation site by immunoblot analysis using phosphorylation site-specific antibody. Detection of GluR1 by phosphospecific antibody to S845 was completely absent in the GluR1-S845A mutant mice (Fig 4.4A, left panel). There was no significant change in the remaining S831 phosphorylation in GluR1-S845A mutants (S845 WT: 100 ± 5% of S845 WT, n = 14; S845A: 145 ± 31% of S845 WT, n = 12; t-test: $p > 0.16$, Fig 4.4A, right panel).

Next, to investigate whether the mutation at GluR1-S845 alters basal synaptic function, we compared AMPAR-mediated mEPSC recorded from layer 2/3 pyramidal neurons between normal reared age matched GluR1-S845A mice and wild type (WT) mice. Again we restricted our investigation to mice between postnatal ages P21and P23. We found that GluR1-S845A mutant mice show a significant increase in mEPSC amplitude in comparison to the their WT counterparts (S845 WT: 9.22 ± 0.53 pA, n = 11; S845A: 11.4 ± 0.9 pA, n = 10; t-test $p < 0.03$; Fig.4. 4C, left panel), without affecting mEPSC frequency (S845 WT: 2.6 ± 0.2 Hz, n = 11; S845A: 2.4 ± 0.3 Hz, n = 10; t-test $p > 0.6$; Fig. 4.4C, right panel) or kinetics. The mEPSC amplitude distribution shifted to the right in the GluR1-S845A mutants towards larger

amplitudes (Fig 4.4B), which was close to being multiplicative (Kolmogrov-Smirnov test: P = 0.049; Fig 4.4D). The increase in mEPSC amplitude without a change in frequency suggests that the locus of change in basal synaptic strength is most probably postsynaptic.

To determine whether the increase in mEPSC amplitude in GluR1-S845A mutants is accompanied by a change in subunit composition of synaptic AMPARs, we compared inward rectification index of evoked AMPAR-EPSCs between wild-type and GluR1-S845A mutants. We found a significant increase in average inward rectification index in the GluR1-S845A mutant mice (S845 WT: 2.07 ± 0.14, n = 5; S845A: 3.41 ± 0.44, n = 8; ttest, $p < 0.01$; Fig 4.4E), which was dependent on the presence of intracellular spermine (Fig. 4.6B). However, the change in subunit composition of synaptic AMPA receptors was not accompanied by alterations in GluR1 (WT = 100 ± 15%, n = 7; S845A = 127 ± 27%, n = 8; t-test: $p > 0.4$) or GluR2 (WT = 100 ± 15%, n =7; S845A = 104 ± 14%, n = 8; t-test: $p > 0.8$) amount at the PSDs (GluR1/GluR2 ratio: WT = 100 ± 5%, n = 7; S845A = 124 ± 20%, n = 8; t-test: $p > 0.2$; Fig. 4.4F), suggesting that the homomeric GluR1 in GluR1-S845A mutants are probably only weakly associated to the PSD.

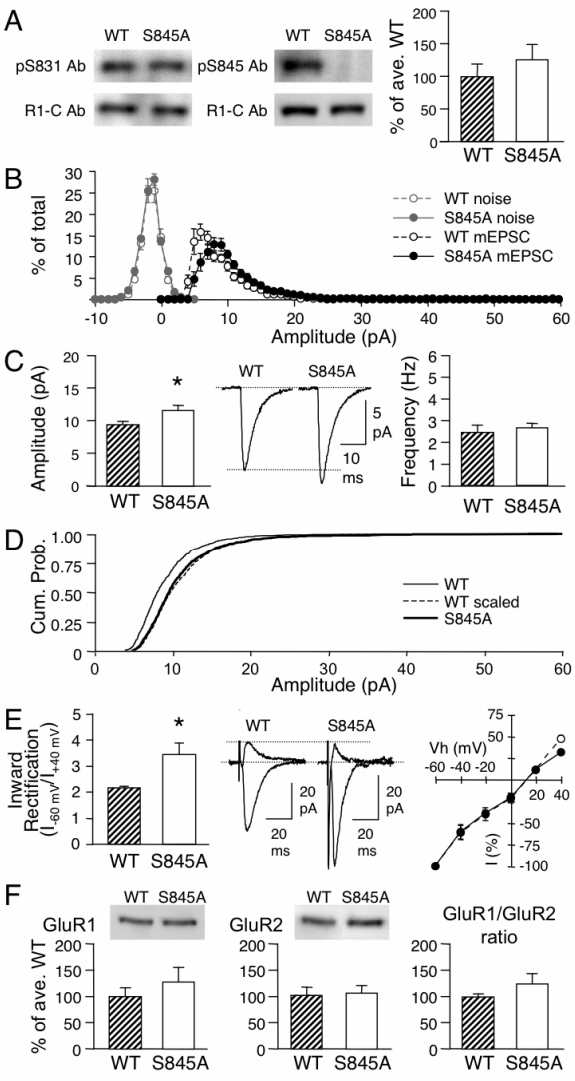

Figure 4. 4. Larger basal mEPSC amplitude in GluR1-S845A mutant mice.

A. Left panel: Immunoblot analysis showing lack of signal on probing visual cortex homogenate obtained from GluR1-S845A mice with phosphospecific antibody to S845 (top lane). Also there is no change in the total GluR1 level indicated by probing the homogenate with antibody specific to the c terminus of GluR1 (bottom lane). Right panel: Bar graph showing a quantification of the above result where there is a trend towards an increase in S831 phosphorylation in GluR1-S845A mutant mice.

B. GluR1-S845A mutant mice had larger mEPSC amplitudes compared to GluR1-S845 WT mice indicated by a shift in amplitude distribution histogram in the GluR1-S845A mice towards larger amplitudes. Distribution histogram of mEPSC amplitudes recorded from GluR1-S845 WT (open black symbols) and GluR1-S845A mutant mice (closed black symbols). The distribution histogram shows that there was no overlap between signal and noise, and that there is no difference in noise levels between the two groups (GluR1-S845 WT noise: open gray symbols, GluR1-S845A noise: closed gray symbols).

C. Left panel: Average mEPSC amplitude of cells from GluR1-S845A mutant mice was larger compared to GluR1-S845 WT. Middle panel: Average mEPSC traces from GluR1-S845 WT (left trace) and GluR1-S845A (right trace) mice. Right panel: Comparison of average mEPSC frequency from cells from GluR1-S845 WT and GluR1-S845A mutant mice.

D. Cumulative probability of mEPSC amplitudes in visual cortex neurons from GluR1-S845 WT (thin black solid line) and GluR1-S845A (thick black solid line). Superimposed on the graph is a cumulative probability of mEPSC amplitudes from GluR1-S845 WT that are multiplied by a factor (1.2) to match the average mEPSC amplitude of GluR1-S845A (WT_{scaled}: black dotted line). The cumulative probability distribution of GluR1-S845A and WT_{scaled} were almost the same (Kolmogorov-Smirnov test: $p = 0.049$) suggesting that most of the changes are likely multiplicative.

E. Left panel: Significant increase in rectification index in GluR1-S845A mutant mice compared to GluR1-S845 WT. Middle panel: Representative AMPAR-mediated current traces for GluR1-S845 WT and GluR1-S845A mutant mice in visual cortical neurons. Right panel: I-V relationship of neurons from GluR1-S845 WT (white circles) is more linear compared to GluR1-S845A (black circles).

F. GluR1, GluR2 and GluR1/2 ratio in PSDs of visual cortex from GluR1-S845A mutant mice did not change when compared to GluR1-S845 WT.

Asterisk: $P < 0.03$ with t-test.

Subsection 5: Visual experience induced scaling is abolished in GluR1-S845A mutant mice.

In order to investigate the effects of visual deprivation and subsequent light exposure in the GluR1-S845A mutant mice we dark reared the mice for 2 days starting at P21 and re-exposed them to light for 1 day. Unlike the effects of dark rearing in the wild type mice, in these mutant mice there was no significant change in mEPSC amplitude with dark rearing or with a subsequent light exposure (S845A: NR: 11.4 ± 0.9 pA, n = 10; DR: 11.7 ± 0.6 pA, n = 11; D+L: 11.7 ± 0.7 pA, n = 12; ANOVA: $F(2,30) = 0.137$, $p > 0.8$; Fig 4.5B, left panel). In addition, visual manipulation did not significantly alter the mEPSC frequency across the 3 groups (S845A: NR: 2.4 ± 0.3 Hz, n = 10; DR: 2.7 ± 0.4 Hz, n = 11; D+L: 3.7 ± 0.4 Hz, n = 12; ANOVA: $F(2,30) = 3.067$, $p > 0.06$; Fig 4.5B, right panel). A lack of change in average mEPSC amplitude in GluR1-S845A mutants with visual manipulations was also evident from no significant alteration in the amplitude distribution histogram across the 3 groups (Fig 4.5A).

Furthermore, 2 days of dark rearing did not modify the AMPA receptor subunit composition at the synaptic surface, as there was no significant change in the inward rectification index (S845A: NR: 3.41 ± 0.44, n = 8; S845A: DR: 2.69 ± 0.41, n = 6; ttest , $p > 0.3$; Fig 4.5C) or the level of GluR1 (WT = 100 ± 16%, n = 7; S845A = 73 ± 13%, n = 8; t-test: $p > 0.2$) or GluR2 (WT = 100 ± 11%, n = 7; S845A = 79 ± 11%, n = 8; t-test: $p > 0.1$) at PSDs (GluR1/GluR2 ratio: WT = 100 ± 22%, n = 7; S845A = 107 ± 29%, n = 8; t-test: $p > 0.8$; Fig. 4.5D) between normal-reared and dark-reared GluR1-S845A mutants.

These results suggest that a lack of S845 phosphorylation site on the GluR1 subunit prevents visual experience-induced homeostatic changes.

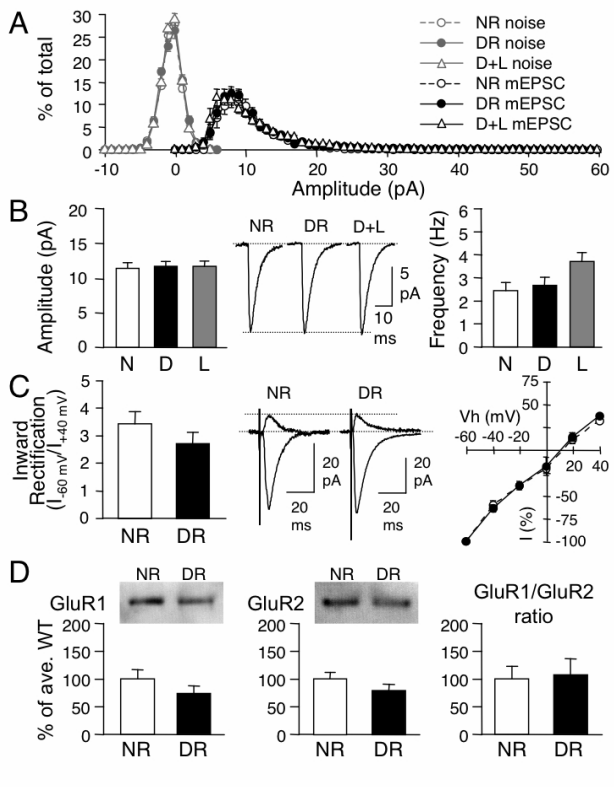

Figure 4.5. Dark rearing induced increase in mEPSC amplitude from GluR1-S845A mutants abolished.

A. No difference in mEPSC amplitude between GluR1-S845A normal reared (GluR1-S845A NR), GluR1-S845A dark reared (GluR1-S831A DR) and GluR1-S845A light exposed (GluR1-S845A D+L) mice indicated by similar and overlapping amplitude distributions across the 3 groups. Distribution histogram of mEPSC amplitudes recorded from GluR1-S845A NR (open black circles), GluR1-S845A DR (closed black circles) and GluR1-S845A D+L mutant mice (open black triangles). The distribution histogram also clearly shows that there was no overlap between signal and noise (GluR1-S845A NR noise: open gray circles, GluR1-S845 DR noise: closed gray circles, GluR1-S845A D+L noise: open gray triangles).

B. Left panel: No change in average mEPSC amplitude of cells from GluR1-S845A NR, GluR1-S845A DR and GluR1-S845A D+L mutant mice. Middle panel: Average mEPSC traces from GluR1-S845A NR (left trace), GluR1-S845A DR (middle trace) and GluR1-S845A D+L (right trace) mice. Right panel: No change in average mEPSC frequency across GluR1-S845 NR, DR, and D+L groups.

C. Left panel: No change in rectification index in GluR1-S845A NR compared to GluR1-S845A DR mutant mice. Middle panel: Representative AMPAR-mediated current traces for GluR1-S845A NR and DR mutant mice in visual cortical neurons. Right panel: No difference in I-V relationship between of neurons from GluR1-S845A NR (white circles) and GluR1-S845A DR (black circles).

D. GluR1, GluR2 and GluR1/2 ratio in PSDs of visual cortex from GluR1-S845A DR mutant mice did not change when compared to GluR1-S845A NR.

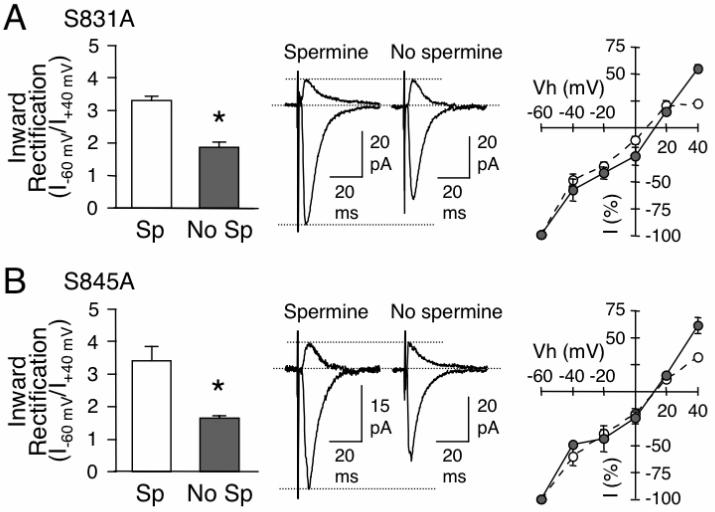

Figure 4.6. Inward rectification is dependent on intracellular spermine.

A. Leftpanel: Inward rectification (IR: I_{-60mV}/I_{+40mV}) of AMPA receptor currents observed in GluR1-S831A NR mutants was abolished when using intracellular solution without spermine (Spermine (Sp): IR = 3.3 ± 0.1, n = 5 cells; No spermine (No Sp): IR = 1.8 ± 0.1, n = 3 cells).
Middle panel: Representative traces of evoked AMPA receptor-mediated currents measured at -60 mV and +40 mV from GluR1-S831A NR mutants recorded with or without spermine inside the recording pipette. Right panel: Comparison of I-V relationship between GluR1-S831A NR mutants recorded with (white circles) and without spermine (black circles).

B. Left panel: Inward rectification (IR: I_{-60mV}/I_{+40mV}) of AMPA receptor currents observed in GluR1-S845A NR mutants was abolished when using intracellular solution without spermine (Spermine (Sp): IR = 3.3 ± 0.1, n = 5 cells; No spermine (No Sp): IR = 1.8 ± 0.1, n = 3 cells).
Middle panel:
Representative traces of evoked AMPA receptor-mediated currents measured at -60 mV and +40 mV from GluR1-S845A NR mutants recorded with or without spermine inside the recording pipette. Right panel: Comparison of I-V relationship between GluR1-S845A NR recorded with (white circles) and without spermine (black circles).

Table 4.1. Neuronal properties.

	Conditions	Rise time 10-90% (ms)	Decay time constant (τ) (ms)	R_{in} (MΩ)	R_{ser} (MΩ)
WT	NR	1.5 ± 0.1	4.7 ± 0.2	413 ± 48	19.1 ± 0.4
	DR	1.5 ± 0.03	3.5 ± 0.2*	336 ± 24	18.4 ± 0.7
S831 WT	NR	1.7 ± 0.1	4.8 ± 0.1	323 ± 14	18.9 ± 0.7
S831A	NR	1.5± 0.1	4.0 ± 0.2*	383 ± 47	19.1 ± 0.8
	DR	1.5 ± 0.1	4.8 ± 0.4	368 ± 32	21.1 ± 0.8
	D+L	1.6 ± 0.1	4.3 ± 0.2	418 ±62	19 ± 1.1
S845 WT	NR	1.6 ± 0.1	4.5 ± 0.3	486 ± 81	19.1 ± 0.5
S845 A	NR	1.7± 0.1	4.7 ± 0.3	303 ± 25	20 ± 0.8
	DR	1.5 ± 0.1	4.1 ± 0.2	449 ± 81	18.1 ± 1.1
	D+L	1.5 ± 0.4	4.5 ± 0.3	383 ± 33	19.1 ± 0.7

* denotes statistically significant difference from NR condition at $P < 0.001$ with t-test .

Section4: Discussion

Our results demonstrate that experience-induced homeostatic plasticity in the superficial layers of mouse visual cortex requires phosphorylation of GluR1 specifically at S845. Mice lacking phosphorylation at S831 on the GluR1 subunit showed a compensatory increase in phosphorylation of S845 basally, which was associated with appearance of GluR2-lacking AMPA receptors at synapses. We believe these are homomeric GluR1 AMPA receptors, because GluR1-S831A mutants have faster mEPSC decay kinetics, which is a characteristic of GluR1 homomers (Mosbacher et al., 1994). In addition, GluR1-S831A mutation led to an

abnormal decrease in mEPSC amplitude in response to dark rearing, which was accompanied by a removal of GluR2-lacking AMPA receptors. On the other hand, mice lacking phosphorylation at S845 did not show significant changes in the phosphorylation of the remaining S831, nevertheless they exhibited a significantly larger mEPSC amplitude and inward rectification index. Importantly, the GluR1-S845A mice failed to show changes in mEPSC amplitude in response to visual manipulations. Collectively, these results provide support to the idea that phosphorylation at S845 on GluR1 is a critical determinant of AMPAR trafficking to the synapse by prolonged manipulation of visual experience.

Both GluR1-S831A and GluR1-S845A mutants showed an increase in basal mEPSC amplitude. In the GluR1-S831A mutants we attribute this elevation to an aberrant up-regulation of phosphorylation at the remaining S845. It has been shown previously that phosphorylation at S845 is involved in trafficking of GluR1 containing AMPARs to the surface (Oh et al., 2006), and ultimately to synapses (Esteban et al., 2003). S845 phosphorylation also increases the mean open probability of the channel (Banke et al., 2000). Therefore, both of these consequences of S845 phosphorylation may account for the observed increase in mEPSC amplitude as well as inward rectification in GluR1-S831A mice. As for the GluR1-S845A mice, the increase in mEPSC amplitude might be associated with the following two possibilities. First, the increase in S831 phosphorylation, though not statistically significant, may have been sufficient to increase mEPSC amplitude since S831 phosphorylation is known to increase single channel conductance of homomeric GluR1 AMPARs (Derkach et al., 1999; Oh and Derkach, 2005). This would also

explain the increase in inward rectification index in the GluR1-S845A mice. Second, a more likely scenario is that the alanine substitution of S845 may prevent these receptors from being tethered intracellularly. There is precedence that mutation of an equivalent phosphorylation site on the GluR4 subunit allows synaptic incorporation of these receptors, which was attributed to untethering of mutated GluR4 from a putative intracellular binding partner (Esteban et al., 2003). Therefore in light of this it is possible that by mutating S845 to an alanine, the GluR1 may be released to the plasma membrane and subsequently diffuse into synapses to participate in synaptic transmission.

Interestingly, the increase in mEPSC amplitude and inward rectification observed basally in GluR1-S831A and GluR1-S845A was not accompanied by changes in GluR1 content at the PSD. This suggests that the homomeric GluR1 receptors, either phosphorylated on S845 (as in the case of GluR1-S831A) or lacking S845 (as in the case of GluR1-S845A), are not stably associated with the PSD, but are present at sites so as to participate in synaptic transmission. A recent single GluR1 tracking study reported that GluR1-containing AMPA receptors can freely diffuse in and out of synapses even within the PSD area (Ehlers et al., 2007). This may represent the unanchored homomeric GluR1 population, which are presumably phosphorylated on the S845. While the GluR1 homomeric receptors lacking S831 or S845 phosphorylation site were able to get into synapses and influence synaptic transmission, our data suggest that S845 phosphorylation alone is not sufficient to allow multiplicative scaling as observed following dark-rearing. A recent view on AMPAR trafficking emphasizes the existence of “slots” or “placeholders” (Shi et al.,

2001; McCormack et al., 2006), which stabilize AMPAR at synapses. Our data is consistent with an interpretation that multiplicative scaling requires a two step process: (1) phosphorylation of GluR1 at S845, which releases homomeric GluR1 from putative intracellular binding partner(s), and (2) generation of "slots" that allow stable incorporation of these homomeric GluR1 at the PSD in a multiplicative manner (Fig 4.7. Model). Under conditions where S845 phosphorylation is increased without the generation of "slots", as we think is the case for the GluR1-S831A mutants, homomeric GluR1 may diffuse into synapses but are not anchored to the PSD, and hence the increase in synaptic transmission does not occur multiplicatively. In the case of the GluR1-S845A mutants, the alanine mutation itself may release the homomeric GluR1 to the plasma membrane, and allow diffusion into synapses. However, presumably new "slots" are not generated, hence the receptors are not associated to the PSD, and the increase in mEPSC does not quite follow the multiplicative scaling rule.

An interesting observation is that GluR1-S831A mutants paradoxically scaled down their mEPSCs when dark-reared, which is contrary to wildtypes which scale up their synapses. This abnormal scaling was associated with a reduction in inward rectification indicative of losing GluR2-lacking receptors from synapses. However, there was no change in either GluR1 or GluR2 content at the PSD. This suggests that the reduction is probably due to the removal of homomeric GluR1 that were diffusing in and out of synapses, but not anchored to the PSD. We are currently testing whether this is due to dephosphorylation of the GluR1-S845, which would allow endocytosis of these receptors (Lee et al., 2003).

Initially studies on Long Term Potentiation (LTP) and Long Term Depression (LTD) outlined a role for S845 phosphorylation in Hebbian synaptic plasticity. It was shown that dephosphorylation of GluR1 at this site is associated with LTD (Kameyama et al., 1998; Lee et al., 1998; Lee et al., 2000), while subsequent studies highlighted the importance of phosphorylation at S845 for LTP (Esteban et al., 2003; Lee et al., 2003). These reports emphasize that the reversible regulation of phosphorylation at S845 which is an important player in bidirectional Hebbian synaptic plasticity. Our results demonstrate the same mechanisms are recruited for homeostatic regulation of synaptic AMPA receptors by visual deprivation. In particular our results show that scaling up of mEPSCs in response to visual deprivation is mediated by an increase in S845 phosphorylation. This implies that despite differences in the trigger both synapse-specific plasticity, like LTP, and homeostatic synaptic scaling are mediated by a common downstream molecular event, namely regulation of GluR1 phosphorylation at S845 and synaptic trafficking of GluR1. It is of interest that GluR1-S845 is a downstream target of various neuromodulatory systems coupled to the PKA signaling pathway. Activation of Gs-coupled receptors such as β-1 adrenergic receptor and D1/D5 receptors readily increases phosphorylation of GluR1 at S845 (Price et al., 1999; Snyder et al., 2000; Chao et al., 2002; Vanhoose and Winder, 2003). In addition, there is evidence that S845 phosphorylation by β adrenergic receptor agonists "primes" AMPA receptors for LTP (Watabe et al., 2000; Seol et al., 2007). Whether dark-rearing induced increase in S845 phosphorylation and synaptic GluR1 will aid in a subsequent LTP expression remains to be examined. However, these molecular events may provide an

alternative explanation for previous studies showing larger LTP in layer 2/3 primary visual cortex following dark-rearing (Kirkwood et al., 1995; Kirkwood et al., 1996).

In conclusion, our results suggest that dark rearing induced synaptic scaling may be a two step process, involving phosphorylation of S845 at GluR1, and modification of the PSD to anchor homomeric GluR1 AMPA receptors in a multiplicative manner. In addition this study demonstrates that regulation of a post-translational mechanism is a common intracellular event that is critical both in experience-induced Hebbian and homeostatic synaptic plasticity.

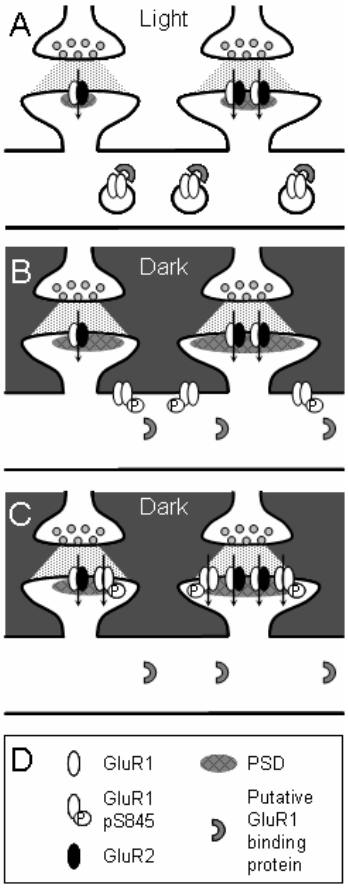

Figure 4.7. Model of 2 step process involved in Synaptic scaling.

A. Synapses with GluR1 and GluR2 containing AMPARs in the PSD in the normal reared condition.

B. After dark rearing Step1 involves an increase in GluR2 lacking AMPARs in the synaptic surface.

C. Step 2 involves a multiplicative increase in AMPARs due to anchoring by a putative GluR1 binding protein.

D. Legend showing what each symbol in the model represents

Chapter 5: Role of AMPAR GluR2 subunit C- terminal in experience-dependent homeostatic plasticity

This manuscript is in preparation.
Putative authors: Anubhuthi Goel, Kevin Snyder, Lihua Song and Hey-Kyoung Lee
My contribution: All the electrophysiological recordings and analyses (Measurement of AMPAR mediated mEPSCs and rectification).

Section1: Introduction.

AMPA receptors are tetrameric channels composed of combinations of glutamate receptor (GluR) subunits 1-4 (Dingledine et al., 1999). In the adult forebrain, AMPA receptor population consists of primarily GluR1/GluR2 and GluR2/GluR3 heteromers with the predominant population being that of GluR1/GluR2 heteromers (Wenthold et al., 1996). Each subunit has a N-terminal domain that binds to glutamate and 4 transmembrane domains (Mayer and Armstrong, 2004). Among the transmembrane domains the second one (M2) forms the pore of the receptor channel and specifies ion selectivity. The majority of the GluR2 subunit undergoes RNA editing within the M2 region wherein, a critical glutamine 607 residue (Q607) is converted to Arginine (R607). This RNA editing, called "Q/R editing", confers distinct physiological properties to AMPA receptors containing the GluR2 subunit, namely impermeability to calcium and resistance to polyamine block (Verdoorn et al., 1991; Washburn et al., 1997). The lack of block by endogenous intracellular polyamine imparts an electrophysiological signature of GluR2-containing AMPA receptors, which display linear I/V curves (Rozov et al., 1998). On the other hand, GluR2-lacking AMPA receptors are blocked by polyamines at positive potentials, and hence display inward

rectifying currents. In addition, GluR2-lacking receptors have a higher single channel conductance (Swanson et al., 1997).

The subunit composition of AMPA receptors also determines the kinetic properties of the AMPA receptor mediated current, wherein GluR1 homomeric AMPA receptors have smaller decay time constant (τ) than heteromeric AMPA receptors (Mosbacher et al., 1994). In cells where GluR2 is one of the predominantly expressed subunit, the preferred and most stable stoichiometry of AMPA receptors are complexes containing 2 GluR1 and 2 GluR2 subunits (Mansour et al., 2001; Brorson et al., 2004). Even though most AMPA receptors exist as heteromers rather than homomers, certain types of neural activity can allow GluR2-lacking AMPARs to express at synapses (Ju et al., 2004; Thiagarajan et al., 2005; Clem and Barth, 2006; Plant et al., 2006; Goel and Lee, 2007).

Each AMPAR subunit also contains a cytoplasmic tail (C-terminal tail), which is distinct, and some subunits have PDZ binding domains which enables these subunits to interact with PDZ domain containing proteins. Depending on the c-tail, different AMPARs are trafficked to synapses via distinct mechanisms. For example, AMPAR subunits with a short c-tail, such as GluR2 and GluR3, can be incorporated to synapses constitutively, while ones with a long c-tail, like GluR1 and GluR4, require synaptic activity (Shi et al., 2001).

GluR2 subunit has 2 important sites on the C terminal tail that mediate direct interactions with several proteins with important functional consequences. One site, which is proximal to the fourth transmembrane domain (M4), binds N-ethylmaleimide-sensitive factor (NSF) and Adaptor protein-2 (AP2). In hippocampal

neurons NSF-GluR2 interaction is essential for regulating the surface expression of AMPA receptors (Nishimune et al., 1998; Luthi et al., 1999; Noel et al., 1999). In particular studies using peptides that out-compete biding of NSF to GluR2 reported a rapid decrease in AMPAR-mediated EPSC amplitude (Nishimune et al., 1998) and an almost complete loss of AMPA receptor expression on the plasma membrane (Noel et al., 1999) surface and synaptic AMPA receptor expression. In addition, further investigations showed that LTD involves the removal of GluR2 containing AMPARs that interact with NSF (Luthi et al., 1999). However, the latter effect may be due to disrupting binding of AP2, which binds to GluR2 at the NSF binding site. AP2 is involved in clathrin dependent endocytosis (Sorkin, 2004), hence may aid clathrin-mediated endocytosis required for AMPAR internalization during LTD (Carroll et al., 1999; Carroll et al., 2001).

The GluR2 subunit also has a PDZ ligand region, which interacts with PDZ domain containing proteins such as Glutamate receptor interacting protein (GRIP) (Dong et al., 1997), AMPAR binding protein (ABP or also known as GRIP2) (Srivastava et al., 1998) and protein interacting with C-kinase- 1 (PICK1) (Dev et al., 1999; Xia et al., 1999). Interestingly, within the PDZ ligand region is a serine residue, S880, which is phosphorylated by PKC (Chung et al., 2000). Phosphorylation of S880 allows GluR2 to preferentially interact with PICK1, and not GRIP (Matsuda et al., 1999; Chung et al., 2000; Matsuda et al., 2000). There is some discrepancy in attributing a role to GluR2/3 interaction with GRIP/ABP and PICK1, since some studies show that GluR2/3 interaction with GRIP/ABP is important for expression of hippocampal LTD (Li et al., 1999; Daw et al., 2000), while others show that it is the PICK1-GluR2

interaction that is critical (Kim et al., 2001; Seidenman et al., 2003). Despite of these differences, it is clear that GluR2 associates with several proteins and these interactions play a role in regulating endocytosis of AMPA receptor.

Since there is little evidence suggesting a role of GluR2 regulation in homeostatic plasticity, I wanted to examine whether GluR2 interaction with PDZ domain proteins may play a role. In order to test this, I used transgenic mice generated in Dr. Richard Huganir's laboratory at the John Hopkins School of Medicine, which lack the last 7 amino acids on the C terminal region of GluR2 and therefore preventing phosphorylation of S880 as well as binding to GRIP/ABP and PICK1 (GluR2 Δ 7 mice) (Gardner et al., 2005).

Section 2: Materials and methods

Subsection 1: Dark rearing animals

Wild-type (GluR2-Δ7 WT) and transgenic mice (GluR2-Δ7) mice were raised under normal lighted environment (12 hr light/12 hr dark cycle). Dark rearing (DR) was initiated at postnatal ages 21 days (P21) for a duration of 2 days, while control (normal-reared) animals were continuously raised in the normal lighted condition for the same duration. The animals in the dark were cared for using infrared vision goggles under dim infrared light. After 2 days of dark-rearing, some of the mice were taken out to the lighted environment for 1 day to study the effect of re-exposure to light.

Subsection 2: Whole cell recording of AMPA receptor mediated EPSCs

The cortical slices were moved to a submersion recording chamber mounted on a stage of an upright microscope (E600 FN, Nikon) equipped with infrared differential interference contrast (IR-DIC). Layer 2/3 pyramidal cells were visually identified and patched using a whole-cell patch pipette (tip resistance: 3-5 MΩ) filled with intracellular solution (130 mM Cs-gluconate, 8 mM KCl, 1 mM EGTA, 10 mM HEPES, 4 mM ATP and 5 mM QX-314; pH 7.4; 285-295 mOsm).

To isolate AMPA receptor-mediated mEPSCs, 1 μM TTX, 20 μM bicuculline, and 100 μM D,L-APV were added to the ACSF (2 ml/min, 30 ± 1˚C), which was continually bubbled with 95% O_2/5% CO_2. mEPSCs were recorded at a holding potential (Vh) of –80 mV using Axopatch-clamp amplifier (Axon Instruments), digitized at 2 kHz by a data acquisition board (National Instruments), and acquired using the Igor Pro™ software (Wave Metrics). Acquired mEPSCs were analyzed using the Mini Analysis Program (Synaptosoft). The threshold for detecting mEPSCs was set at 3 times the Root Mean Square (RMS) noise. There was no significant difference in RMS noise between the experimental groups. There was no significant difference in RMS noise between the experimental groups (GluR2Δ7 WT NR =1.6 ± 0.1; n =10; GluR2Δ7 WT DR =1.8 ± 0.04, n = 6; ttest, p > 0.1: GluR2Δ7 WT NR = 1.6 ± 0.07, n = 10; GluR2Δ7 NR = 1.7 ± 0.05, n = 9; t-test, p > 0.5: GluR2Δ7 NR = 1.7 ± 0.05, n = 9; GluR2Δ7 DR = 1.7 ± 0.05, n = 14, GluR2Δ7 D+L= 1.6 ± 0.07, n = 10; ANOVA, F(2,30) = 1.204, p > 0.2). A possibility of dendritic filtering was assessed by plotting mEPSC amplitude against mEPSC rise time. Cells showing a negative correlation between mEPSC amplitude and rise time (i.e. dendritic filtering

present) were excluded from analysis, as well as mEPSCs with greater than 3 msec rise time (measured between 10-90% of amplitude). Average mEPSC amplitude and frequency were calculated and compared across different experimental groups using one-factor ANOVA or unpaired Student's t-test. Only the cells and recording conditions that meet the following criteria were studied: Vm $\leq$ –65 mV, input R $\geq$ 200 MΩ, series R $\leq$ 25 MΩ. Cells were discarded if input R or series R changed more than 15%. Junction potentials were typically less than 5 mV, and were left uncompensated.

Evoked AMPA receptor-mediated synaptic currents (EPSCs) were measured from layer 2/3 pyramidal cells of either visual or somatosensory cortices in response to stimulation through an electrode (concentric bipolar, FHC) placed in layer 4. To isolate the AMPA receptor component, 100 μM D, L-APV and 100 μM bicuculline were added to the bath solution. The concentration of $CaCl_2$ and $MgCl_2$ in the ACSF were changed to 4 mM and 2 mM, respectively, to prevent polysynaptic responses upon stimulation in the presence of bicuculline. Intracellular recording solution containing 200 μM spermine (in 90 mM $CsMeSO_3H$, 5 mM $MgCl_2$, 8 mM NaCl, 10 mM EGTA, 20 mM HEPES, 1 mM QX-314, 0.5 mM Na_3GTP, and 2 mM Mg•ATP, pH 7.2, 250-270 mOsm) was used. For generating I-V curves for rectification measurements, cells were held at –60, –40, –20, 0, +20 and +40 mV. Inward Rectification (IR) was calculated by dividing the absolute amplitude of average EPSC measured at –60 mV by that at +40 mV. There were no significant differences in calculated reversal potentials between groups. Reversal potentials were calculated using equations generated by fitting a linear regression curve to the current values

collected at negative holding potentials. Only the cells and recording conditions that meet the following criteria were studied: Vm ≤ –65 mV, input R ≥ 100 MΩ, series R ≤ 20 MΩ. Cells were discarded if input R or series R changed more than 15%. Junction potentials were typically less than 5 mV, and were left uncompensated.

Section 3: Results

Subsection 1: Dark rearing leads to an increase in mEPSC amplitude in wild-type mice.

Previous work from this lab has shown that dark rearing wild type mice for 2 days is necessary and sufficient to maximally scale up the mEPSC amplitudes of pyramidal neurons in layer 2/3 of visual cortex ((Goel and Lee, 2007), reported in chapter 3). Since 2 days of dark rearing at P21 produced significant and robust homeostatic changes we restricted our experiments in this study within that age group. In order to ensure that the wild type mice with the same genetic background as the mutant mice showed visual deprivation induced synaptic scaling we dark reared P21 GluR2 WT mice for 2 days. Consistent with our pervious work ((Goel and Lee, 2007), shown in chapter 3) visual deprivation for 2 days significantly increased the mEPSC amplitude (GluR2 WT: NR: GluR2-WT : 9.8 ± 0.5 pA, n = 10 ; DR: 14.4 ± 1.4 pA, n = 6; t-test $p < 0.04$, Fig 5.2a, left panel) with no change in frequency (GluR2 WT: NR: 4.3 ± 0.8 Hz, n = 10; DR: 3.8 ± 0.4 Hz, n = 6; t-test $p > 0.7$, Fig 5.2a, right panel) or kinetics (Fig 5.2a , middle panel).

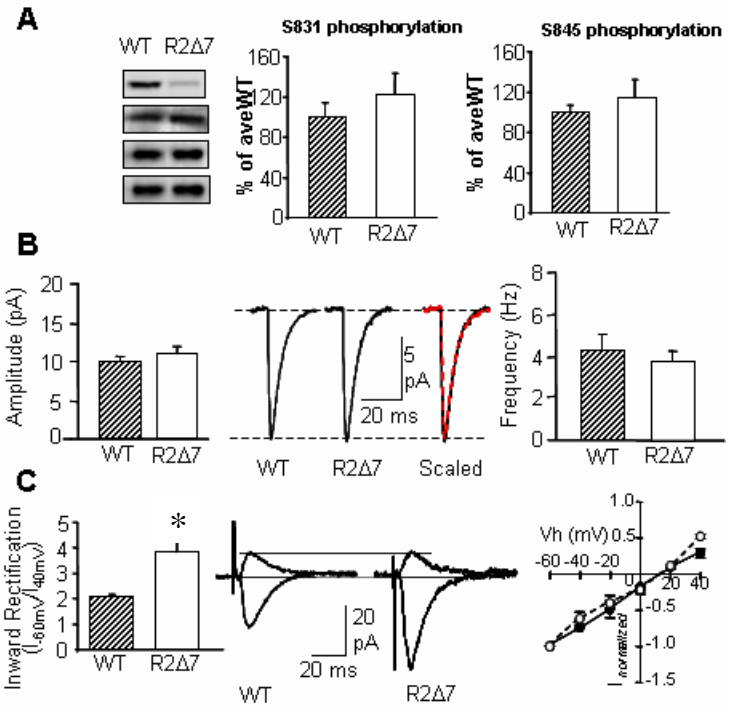

Figure 5.1. No change in mEPSC amplitude in the GluR2-Δ7.

Detection of GluR2/3 by an antibody specific to C terminus of GluR2/3 was absent in GluR2-Δ7 mice.

A. Left panel: Immunoblot analysis showing a greater reduction of signal when probing visual cortex homogenate obtained from GluR2-Δ7 mice with antibody recognizing c termini of GluR2 and GluR3 (topmost lane). The residual signal is likely the GluR3 subunit. Note that there is no change in the phosphorylation of GluR1 using phosphospecific antibody to S831 and S845 (second and third lane). Also total GluR1 level indicated by probing the homogenate with antibody specific to the c terminus of GluR1 (bottom lane) was unchanged. Middle panel: Bar graph showing a quantification of the above result where there is no change in S831 phosphorylation in GluR2-Δ7 mutant mice. Right panel: Bar graph showing a quantification of the above result where there is no change in S845 phosphorylation in GluR2-Δ7 mutant mice.

B. No change in mEPSC amplitude between GluR2-Δ7 mutant mice and wild-type (WT) mice. Left panel: No difference between average mEPSC amplitude of cells from GluR2-Δ7 mutant mice and WT. Middle panel: Average mEPSC traces from GluR1-S831 WT (left trace) and GluR1-S831A (right trace) mice. "Scaled" indicates the WT mEPSC average trace scaled (red trace) to match in amplitude to that of GluR2-Δ7 and superimposed on the GluR2-Δ7 average trace (black trace). Note that there was no difference in mEPSC kinetics. Right panel: Comparison of average mEPSC frequency from cells from WT and GluR2-Δ7 mutant mice.

C. Larger inward rectification of current through synaptic AMPARs in GluR2-Δ7 mutant mice. Left panel: Significant increase in inward rectification index (I_{-60mV}/I_{+40mV}) in GluR2-Δ7 mutant mice compared to WT. Middle panel: Representative AMPAR-mediated current traces for WT and GluR2-Δ7 mutant mice in visual cortical neurons. Right panel: Comparison of I-V relationship between neurons from WT (white circles) and GluR2-Δ7 (black circles). Note that the I/V relationship is more linear in WT mice.

Asterisk: $P < 0.03$ with t-test.

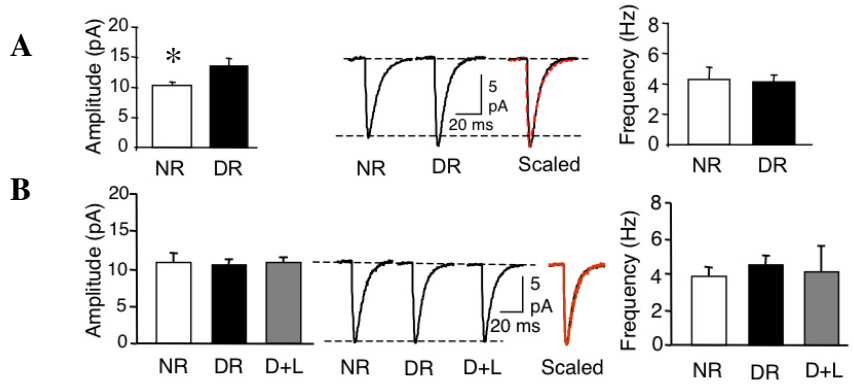

Figure 5. 2. Visual deprivation dependent increase in mEPSC amplitude is abolished in GluR2-Δ7 mutant mice

A. Wild-type (WT) mice dark reared (DR) for 2 days from P21-23 had larger mEPSC amplitudes compared to normal reared (NR) mice.
Left panel**:** Average mEPSC amplitude of cells from WT DR mice was larger than the NR counterparts. Middle panel: Average mEPSC traces from WT NR (left trace) and WT DR (right trace) mice. "Scaled" indicates the NR mEPSC average trace scaled (red trace) and superimposed on the 2 days DR average trace (black trace). Right panel: Comparison of average mEPSC frequency from cells from WT NR and DR mice.

B. Lack of change in mEPSC amplitude with visual experience in GluR2-Δ7 mutants.
Left panel: No difference in average mEPSC amplitude between normal reared (NR), dark reared (DR) and dark reared followed by light exposed (D+L) GluR2-Δ7 mutants mice .
Middle panel: Average mEPSC traces from NR (left trace), DR (middle trace) mice and D+L (right trace). "Scaled" indicates the average mEPSC traces of NR (red solid line trace) and D+L (red dotted line trace) scaled and superimposed on the DR average trace (black trace). Note no difference in mEPSC kinetics across the three groups.

Asterisk: $P < 0.04$ with t-test.

Subsection 2: No change in basal mEPSC amplitude in layer 2/3 visual cortical neurons in GluR2-Δ7 mutant mice.

In GluR2-Δ7 mutants, we first confirmed the mutation of the phosphorylation site by immunoblot analysis. The majority of signal detected by an antibody against C-terminal of GluR2/3 was absent in the GluR2-Δ7 mutant mice (Fig 5.1a, left panel). To examine whether the lack of 7 amino acids on the GluR2 C-terminal would affect GluR1 regulation, we measured GluR1 phosphorylation levels using phosphorylation site specific antibodies. There was no change, in the phosphorylation sites S831 and S845 site on the GluR1 subunit in GluR2-Δ7 mutants (S831 phosphorylation: GluR2-WT : 100 ± 13% of GluR2-WT , n = 6 ; GluR2-Δ7 : 122 ± 20% of GluR2-WT , n = 9 ; t-test: $p > 0.4$, Fig 5.1a, middle panel; S845 phosphorylation : GluR2-WT : 100 ± 7.2 % of GluR2-WT, n = 8 ; GluR2-Δ7: 113 ± 18% of GluR2-WT, n = 7 ; t-test: $p > 0.5$, Fig 5.1a, middle and right panel).

To examine whether the mutation itself affects basal synaptic transmission, we compared mEPSCs between GluR2-WT and GluR2-Δ7 mutant mice. We found that there was no difference in mEPSC amplitude (GluR2-WT: 9.8 ± 0.5 pA, n = 10; GluR2-Δ7: 10.8 ± 1.2 pA, n = 9; t-test $p > 0.6$; Fig. 5.1b, left panel), frequency (GluR2-WT: 4.3 ± 0.8 Hz, n = 10; GluR2-Δ7: 3.9 ± 0.5 Hz, n = 9; t-test $p > 0.7$; Fig. 5.1b, right panel), or kinetics (Fig 5.1b, middle panel) between GluR2-WT and GluR2-Δ7 mutant mice. These results show that the mutation had no effect on the number of postsynaptic receptors, nevertheless it does not rule out the possibility that there might be a change in the subunit composition of synaptic AMPA receptors. To test this we assessed the composition of AMPA receptors at the synapse electrophysiologically by determining the inward rectification index (IR: I_{-60mV}/I_{+40mV}, see methods) of AMPAR-mediated synaptic responses evoked by layer 4

stimulation. GluR1-S831A mutant mice showed larger inward rectification of AMPA receptor current compared to the wild type counterparts (GluR2 WT = 2.09 ± 0.1, n = 4; GluR2-Δ7 = 3.8 ± 0.5, n = 5; t-test, $p < 0.03$; Fig 5.1c.). These results suggest that lacking the last 7 amino acids on the GluR2 subunit probably prevents the incorporation of GluR2 containing AMPAR receptors under basal conditions.

Subsection 3: Visual experience induced synaptic scaling is abolished in GluR2-Δ7 mutant mice.

Next, we wanted to investigate whether visual experience-induced homeostatic synaptic plasticity is affected in the GluR2-Δ7 mutants. We visually deprived the GluR2-Δ7 mutant mice for 2 days from P21-P23 and the re-exposed them to light for 1 day. Unlike the effects of dark rearing in the wild type mice, the GluR2-Δ7 mutant mice dark rearing there was no significant change in mEPSC amplitude with dark rearing or with a subsequent light exposure (GluR2-Δ7: NR: 10.8 ± 1.2 pA, n = 9; DR: 10.5 ± 0.5 pA, n = 14; D+L: 10.8 ± 0.7 pA, n = 10; ANOVA: $F(2,30) = 0.037$, $p > 0.9$; Fig 5.2b. left panel). Again, along with lack of changes in mEPSC amplitude there were no alterations in mEPSC frequency (GluR2-Δ7: NR: 3.9 ± 0.5 Hz, n = 9; DR: 4.6 ± 0.4 Hz, n = 14; D+L: 4.2 ± 1.4 Hz, n = 10; ANOVA: $F(2,30) = 0.187$, $p > 0.8$; Fig 5.2b, right panel) or kinetics (Fig 5.2b, middle panel). In conclusion, these results suggest that the presence of the last seven amino acids on the GluR2 C terminal is necessary for visual experience-dependent changes in AMPAR-mEPSCs in the visual cortex.

Section 4: Discussion

This study was aimed at understanding the role of the GluR2 subunit in mediating visual deprivation induced homeostatic synaptic plasticity. Our results show that interactions mediated by the last seven amino acids on the c-terminal of the GluR2 subunit are involved in visual experience-induced changes in synaptic strength in the superficial layers of mouse visual cortex. We found that there is no basal change in AMPA receptor-mediated mEPSC amplitude or frequency in the GluR2-Δ7 mutant mice. However, there was an increase in the synaptic GluR1/GluR2 ratio, indicative of a modification in subunit composition in these mutants. The lack of the last 7 amino acids on the GluR2 tail also abolished experience-induced change in AMPA receptor number, function and subunit composition. These results suggest that the GluR2 tail is involved in synaptic scaling.

The basal synaptic strength in GluR2-Δ7 mutant mice was unaffected, despite the fact that they have reduced copies of GluR2 as apparent from displaying inward rectifying AMPA receptor current. This suggests that there is a possible decrease in the number of synaptic AMPA receptors. The reason is that GluR2-lacking AMPA receptors have a higher single channel conductance (Swanson et al., 1997), and is known to increase the amplitude of EPSCs (Liu and Cull-Candy, 2000; Liu and Cull-Candy, 2002). Therefore, the observed increase in inward rectification in GluR2-Δ7 mutant mice should have been accompanied by larger mEPSCs. The fact that we did not observe changes in mEPSC amplitude in GluR2-Δ7 mutant mice, suggest that there may be a decrease in synaptic AMPA receptor number.

The presence of GluR2 in an AMPA receptor complex, not only affects biophysical properties like Ca^{2+} permeability, sensitivity to polyamines, and mean single channel conductance, it also alters the receptor function by interacting with several intracellular proteins via its extreme C-tail PDZ ligand (-$SVKI_{COOH}$). There is evidence showing that the expression of hippocampal LTD requires interaction between GluR2/3 and GRIP/ABP (Li et al., 1999; Daw et al., 2000). Also a few studies emphasize that PICK1-GluR2 interaction is critical for LTD expression (Kim et al., 2001; Seidenman et al., 2003). The GluR2 c-terminal also has a phosphorylation site at S880, which is phosphorylated by PKC (Chung et al., 2000). Phosphorylation of S880 allows GluR2 to preferentially interact with PICK1, and not GRIP (Matsuda et al., 1999; Chung et al., 2000; Matsuda et al., 2000). Hence all of these studies suggest that GluR2 seems to play an important role in AMPA receptor endocytosis. In the GluR2-Δ7 mutant mice the interaction with these PDZ binding partners is absent, which implies that mechanisms regulating endocytosis are lacking. This deficit in endocytotic mechanism might be responsible for the lack of decrease in mEPSC amplitude with light exposure.

It is interesting that not only was the light exposure induced decrease in synaptic strength abolished, but the dark rearing induced increase in synaptic strength was also absent. Several studies have shown that activity deprivation causes an increase in GluR2 lacking AMPA receptors at the synaptic surface (O'Brien et al., 1998; Ju et al., 2004; Thiagarajan et al., 2005; Goel et al., 2006; Sutton et al., 2006). In the GluR2-Δ7 mice there is a basal increase in GluR1/GluR2 ratio, which possible prevents further addition of GluR2 lacking AMPARs to the surface and hence there is a lack of

increase in synaptic strength with dark rearing. This could be due to the fact that there is calcium entering through the Ca^{2+} permeable AMPA receptors, which prevents insertion of AMPA receptors into the synapse. A recent study demonstrates that GluR2-PICK1 interaction plays an important role in LTP (Terashima et al., 2008). Hence, it is possible that the absence of scaling up in GluR2-Δ7 mutants maybe be due to the lack of PICK-1 dependent synaptic targeting of AMPA receptors.

It is important to know that there are several other studies that use GluR2 and GluR3 knockout mice to investigate the importance of activity dependent AMPAR internalization and trafficking in the hippocampus. Their results show imply that GluR2-dependent mechanisms may not be necessary for activity-dependent trafficking and recycling in the hippocampus. Transgenic mice lacking GluR2/3 show normal endocytosis of AMPA receptors upon NMDAR activation, and normal recycling of AMPA receptors back to the plasma membrane (Biou et al., 2008). Another study also using mutant mice that lack GluR2 and GluR3 shows that activity dependent changes like LTP, LTD, depotentiation and dedepression do not require GluR2/3 dependent mechanisms (Meng et al., 2003). A recent study shows that AMPAR trafficking to the synapse is not dependent on the selective interaction between intracellular proteins and GluR2 but rather on the binding between any of the GluR subunits to one or more proteins (Panicker et al., 2008). Contrary to these implications that undermine the importance of GluR2, one study showed that GluR2 lacking mice show enhanced LTP in the hippocampus (Jia et al., 1996). Importantly an investigation of calcium-permeable AMPA receptor plasticity (CARP) at cerebellar granule cell-stellate cell synapses using GluR2-Δ7 mutant mice showed

that this form of plasticity requires the GluR2 PDZ ligand (Gardner et al., 2005). And there are clear indications that the GluR2-PDZ interaction is necessary for cerebellar LTD (Steinberg et al., 2006).

Though, it seems that there is no consensus on the role of GluR2, the results seem to vary depending upon the brain region and the experimental protocols used. Nevertheless, our results support the view that GluR2 PDZ ligand mediated signaling is involved in mediating activity-dependent homeostatic regulation of synaptic strength in the superficial layers of the visual cortex. How this mechanism interacts with GluR1-dependent mechanisms of synaptic scaling remains to be examined.

Chapter 6: Conclusion

In my thesis work I have focused on understanding the cellular and molecular mechanisms involved in homeostatic synaptic plasticity like synaptic scaling. In this

chapter the important conclusions and implications of this research work are described.

Prolonged increase in activity can lead to uncontrolled increase in firing rate and eventually render a neuronal network unstable. Hence homeostatic mechanisms like synaptic scaling are required to stabilize interconnected populations of neurons. According to the synaptic scaling model a chronic decrease in activity leads to an increase in strength of all the excitatory synapses while a prolonged increase in activity is compensated for by a decrease in strength of all the synapses. Hence synaptic scaling is a form of cortical adaptation that occurs and this is executed by alterations in AMPA receptor-mediated synaptic gain (Turrigiano and Nelson, 2000). While several reports have used in vitro preparations to show homeostatic changes in synaptic gain (Lissin et al., 1998; O'Brien et al., 1998; Turrigiano et al., 1998; Ju et al., 2004; Thiagarajan et al., 2005), few studies have undertaken in vivo manipulations to study synaptic scaling, particularly in the cortex (Desai et al., 2002; Maffei et al., 2004). Most importantly the molecular machinery and intracellular signaling events involved are largely unknown. Therefore I attempted to study the molecular events that are involved in homeostatic regulation of synaptic transmission by visual experience in rodents. To do this, I used dark rearing as a means to alter visual experience of the animals, and then assayed the resulting changes in AMPA receptor-mediated synaptic transmission in the visual cortex. Previous reports show that Hebbian modifications like Long Term Potentiation (LTP) and Long Term Depression (LTD) can be induced in layer 2/3 synapses in the juvenile and adult visual cortex. Therefore, I determined this would be a good set of synapses to

examine visual experience-dependent homeostatic plasticity, which would provide stability to a network that undergo Hebbian plasticity.

In the following sections I discuss the results obtained from this study.

Mechanisms of Cross-Modal homeostatic plasticity

My initial studies were done in rats where I dark reared them for 1 week and then re-exposed them to light for 2 days in order to see if the changes that occur with dark rearing were reversible. I found that dark rearing caused an increase in mEPSC amplitude, without a change in frequency or kinetics in layer 2/3 visual cortical neurons. This increase in amplitude was readily reversed with two days of light exposure. Interestingly, I found that visual deprivation caused a significant decrease in mEPSC amplitude in the somatosensory and auditory cortices. Again there was no change in mEPSC frequency or kinetics. This reduction in amplitude was bidirectional since the amplitude following light exposure increased to similar levels as normal reared animals. The cross modal modifications that occurred in the other primary sensory cortices implied that the activity in these cortices was probably increased as a result of dark-rearing. This could be because the dark reared animals were probably relying on their somatosensory and auditory input or perception, which could have led to a decrease in synaptic strength.

The cross-modal plasticity induced in somatosensory cortex could be due to altered cortical processing of tactile inputs (i.e. top-down) or due to differences in tactile experience (i.e. bottom-up). There is evidence suggesting that top-down signals that originate in multimodal areas may utilize information from the primary sensory

cortices (Macaluso et al., 2000). The hierarchical organization of the visual system and studies from visual attention suggest that there are top-down forces in operation and hence the prediction would be that cross modal effects are most likely to occur in higher sensory areas. However, cross modal effects could also be mediated by bottom–up processes (Schroeder and Foxe, 2005). Some groups believe that cross modal plasticity may be mediated by synaptic modifications occurring in the sub-cortical connections (Sur and Leamey, 2001). It is unknown whether the cross-modal plasticity observed following dark-rearing is due to top-down or bottom-up inputs. However, it is possible to speculate that mechanistically, a top-down model would engage intracortical inputs, while bottom-up activation involves thalamocortical inputs. There is a recent cross modal study which shows that blindfolded subjects when asked to do a tactile discrimination task utilized a combination of direct primary visual cortex activation and top down suppression of extrastriate cortex (Merabet et al., 2007). In any case, a change in mEPSC amplitude without an alteration in frequency implied that the locus of cross-modal changes is postsynaptic. In addition this modification of synaptic strength was multiplicative as shown by Turrigiano, 1998, which suggests that receptors are added to synapses in proportion to their original strength. Also it is important to realize that unlike Hebbian modifications, which are synapse-specific, homeostatic synaptic modifications are global and affect all synapses.

The changes in mEPSC size by visual experience were associated with similar bidirectional modifications in subunit composition of AMPA receptors. Dark-rearing caused a significant increase in GluR2-lacking AMPA receptors at visual cortex

synapses, which was reversed by light exposure. This increase in GluR1/GluR2 ratio is likely mediated by an elevation in phosphorylation at S845 on GluR1. This is because dark rearing for a week in rats was associated with an increase in S845 phosphorylation in the visual cortex. Similarly, in the somatosensory cortex dark rearing followed by light exposure caused a significant increase in AMPA mediated mEPSCs accompanied by an elevation in GluR1/GluR2 ratio and an up-regulation of S845 phosphorylation. Hence, in both the visual and the somatosensory cortices an increase in synaptic strength correlated with an elevation in S845 phosphorylation along with a greater proportion of GluR1 containing AMPA receptors. This is analogous to previous studies that have shown that an increase in S845 phosphorylation causes an up-regulation of GluR1 containing AMPA receptors at the synapses (Esteban et al., 2003). Collectively, these results imply that visual experience causes a homeostatic modification in AMPA mediated synaptic strength, which is associated with an increase in AMPA receptors with a higher conductance at synapses. Most importantly and interestingly, the change in visual environment homeostatically modified synapses across different primary sensory cortices, but not in the frontal cortex.

Mechanisms of visual deprivation induced synaptic scaling in adult visual cortex

Experience-dependent Hebbian modifications like Long Term Potentiation (LTP) and Long Term Depression (LTD) are known to persist through adulthood in layer 2/3 of the visual cortex (Jiang et al., 2007). In addition ocular dominance (OD) plasticity which is mediated by LTP and LTD occurs to a substantial extent in adult visual cortex (Sawtell et al., 2003; Pham et al., 2004; Tagawa et al., 2005). Hence to

counterbalance the destabilizing effects of LTP and LTD, homeostatic mechanism like synaptic scaling must operate in adults as well. To determine this, we investigated the effects of prolonged visual deprivation in adult mice. We found that 2 days of dark rearing causes a robust, maximal and reversible increase in mEPSC amplitude in layer 2/3 of juvenile mouse visual cortex. Similar to our study in rats, I found that this occurred without a change in frequency or kinetics. Similar to the results from rats, the increase in mEPSC amplitude with dark-rearing was multiplicative. Dark-rearing adult mice also showed similar homeostatic alterations, which were postsynaptic, but these modifications in synaptic strength were not multiplicative. This suggests that in response to prolonged visual deprivation the synapses in the adult visual cortex do undergo homeostatic increase in synaptic strength but the mechanisms of receptor addition might be different. This non-multiplicative scaling is in contrast to the previous results in juvenile rats and mice (chapter 2 and 3), as well as initial descriptions of homeostatic synaptic scaling (Turrigiano et al., 1998; Desai et al., 2002). My results on visual deprivation in adults suggests that all synapses on a cell do not scale up or down with the same multiplicative factor. Other studies using hippocampal cultures also showed that homeostatic changes differentially modify subsets of synapses, which implies that it does not follow a strict global multiplicative mechanism (Thiagarajan et al., 2005). We found that experience-induced reversible homeostatic plasticity in visual cortex occurs via a global multiplicative mechanism in young animals (P23), but not in adults (especially at P97), suggesting that age may be a determining factor. Similarly, a recent study demonstrated that an increase in the *in vitro* age of neuronal cultures

causes the expression locus of homeostatic plasticity to shift from predominantly postsynaptic to having both pre- and postsynaptic components (Wierenga et al., 2006). Interestingly, spines turnover more slowly in the visual cortex of adult mice (Grutzendler et al., 2002; Holtmaat et al., 2005), implying that there may be a smaller proportion of dynamic synapses which undergo activity-dependent modifications. Therefore, it is possible that visual-experience may preferentially affect this dynamic population of synapses in adult cortex. Also recent studies highlighted that synapses on neocortical neurons may utilize different rules for inducing synaptic plasticity depending on their dendritic location (Froemke et al., 2005; Gordon et al., 2006; Letzkus et al., 2006; Sjostrom and Hausser, 2006). Therefore, it is also plausible that there may be select dendritic compartments that undergo homeostatic plasticity in adults. All of these different studies emphasize that as the animals mature the computational requirements that the neuronal networks need to fulfill becomes diverse. This diversity along with alterations in the plastic nature of juvenile and adult visual cortex can attribute to differences in mechanisms that maintain homeostasis in the mature animals.

Role of homeostatic modifications in response to dark rearing

Hubel and Wiesel and several other groups established decades ago that the visual cortex is highly susceptible to visual experience during a certain phase of visual development which they called the "critical period" (Wiesel and Hubel, 1963; LeVay et al., 1980; Hubel, 1982; Mower et al., 1983; Gordon and Stryker, 1996). Work by Mower and others has shown that dark-rearing can extend this critical period. According to Mower et al. (1983) dark-rearing from birth maintained the visual

cortex in a highly plastic state and this plasticity was diminished by a very brief visual experience. Subsequent work over the years has shown that the adult visual cortex can also be modified by experience (Sawtell et al., 2003; Pham et al., 2004; Tagawa et al., 2005; Jiang et al., 2007). In particular He et al, 2006 showed that preceding monocular deprivation with ten days of dark rearing caused a robust shift in OD plasticity even in adult visual cortex. Hence this work and the studies on critical period elongation suggest that lack of visual experience renders the cortex plastic. Previously, it has been shown that dark-rearing causes a shift in the "modification threshold (θ_M)" thus making it easier to induce LTP in the cortex while making it harder to induce LTD (Kirkwood et al., 1996). He et al, 2006 also show that the visual deprivation preceding monocular deprivation causes a decrease in $GABA_A$ relative to AMPA receptors and an increase in NR2b/NR2a. Both of these changes would cause a shift in modification threshold favoring LTP.

It is also possible that dark rearing causes an increase in synaptic GluR1-containing AMPA receptors, which due to the elevation in number and the increased single channel conductance, can cause better summation of synaptic current, eventually favoring LTP. Therefore, it is possible to speculate that prolonged period of visual deprivation can bring about a homeostatic modification, which can occur potentially due to either sliding threshold or synaptic scaling mechanism or some combination of both.

My results showed that synaptic scaling might be one of the mechanisms by which dark rearing endows the cortex with enhanced plasticity. Nevertheless it is important to realize that normal visual development is important since prolonged visual

deprivation during the critical period of development causes poorly developed receptive fields (Mower et al., 1983) and cortical physiology is not recovered (Hubel and Wiesel, 1970). It is known that initially during development the receptive fields are broad and less well defined. As the visual cortex matures with age and experience the receptive fields become more precise and sharply tuned. Due to the global nature of synaptic scaling dark rearing will cause an increase in synaptic strength across all the synapses, which can be correlated with the broad, less specific receptive fields.

Role of GluR1 and GluR2 mediated signaling in synaptic scaling

The effects of visual deprivation in rats and mice caused an up regulation of AMPA receptors at the surface. Pharmacological manipulations have previously shown that activity deprivation caused an increase in surface accumulation of AMPA receptors due to an increase in receptor half life (O'Brien et al., 1998). However visual deprivation in rats (chapter 2) did not change the total GluR1 or GluR2 indicating that the increase in GluR1/GluR2 ratio we saw at the PSD is likely due to an increase in trafficking of AMPARs to synapses. Phosphorylation at S845 is implicated in trafficking AMPA receptors to the synaptic surface (Esteban et al., 2003). Our results demonstrating that dark rearing increases phosphorylation of GluR1-S845 is consistent with the possiblity that the effects of visual deprivation are mediated by an increase in trafficking of GluR1 containing AMPA receptors. The involvement of S845 phosphorylation is further exemplified by our results from the GluR1-S831A mutants where an up-regulation in basal S845 phosphorylation correlated with an increase in mEPSC amplitude. In addition, in the GluR1-S845A

mutants, that lack this phosphorylation site, does not scale up excitatory synapses with dark rearing. Therefore, a key molecular event that play a critical role in visual deprivation induced synaptic scaling seems to be a post-translational modification of AMPA receptors by phosphorylation.

We also demonstrate that visual experience induced modifications in synaptic strength require signaling mediated by the GluR2 C-terminal. Evidence from work on LTD suggested that regulation via GluR2 is important for AMPA receptor endocytosis (Li et al., 1999; Daw et al., 2000; Kim et al., 2001; Seidenman et al., 2003). Hence in view of previous work and our results we had hypothesized that while GluR1 mechanisms are involved in scaling up, GluR2 mediated mechanisms are probably involved in scaling down. However, during the course of my study, I have unraveled that there might be some level of interaction occurring between GluR1 and GluR2 mediated mechanisms. Also, it is possible that the previous history of synaptic plasticity may be an important determinant for inducing further modification at synapses. For example, in dark-reared GluR1-S831A mutants the synaptic strength is decreased and there is no subsequent decrease in synaptic strength following light exposure despite the fact that signaling via GluR2 is intact. Hence this implies that the previous history of synaptic strength might be important. Also in the GluR1-S845A mutants there is an increase in basal synaptic strength which remains elevated even after dark rearing. Nevertheless despite the enhanced synaptic strength and available GluR2 signaling mechanisms there is no reduction in mEPSC amplitude with light exposure. This again implies that the lack of signaling via GluR1 somehow prevents GluR2 mediated endocytosis. The interaction between GluR1 and GluR2

signaling mechanisms is also evident in the GluR2-Δ7 mutants. In these mutants the lack of last seven amino acids on the GluR2 c-tail is probably associated with the basal increase in GluR2-lacking AMPA receptors as determined electrophysiologically. Nevertheless, this was not accompanied by an increase in mEPSC amplitude, indicating that there is probably a decrease in synaptic receptor number. Moreover despite having intact signaling via GluR1 the lack of the GluR2 C-tail mediated mechanisms prevented any further insertion of AMPA receptors with dark rearing. Therefore, these results suggest that there is as of unknown mechanism in which GluR2 c-terminal mediated signal can regulate GluR1-dependent insertion of synaptic AMPA receptors, which ultimately leads to an increase in synaptic strength.

While I have evidence suggesting GluR1 regulation in mediating the increase in mEPSC amplitude with visual deprivation, the mechanism involved in scaling down is still unresolved. The decrease in mEPSC amplitude in visual cortex when dark-reared mice are re-exposed to light was associated with a decrease in the synaptic GluR1/GluR2 ratio, but an analysis of PSDs did not show a significant change in the GluR2 levels. Hence this study shows that scaling down is definitely due to a decrease in receptor number and change in subunit composition but the intracellular mechanisms involved are still undetermined.

Multiplicative synaptic scaling

In this study I have shown that visual experience causes a scaling up or down of the quantal amplitude of all synapses on a postsynaptic neuron. This adjustment in

synaptic strength can be multiplicative or additive. A multiplicative modification implies that the number or receptors added or removed are proportional to the initial strength of the synapse. An additive modification adds or subtracts the same amount from each synapse. Both multiplicative and additive adjustments can bring about synaptic modifications in response to chronic changes in activity. Initial work that demonstrated the phenomenon of synaptic scaling showed that synapses are scaled bidirectionally in a multiplicative manner (Turrigiano et al.,1998). The advantage of multiplicative scaling is that since receptor addition or removal is proportional to the initial strength, this modification leaves relative differences in synaptic weight across the numerous synapses unchanged. Hence this homogenous change in quantal amplitude can sustain patterns of synaptic change that underlie cellular learning and memory. In contrast, work using hippocampal cultures showed that homeostatic changes differentially modify subsets of synapses, which implies that it does not follow a strict global multiplicative mechanism (Thiagarajan et al., 2005). I found that in juvenile visual cortex the synaptic scaling is multiplicative. In the adults (P38) immediately after the closure of the classical critical period (~P35) visual deprivation induced increase in quantal amplitude is multiplicative while scaling down is not. Changes in visual experience in 3 month old mice, which are well beyond the closure of the classical critical period, causes synaptic adjustments which are non-multiplicative. It is possible that with age the rules governing modification of synaptic strength change. Also as I mentioned in the introduction there are other mechanisms that can bring about homeostasis and hence there might be changes in intrinsic excitability or inhibition that maintains homeostasis in adult visual cortex.

Interestingly, I found that phosphorylation of S845 on the GluR1 subunit alone is not sufficient to produce multiplicative scaling suggesting that additional mechanisms are at play.

Mechanisms involved in scaling up and scaling down of synaptic strength are asymmetric

It is interesting that there seems to be an asymmetry in the cellular events mediating scaling up versus scaling down. This is evident at the level of S845 phosphorylation and the multiplicative nature of receptor insertion. Our results demonstrate that a post-translational modification of AMPA receptors, namely, S845 phosphorylation is associated with an increase in synaptic strength while a decrease in synaptic strength is not accompanied by a change in GluR1 phosphorylation. Also in the adult visual cortex dark rearing associated with scaling up is accompanied by a multiplicative increase in mEPSC amplitude while light exposure induced decrease in synaptic strength is not multiplicative. While there are data supporting reversible changes in AMPA receptor subunit composition (Thiagarajan et al., 2005; Goel et al., 2006), and CaMKIIalpha/CaMKIIbeta ratio (Thiagarajan et al., 2002) during bidirectional homeostatic plasticity, recent evidence supports the notion of asymmetry in molecular mechanisms. For instance, a recent study demonstrated that tumor-necrosis factor-α (TNF-α) is only involved in synaptic scaling up of excitatory synaptic transmission by inactivity, but not for scaling down synapses by enhanced activity in hippocampal cultures (Stellwagen and Malenka, 2006). In contrast, activity-regulated cytoskeletal protein/activity-regulated gene 3.1 (Arc/Arg 3.1), which is an immediate early gene

rapidly up-regulated by neural activity (Lyford et al., 1995), has been shown to be involved in scaling down synapses. This asymmetry in the mechanisms may arise as a result of difference in the induction signals, which triggers scaling up or scaling down. It is clear from my data that scaling up synapses in the visual cortex requires longer duration of activity manipulation than that required for scaling down synapses. This implies that the induction of scaling up requires longer duration of activity integration. Hence the molecular "read-out" of activity changes should be different for scaling up versus down.

A common downstream mechanism shared by both Hebbian and non-Hebbian synaptic modifications.

It is quite interesting that Hebbian and homeostatic alterations at synapses seems to recruit common downstream mechanisms for expression. A prolonged (in the order of days) increase in activity (chapter 2 and 3), which likely is manifested in an elevation in postsynaptic depolarization (Leslie et al., 2001), causes an upregulation of GluR1, which is a common downstream mechanism shared by both Hebbian modifications and synaptic scaling phenomenon. Hence in response to a transient elevation in activity, that can induce LTP, there is an increase in synaptic GluR1 that is synapse-specific and requires prior S845 phosphorylation. A continued increase in activity causes an elevation in S845 phosphorylation and an up-regulation of AMPA receptor insertion across the majority of, if not all, synapses. In response to this prolonged activity the receptor addition becomes multiplicative by the action of another mechanism. Importantly, in synaptic scaling the increase in S845 phosphorylation

mediates only part of the increase in mEPSC amplitude and we think that it is the primary step involved in increasing excitatory synaptic strenght. The fact that insertion of AMPA receptors is mediated by a common mechanism is advantageous in that there is conservation of cellular and molecular resources.

Bibliography

Abbott LF, Nelson SB (2000) Synaptic plasticity: taming the beast. Nat Neurosci 3 Suppl:1178-1183.

Artola A, Singer W (1993) Long-term depression of excitatory synaptic transmission and its relationship to long-term potentiation. Trends Neurosci 16:480-487.

Axelsson J, Thesleff S (1959) A study of supersensitivity in denervated mammalian skeletal muscle. J Physiol 147:178-193.

Bacci A, Coco S, Pravettoni E, Schenk U, Armano S, Frassoni C, Verderio C, De Camilli P, Matteoli M (2001) Chronic blockade of glutamate receptors enhances presynaptic release and downregulates the interaction between synaptophysin-synaptobrevin-vesicle-associated membrane protein 2. J Neurosci 21:6588-6596.

Banke TG, Bowie D, Lee H, Huganir RL, Schousboe A, Traynelis SF (2000) Control of GluR1 AMPA receptor function by cAMP-dependent protein kinase. J Neurosci 20:89-102.

Bavelier D, Neville HJ (2002) Cross-modal plasticity: where and how? Nat Rev Neurosci 3:443-452.

Bear MF, Cooper LN, Ebner FF (1987) A physiological basis for a theory of synapse modification. Science 237:42-48.

Beattie EC, Stellwagen D, Morishita W, Bresnahan JC, Ha BK, Von Zastrow M, Beattie MS, Malenka RC (2002) Control of synaptic strength by glial TNFalpha. Science 295:2282-2285.

Bekkers JM, Stevens CF (1994) The nature of quantal transmission at central excitatory synapses. Adv Second Messenger Phosphoprotein Res 29:261-273.

Benevento LA, Bakkum BW, Port JD, Cohen RS (1992) The effects of dark-rearing on the electrophysiology of the rat visual cortex. Brain Res 572:198-207.

Berardi N, Pizzorusso T, Maffei L (2000) Critical periods during sensory development. Curr Opin Neurobiol 10:138-145.

Berardi N, Pizzorusso T, Maffei L (2004) Extracellular matrix and visual cortical plasticity: freeing the synapse. Neuron 44:905-908.

Berg DK, Hall ZW (1975) Increased extrajunctional acetylcholine sensitivity produced by chronic acetylcholine sensitivity produced by chronic post-synaptic neuromuscular blockade. J Physiol 244:659-676.

Bi GQ, Poo MM (1998) Synaptic modifications in cultured hippocampal neurons: dependence on spike timing, synaptic strength, and postsynaptic cell type. J Neurosci 18:10464-10472.

Bienenstock EL, Cooper LN, Munro PW (1982) Theory for the development of neuron selectivity: orientation specificity and binocular interaction in visual cortex. J Neurosci 2:32-48.

Biou V, Bhattacharyya S, Malenka RC (2008) Endocytosis and recycling of AMPA receptors lacking GluR2/3. Proc Natl Acad Sci U S A 105:1038-1043.

Bliss TV, Gardner-Medwin AR (1973) Long-lasting potentiation of synaptic transmission in the dentate area of the unanaestetized rabbit following stimulation of the perforant path. J Physiol 232:357-374.

Bliss TV, Collingridge GL (1993) A synaptic model of memory: long-term potentiation in the hippocampus. Nature 361:31-39.
Blue ME, Parnavelas JG (1983) The formation and maturation of synapses in the visual cortex of the rat. I. Qualitative analysis. J Neurocytol 12:599-616.
Brocke L, Chiang LW, Wagner PD, Schulman H (1999) Functional implications of the subunit composition of neuronal CaM kinase II. J Biol Chem 274:22713-22722.
Brorson JR, Li D, Suzuki T (2004) Selective expression of heteromeric AMPA receptors driven by flip-flop differences. J Neurosci 24:3461-3470.
Buchel C (1998) Functional neuroimaging studies of Braille reading: cross-modal reorganization and its implications. Brain 121 (Pt 7):1193-1194.
Burrone J, O'Byrne M, Murthy VN (2002) Multiple forms of synaptic plasticity triggered by selective suppression of activity in individual neurons. Nature 420:414-418.
Cancedda L, Putignano E, Impey S, Maffei L, Ratto GM, Pizzorusso T (2003) Patterned vision causes CRE-mediated gene expression in the visual cortex through PKA and ERK. J Neurosci 23:7012-7020.
Carmignoto G, Vicini S (1992) Activity-dependent decrease in NMDA receptor responses during development of the visual cortex. Science 258:1007-1011.
Carroll RC, Beattie EC, von Zastrow M, Malenka RC (2001) Role of AMPA receptor endocytosis in synaptic plasticity. Nat Rev Neurosci 2:315-324.
Carroll RC, Lissin DV, von Zastrow M, Nicoll RA, Malenka RC (1999) Rapid redistribution of glutamate receptors contributes to long-term depression in hippocampal cultures. Nat Neurosci 2:454-460.
Chao SZ, Ariano MA, Peterson DA, Wolf ME (2002) D1 dopamine receptor stimulation increases GluR1 surface expression in nucleus accumbens neurons. J Neurochem 83:704-712.
Cho K, Aggleton JP, Brown MW, Bashir ZI (2001) An experimental test of the role of postsynaptic calcium levels in determining synaptic strength using perirhinal cortex of rat. J Physiol 532:459-466.
Chung HJ, Xia J, Scannevin RH, Zhang X, Huganir RL (2000) Phosphorylation of the AMPA receptor subunit GluR2 differentially regulates its interaction with PDZ domain-containing proteins. J Neurosci 20:7258-7267.
Clem RL, Barth A (2006) Pathway-specific trafficking of native AMPARs by in vivo experience. Neuron 49:663-670.
Crowley JC, Katz LC (2000) Early development of ocular dominance columns. Science 290:1321-1324.
Cummings JA, Mulkey RM, Nicoll RA, Malenka RC (1996) Ca2+ signaling requirements for long-term depression in the hippocampus. Neuron 16:825-833.
Czepita D, Reid SN, Daw NW (1994) Effect of longer periods of dark rearing on NMDA receptors in cat visual cortex. J Neurophysiol 72:1220-1226.
Davis GW, Goodman CS (1998) Synapse-specific control of synaptic efficacy at the terminals of a single neuron. Nature 392:82-86.
Daw MI, Chittajallu R, Bortolotto ZA, Dev KK, Duprat F, Henley JM, Collingridge GL, Isaac JT (2000) PDZ proteins interacting with C-terminal GluR2/3 are

involved in a PKC-dependent regulation of AMPA receptors at hippocampal synapses. Neuron 28:873-886.
Daw NW, Fox K, Sato H, Czepita D (1992) Critical period for monocular deprivation in the cat visual cortex. J Neurophysiol 67:197-202.
De Gois S, Schafer MK, Defamie N, Chen C, Ricci A, Weihe E, Varoqui H, Erickson JD (2005) Homeostatic scaling of vesicular glutamate and GABA transporter expression in rat neocortical circuits. J Neurosci 25:7121-7133.
Derkach V, Barria A, Soderling TR (1999) Ca2+/calmodulin-kinase II enhances channel conductance of alpha-amino-3-hydroxy-5-methyl-4-isoxazolepropionate type glutamate receptors. Proc Natl Acad Sci U S A 96:3269-3274.
Desai NS, Rutherford LC, Turrigiano GG (1999) Plasticity in the intrinsic excitability of cortical pyramidal neurons. Nat Neurosci 2:515-520.
Desai NS, Cudmore RH, Nelson SB, Turrigiano GG (2002) Critical periods for experience-dependent synaptic scaling in visual cortex. Nat Neurosci 5:783-789.
Dev KK, Nishimune A, Henley JM, Nakanishi S (1999) The protein kinase C alpha binding protein PICK1 interacts with short but not long form alternative splice variants of AMPA receptor subunits. Neuropharmacology 38:635-644.
Diamond ME, Armstrong-James M, Ebner FF (1993) Experience-dependent plasticity in adult rat barrel cortex. Proc Natl Acad Sci U S A 90:2082-2086.
Dingledine R, Borges K, Bowie D, Traynelis SF (1999) The glutamate receptor ion channels. Pharmacol Rev 51:7-61.
Dong H, O'Brien RJ, Fung ET, Lanahan AA, Worley PF, Huganir RL (1997) GRIP: a synaptic PDZ domain-containing protein that interacts with AMPA receptors. Nature 386:279-284.
Dudek SM, Bear MF (1992) Homosynaptic long-term depression in area CA1 of hippocampus and effects of N-methyl-D-aspartate receptor blockade. Proceedings of the National Academy of Sciences 89:4363-4367.
Ehlers MD, Heine M, Groc L, Lee MC, Choquet D (2007) Diffusional trapping of GluR1 AMPA receptors by input-specific synaptic activity. Neuron 54:447-460.
Esteban JA, Shi SH, Wilson C, Nuriya M, Huganir RL, Malinow R (2003) PKA phosphorylation of AMPA receptor subunits controls synaptic trafficking underlying plasticity. Nat Neurosci 6:136-143.
Feldman DE (2000) Timing-based LTP and LTD at vertical inputs to layer II/III pyramidal cells in rat barrel cortex. Neuron 27:45-56.
Flint AC, Maisch US, Weishaupt JH, Kriegstein AR, Monyer H (1997) NR2A subunit expression shortens NMDA receptor synaptic currents in developing neocortex. J Neurosci 17:2469-2476.
Fox K (1992) A critical period for experience-dependent synaptic plasticity in rat barrel cortex. J Neurosci 12:1826-1838.
Fox K (2002) Anatomical pathways and molecular mechanisms for plasticity in the barrel cortex. Neuroscience 111:799-814.
Fox K, Daw N, Sato H, Czepita D (1991) Dark-rearing delays the loss of NMDA receptor function in kitten visual cortex. Nature 350:342-344.

Frenkel MY, Bear MF (2004) How monocular deprivation shifts ocular dominance in visual cortex of young mice. Neuron 44:917-923.
Froemke RC, Poo MM, Dan Y (2005) Spike-timing-dependent synaptic plasticity depends on dendritic location. Nature 434:221-225.
Gardner SM, Takamiya K, Xia J, Suh JG, Johnson R, Yu S, Huganir RL (2005) Calcium-permeable AMPA receptor plasticity is mediated by subunit-specific interactions with PICK1 and NSF. Neuron 45:903-915.
Glazewski S, Chen CM, Silva A, Fox K (1996) Requirement for alpha-CaMKII in experience-dependent plasticity of the barrel cortex. Science 272:421-423.
Goel A, Lee HK (2007) Persistence of experience-induced homeostatic synaptic plasticity through adulthood in superficial layers of mouse visual cortex. J Neurosci 27:6692-6700.
Goel A, Jiang B, Xu LW, Song L, Kirkwood A, Lee HK (2006) Cross-modal regulation of synaptic AMPA receptors in primary sensory cortices by visual experience. Nat Neurosci 9:1001-1003.
Goldreich D, Kanics IM (2003) Tactile acuity is enhanced in blindness. J Neurosci 23:3439-3445.
Gordon JA, Stryker MP (1996) Experience-dependent plasticity of binocular responses in the primary visual cortex of the mouse. J Neurosci 16:3274-3286.
Gordon U, Polsky A, Schiller J (2006) Plasticity compartments in basal dendrites of neocortical pyramidal neurons. J Neurosci 26:12717-12726.
Grutzendler J, Kasthuri N, Gan WB (2002) Long-term dendritic spine stability in the adult cortex. Nature 420:812-816.
Guire ES, Lickey ME, Gordon B (1999) Critical period for the monocular deprivation effect in rats: assessment with sweep visually evoked potentials. J Neurophysiol 81:121-128.
Hayashi Y, Shi SH, Esteban JA, Piccini A, Poncer JC, Malinow R (2000) Driving AMPA receptors into synapses by LTP and CaMKII: requirement for GluR1 and PDZ domain interaction. Science 287:2262-2267.
He HY, Hodos W, Quinlan EM (2006) Visual deprivation reactivates rapid ocular dominance plasticity in adult visual cortex. J Neurosci 26:2951-2955.
Hebb DO (1949) Organization of Behavior. New York: John Wiley and Sons.
Hensch TK, Fagiolini M, Mataga N, Stryker MP, Baekkeskov S, Kash SF (1998) Local GABA circuit control of experience-dependent plasticity in developing visual cortex. Science 282:1504-1508.
Hoffman DA, Sprengel R, Sakmann B (2002) Molecular dissection of hippocampal theta-burst pairing potentiation. Proc Natl Acad Sci U S A 99:7740-7745.
Holtmaat A, Wilbrecht L, Knott GW, Welker E, Svoboda K (2006) Experience-dependent and cell-type-specific spine growth in the neocortex. Nature 441:979-983.
Holtmaat AJ, Trachtenberg JT, Wilbrecht L, Shepherd GM, Zhang X, Knott GW, Svoboda K (2005) Transient and persistent dendritic spines in the neocortex in vivo. Neuron 45:279-291.
Hou Q, Zhang D, Jarzylo L, Huganir RL, Man HY (2008) Homeostatic regulation of AMPA receptor expression at single hippocampal synapses. Proc Natl Acad Sci U S A 105:775-780.

Huang ZJ, Kirkwood A, Pizzorusso T, Porciatti V, Morales B, Bear MF, Maffei L, Tonegawa S (1999) BDNF regulates the maturation of inhibition and the critical period of plasticity in mouse visual cortex. Cell 98:739-755.

Hubel DH (1982) Exploration of the primary visual cortex, 1955-78. Nature 299:515-524.

Hubel DH, Wiesel TN (1970) The period of susceptibility to the physiological effects of unilateral eye closure in kittens. J Physiol 206:419-436.

Isackson PJ, Huntsman MM, Murray KD, Gall CM (1991) BDNF mRNA expression is increased in adult rat forebrain after limbic seizures: temporal patterns of induction distinct from NGF. Neuron 6:937-948.

Jia Z, Agopyan N, Miu P, Xiong Z, Henderson J, Gerlai R, Taverna FA, Velumian A, MacDonald J, Carlen P, Abramow-Newerly W, Roder J (1996) Enhanced LTP in mice deficient in the AMPA receptor GluR2. Neuron 17:945-956.

Jiang B, Trevino M, Kirkwood A (2007) Sequential development of long-term potentiation and depression in different layers of the mouse visual cortex. J Neurosci 27:9648-9652.

Ju W, Morishita W, Tsui J, Gaietta G, Deerinck TJ, Adams SR, Garner CC, Tsien RY, Ellisman MH, Malenka RC (2004) Activity-dependent regulation of dendritic synthesis and trafficking of AMPA receptors. Nat Neurosci 7:244-253.

Kameyama K, Lee HK, Bear MF, Huganir RL (1998) Involvement of a postsynaptic protein kinase A substrate in the expression of homosynaptic long-term depression. Neuron 21:1163-1175.

Karni A, Sagi D (1991) Where practice makes perfect in texture discrimination: evidence for primary visual cortex plasticity. Proc Natl Acad Sci U S A 88:4966-4970.

Kato K, Sekino Y, Takahashi H, Yasuda H, Shirao T (2007) Increase in AMPA receptor-mediated miniature EPSC amplitude after chronic NMDA receptor blockade in cultured hippocampal neurons. Neurosci Lett 418:4-8.

Katz LC, Shatz CJ (1996) Synaptic activity and the construction of cortical circuits. Science 274:1133-1138.

Kim CH, Chung HJ, Lee HK, Huganir RL (2001) Interaction of the AMPA receptor subunit GluR2/3 with PDZ domains regulates hippocampal long-term depression. Proc Natl Acad Sci U S A 98:11725-11730.

Kirkwood A, Bear MF (1994) Hebbian synapses in visual cortex. J Neurosci 14:1634-1645.

Kirkwood A, Lee HK, Bear MF (1995) Co-regulation of long-term potentiation and experience-dependent synaptic plasticity in visual cortex by age and experience. Nature 375:328-331.

Kirkwood A, Rioult MC, Bear MF (1996) Experience-dependent modification of synaptic plasticity in visual cortex. Nature 381:526-528.

Kirkwood A, Dudek SM, Gold JT, Aizenman CD, Bear MF (1993) Common forms of synaptic plasticity in the hippocampus and neocortex in vitro. Science 260:1518-1521.

Konorski J, Szwejkowska G (1953) [Chronic extinction and restoration of conditioned reflexes.]. Acta Physiol Pol 4:37-51.

Konorski J, Stepien L, Brutkowski S, Lawicka W, Stepien I (1952) [Effect of partial removal of frontal and parietal lobes on conditioned motor reflexes.]. Neurol Neurochir Psychiatr Pol 2:197-210.
Kriegstein AR (1987) Synaptic responses of cortical pyramidal neurons to light stimulation in the isolated turtle visual system. J Neurosci 7:2488-2492.
Lee HK, Kameyama K, Huganir RL, Bear MF (1998) NMDA induces long-term synaptic depression and dephosphorylation of the GluR1 subunit of AMPA receptors in hippocampus. Neuron 21:1151-1162.
Lee HK, Barbarosie M, Kameyama K, Bear MF, Huganir RL (2000) Regulation of distinct AMPA receptor phosphorylation sites during bidirectional synaptic plasticity. Nature 405:955-959.
Lee HK, Takamiya K, Han JS, Man H, Kim CH, Rumbaugh G, Yu S, Ding L, He C, Petralia RS, Wenthold RJ, Gallagher M, Huganir RL (2003) Phosphorylation of the AMPA receptor GluR1 subunit is required for synaptic plasticity and retention of spatial memory. Cell 112:631-643.
Leslie KR, Nelson SB, Turrigiano GG (2001) Postsynaptic depolarization scales quantal amplitude in cortical pyramidal neurons. J Neurosci 21:RC170.
Lessard N, Pare M, Lepore F, Lassonde M (1998) Early-blind human subjects localize sound sources better than sighted subjects. Nature 395:278-280.
Letzkus JJ, Kampa BM, Stuart GJ (2006) Learning rules for spike timing-dependent plasticity depend on dendritic synapse location. J Neurosci 26:10420-10429.
LeVay S, Wiesel TN, Hubel DH (1980) The development of ocular dominance columns in normal and visually deprived monkeys. J Comp Neurol 191:1-51.
Li P, Kerchner GA, Sala C, Wei F, Huettner JE, Sheng M, Zhuo M (1999) AMPA receptor-PDZ interactions in facilitation of spinal sensory synapses. Nat Neurosci 2:972-977.
Lissin DV, Gomperts SN, Carroll RC, Christine CW, Kalman D, Kitamura M, Hardy S, Nicoll RA, Malenka RC, von Zastrow M (1998) Activity differentially regulates the surface expression of synaptic AMPA and NMDA glutamate receptors. Proc Natl Acad Sci U S A 95:7097-7102.
Liu G, Choi S, Tsien RW (1999) Variability of neurotransmitter concentration and nonsaturation of postsynaptic AMPA receptors at synapses in hippocampal cultures and slices. Neuron 22:395-409.
Liu SJ, Cull-Candy SG (2002) Activity-dependent change in AMPA receptor properties in cerebellar stellate cells. J Neurosci 22:3881-3889.
Liu SQ, Cull-Candy SG (2000) Synaptic activity at calcium-permeable AMPA receptors induces a switch in receptor subtype. Nature 405:454-458.
Luthi A, Chittajallu R, Duprat F, Palmer MJ, Benke TA, Kidd FL, Henley JM, Isaac JT, Collingridge GL (1999) Hippocampal LTD expression involves a pool of AMPARs regulated by the NSF-GluR2 interaction. Neuron 24:389-399.
Lyford GL, Yamagata K, Kaufmann WE, Barnes CA, Sanders LK, Copeland NG, Gilbert DJ, Jenkins NA, Lanahan AA, Worley PF (1995) Arc, a growth factor and activity-regulated gene, encodes a novel cytoskeleton-associated protein that is enriched in neuronal dendrites. Neuron 14:433-445.
Macaluso E, Frith CD, Driver J (2000) Modulation of human visual cortex by crossmodal spatial attention. Science 289:1206-1208.

Maffei A, Nelson SB, Turrigiano GG (2004) Selective reconfiguration of layer 4 visual cortical circuitry by visual deprivation. Nat Neurosci 7:1353-1359.
Magee JC (2003) A prominent role for intrinsic neuronal properties in temporal coding. Trends Neurosci 26:14-16.
Malenka RC, Bear MF (2004) LTP and LTD: an embarrassment of riches. Neuron 44:5-21.
Man HY, Wang Q, Lu WY, Ju W, Ahmadian G, Liu L, D'Souza S, Wong TP, Taghibiglou C, Lu J, Becker LE, Pei L, Liu F, Wymann MP, MacDonald JF, Wang YT (2003) Activation of PI3-kinase is required for AMPA receptor insertion during LTP of mEPSCs in cultured hippocampal neurons. Neuron 38:611-624.
Mansour M, Nagarajan N, Nehring RB, Clements JD, Rosenmund C (2001) Heteromeric AMPA receptors assemble with a preferred subunit stoichiometry and spatial arrangement. Neuron 32:841-853.
Matsuda S, Mikawa S, Hirai H (1999) Phosphorylation of serine-880 in GluR2 by protein kinase C prevents its C terminus from binding with glutamate receptor-interacting protein. J Neurochem 73:1765-1768.
Matsuda S, Launey T, Mikawa S, Hirai H (2000) Disruption of AMPA receptor GluR2 clusters following long-term depression induction in cerebellar Purkinje neurons. Embo J 19:2765-2774.
Mayer ML, Armstrong N (2004) Structure and function of glutamate receptor ion channels. Annu Rev Physiol 66:161-181.
McCormack SG, Stornetta RL, Zhu JJ (2006) Synaptic AMPA receptor exchange maintains bidirectional plasticity. Neuron 50:75-88.
McGee AW, Yang Y, Fischer QS, Daw NW, Strittmatter SM (2005) Experience-driven plasticity of visual cortex limited by myelin and Nogo receptor. Science 309:2222-2226.
Meng Y, Zhang Y, Jia Z (2003) Synaptic transmission and plasticity in the absence of AMPA glutamate receptor GluR2 and GluR3. Neuron 39:163-176.
Merabet LB, Swisher JD, McMains SA, Halko MA, Amedi A, Pascual-Leone A, Somers DC (2007) Combined activation and deactivation of visual cortex during tactile sensory processing. J Neurophysiol 97:1633-1641.
Miller KD (1996) Synaptic economics: competition and cooperation in synaptic plasticity. Neuron 17:371-374.
Monyer H, Burnashev N, Laurie DJ, Sakmann B, Seeburg PH (1994) Developmental and regional expression in the rat brain and functional properties of four NMDA receptors. Neuron 12:529-540.
Mosbacher J, Schoepfer R, Monyer H, Burnashev N, Seeburg PH, Ruppersberg JP (1994) A molecular determinant for submillisecond desensitization in glutamate receptors. Science 266:1059-1062.
Mower GD, Christen WG, Caplan CJ (1983) Very brief visual experience eliminates plasticity in the cat visual cortex. Science 221:178-180.
Murthy VN, Schikorski T, Stevens CF, Zhu Y (2001) Inactivity produces increases in neurotransmitter release and synapse size. Neuron 32:673-682.

Nishimune A, Isaac JT, Molnar E, Noel J, Nash SR, Tagaya M, Collingridge GL, Nakanishi S, Henley JM (1998) NSF binding to GluR2 regulates synaptic transmission. Neuron 21:87-97.
Noel J, Ralph GS, Pickard L, Williams J, Molnar E, Uney JB, Collingridge GL, Henley JM (1999) Surface expression of AMPA receptors in hippocampal neurons is regulated by an NSF-dependent mechanism. Neuron 23:365-376.
O'Brien RJ, Kamboj S, Ehlers MD, Rosen KR, Fischbach GD, Huganir RL (1998) Activity-dependent modulation of synaptic AMPA receptor accumulation. Neuron 21:1067-1078.
Oh MC, Derkach VA (2005) Dominant role of the GluR2 subunit in regulation of AMPA receptors by CaMKII. Nat Neurosci 8:853-854.
Oh MC, Derkach VA, Guire ES, Soderling TR (2006) Extrasynaptic membrane trafficking regulated by GluR1 serine 845 phosphorylation primes AMPA receptors for long-term potentiation. J Biol Chem 281:752-758.
Okuda T, Yu LM, Cingolani LA, Kemler R, Goda Y (2007) beta-Catenin regulates excitatory postsynaptic strength at hippocampal synapses. Proc Natl Acad Sci U S A 104:13479-13484.
Panicker S, Brown K, Nicoll RA (2008) Synaptic AMPA receptor subunit trafficking is independent of the C terminus in the GluR2-lacking mouse. Proc Natl Acad Sci U S A 105:1032-1037.
Passafaro M, Piech V, Sheng M (2001) Subunit-specific temporal and spatial patterns of AMPA receptor exocytosis in hippocampal neurons. Nat Neurosci 4:917-926.
Pawlak V, Schupp BJ, Single FN, Seeburg PH, Kohr G (2005) Impaired synaptic scaling in mouse hippocampal neurones expressing NMDA receptors with reduced calcium permeability. J Physiol 562:771-783.
Pellegrini-Giampietro DE, Gorter JA, Bennett MV, Zukin RS (1997) The GluR2 (GluR-B) hypothesis: Ca(2+)-permeable AMPA receptors in neurological disorders. Trends Neurosci 20:464-470.
Penn AA, Riquelme PA, Feller MB, Shatz CJ (1998) Competition in retinogeniculate patterning driven by spontaneous activity. Science 279:2108-2112.
Pham TA, Graham SJ, Suzuki S, Barco A, Kandel ER, Gordon B, Lickey ME (2004) A semi-persistent adult ocular dominance plasticity in visual cortex is stabilized by activated CREB. Learn Mem 11:738-747.
Pizzorusso T, Medini P, Berardi N, Chierzi S, Fawcett JW, Maffei L (2002) Reactivation of ocular dominance plasticity in the adult visual cortex. Science 298:1248-1251.
Plant K, Pelkey KA, Bortolotto ZA, Morita D, Terashima A, McBain CJ, Collingridge GL, Isaac JT (2006) Transient incorporation of native GluR2-lacking AMPA receptors during hippocampal long-term potentiation. Nat Neurosci 9:602-604.
Polley DB, Kvasnak E, Frostig RD (2004) Naturalistic experience transforms sensory maps in the adult cortex of caged animals. Nature 429:67-71.
Price CJ, Kim P, Raymond LA (1999) D1 dopamine receptor-induced cyclic AMP-dependent protein kinase phosphorylation and potentiation of striatal glutamate receptors. J Neurochem 73:2441-2446.

Quinlan EM, Olstein DH, Bear MF (1999a) Bidirectional, experience-dependent regulation of N-methyl-D-aspartate receptor subunit composition in the rat visual cortex during postnatal development. Proc Natl Acad Sci U S A 96:12876-12880.

Quinlan EM, Philpot BD, Huganir RL, Bear MF (1999b) Rapid, experience-dependent expression of synaptic NMDA receptors in visual cortex in vivo. Nat Neurosci 2:352-357.

Rauschecker JP, Tian B, Korte M, Egert U (1992) Crossmodal changes in the somatosensory vibrissa/barrel system of visually deprived animals. Proc Natl Acad Sci U S A 89:5063-5067.

Rema V, Armstrong-James M, Jenkinson N, Ebner FF (2006) Short exposure to an enriched environment accelerates plasticity in the barrel cortex of adult rats. Neuroscience 140:659-672.

Rozov A, Zilberter Y, Wollmuth LP, Burnashev N (1998) Facilitation of currents through rat Ca2+-permeable AMPA receptor channels by activity-dependent relief from polyamine block. J Physiol 511 (Pt 2):361-377.

Rutherford LC, Nelson SB, Turrigiano GG (1998) BDNF has opposite effects on the quantal amplitude of pyramidal neuron and interneuron excitatory synapses. Neuron 21:521-530.

Sawtell NB, Frenkel MY, Philpot BD, Nakazawa K, Tonegawa S, Bear MF (2003) NMDA receptor-dependent ocular dominance plasticity in adult visual cortex. Neuron 38:977-985.

Scheiffele P (2003) Cell-cell signaling during synapse formation in the CNS. Annu Rev Neurosci 26:485-508.

Schroeder CE, Foxe J (2005) Multisensory contributions to low-level, 'unisensory' processing. Curr Opin Neurobiol 15:454-458.

Seidenman KJ, Steinberg JP, Huganir R, Malinow R (2003) Glutamate receptor subunit 2 Serine 880 phosphorylation modulates synaptic transmission and mediates plasticity in CA1 pyramidal cells. J Neurosci 23:9220-9228.

Seol GH, Ziburkus J, Huang S, Song L, Kim IT, Takamiya K, Huganir RL, Lee HK, Kirkwood A (2007) Neuromodulators control the polarity of spike-timing-dependent synaptic plasticity. Neuron 55:919-929.

Sermasi E, Tropea D, Domenici L (1999) Long term depression is expressed during postnatal development in rat visual cortex: a role for visual experience. Brain Res Dev Brain Res 113:61-65.

Shepherd JD, Rumbaugh G, Wu J, Chowdhury S, Plath N, Kuhl D, Huganir RL, Worley PF (2006) Arc/Arg3.1 Mediates Homeostatic Synaptic Scaling of AMPA Receptors. Neuron 52:475-484.

Shi S, Hayashi Y, Esteban JA, Malinow R (2001) Subunit-specific rules governing AMPA receptor trafficking to synapses in hippocampal pyramidal neurons. Cell 105:331-343.

Sjostrom PJ, Hausser M (2006) A cooperative switch determines the sign of synaptic plasticity in distal dendrites of neocortical pyramidal neurons. Neuron 51:227-238.

Snyder GL, Allen PB, Fienberg AA, Valle CG, Huganir RL, Nairn AC, Greengard P (2000) Regulation of phosphorylation of the GluR1 AMPA receptor in the

neostriatum by dopamine and psychostimulants in vivo. J Neurosci 20:4480-4488.
Sorkin A (2004) Cargo recognition during clathrin-mediated endocytosis: a team effort. Curr Opin Cell Biol 16:392-399.
Srivastava S, Osten P, Vilim FS, Khatri L, Inman G, States B, Daly C, DeSouza S, Abagyan R, Valtschanoff JG, Weinberg RJ, Ziff EB (1998) Novel anchorage of GluR2/3 to the postsynaptic density by the AMPA receptor-binding protein ABP. Neuron 21:581-591.
Steinberg JP, Takamiya K, Shen Y, Xia J, Rubio ME, Yu S, Jin W, Thomas GM, Linden DJ, Huganir RL (2006) Targeted in vivo mutations of the AMPA receptor subunit GluR2 and its interacting protein PICK1 eliminate cerebellar long-term depression. Neuron 49:845-860.
Stellwagen D, Malenka RC (2006) Synaptic scaling mediated by glial TNF-alpha. Nature 440:1054-1059.
Stern EA, Maravall M, Svoboda K (2001) Rapid development and plasticity of layer 2/3 maps in rat barrel cortex in vivo. Neuron 31:305-315.
Sur M, Leamey CA (2001) Development and plasticity of cortical areas and networks. Nat Rev Neurosci 2:251-262.
Sutton MA, Ito HT, Cressy P, Kempf C, Woo JC, Schuman EM (2006) Miniature neurotransmission stabilizes synaptic function via tonic suppression of local dendritic protein synthesis. Cell 125:785-799.
Swanson GT, Kamboj SK, Cull-Candy SG (1997) Single-channel properties of recombinant AMPA receptors depend on RNA editing, splice variation, and subunit composition. J Neurosci 17:58-69.
Tagawa Y, Kanold PO, Majdan M, Shatz CJ (2005) Multiple periods of functional ocular dominance plasticity in mouse visual cortex. Nat Neurosci 8:380-388.
Terashima A, Pelkey KA, Rah JC, Suh YH, Roche KW, Collingridge GL, McBain CJ, Isaac JT (2008) An essential role for PICK1 in NMDA receptor-dependent bidirectional synaptic plasticity. Neuron 57:872-882.
Thiagarajan TC, Piedras-Renteria ES, Tsien RW (2002) alpha- and betaCaMKII. Inverse regulation by neuronal activity and opposing effects on synaptic strength. Neuron 36:1103-1114.
Thiagarajan TC, Lindskog M, Tsien RW (2005) Adaptation to synaptic inactivity in hippocampal neurons. Neuron 47:725-737.
Trachtenberg JT, Chen BE, Knott GW, Feng G, Sanes JR, Welker E, Svoboda K (2002) Long-term in vivo imaging of experience-dependent synaptic plasticity in adult cortex. Nature 420:788-794.
Turrigiano G, Abbott LF, Marder E (1994) Activity-dependent changes in the intrinsic properties of cultured neurons. Science 264:974-977.
Turrigiano G, LeMasson G, Marder E (1995) Selective regulation of current densities underlies spontaneous changes in the activity of cultured neurons. J Neurosci 15:3640-3652.
Turrigiano GG, Nelson SB (2000) Hebb and homeostasis in neuronal plasticity. Curr Opin Neurobiol 10:358-364.
Turrigiano GG, Nelson SB (2004) Homeostatic plasticity in the developing nervous system. Nat Rev Neurosci 5:97-107.

Turrigiano GG, Leslie KR, Desai NS, Rutherford LC, Nelson SB (1998) Activity-dependent scaling of quantal amplitude in neocortical neurons. Nature 391:892-896.
Vanhoose AM, Winder DG (2003) NMDA and beta1-adrenergic receptors differentially signal phosphorylation of glutamate receptor type 1 in area CA1 of hippocampus. J Neurosci 23:5827-5834.
Verdoorn TA, Burnashev N, Monyer H, Seeburg PH, Sakmann B (1991) Structural determinants of ion flow through recombinant glutamate receptor channels. Science 252:1715-1718.
Vicini S, Wang JF, Li JH, Zhu WJ, Wang YH, Luo JH, Wolfe BB, Grayson DR (1998) Functional and pharmacological differences between recombinant N-methyl-D-aspartate receptors. J Neurophysiol 79:555-566.
Wallace H, Glazewski S, Liming K, Fox K (2001) The role of cortical activity in experience-dependent potentiation and depression of sensory responses in rat barrel cortex. J Neurosci 21:3881-3894.
Wallace W, Bear MF (2004) A morphological correlate of synaptic scaling in visual cortex. J Neurosci 24:6928-6938.
Washburn MS, Numberger M, Zhang S, Dingledine R (1997) Differential dependence on GluR2 expression of three characteristic features of AMPA receptors. J Neurosci 17:9393-9406.
Watabe AM, Zaki PA, O'Dell TJ (2000) Coactivation of beta-adrenergic and cholinergic receptors enhances the induction of long-term potentiation and synergistically activates mitogen-activated protein kinase in the hippocampal CA1 region. J Neurosci 20:5924-5931.
Watt AJ, van Rossum MC, MacLeod KM, Nelson SB, Turrigiano GG (2000) Activity coregulates quantal AMPA and NMDA currents at neocortical synapses. Neuron 26:659-670.
Wenthold RJ, Petralia RS, Blahos J, II, Niedzielski AS (1996) Evidence for multiple AMPA receptor complexes in hippocampal CA1/CA2 neurons. J Neurosci 16:1982-1989.
Wierenga CJ, Ibata K, Turrigiano GG (2005) Postsynaptic expression of homeostatic plasticity at neocortical synapses. J Neurosci 25:2895-2905.
Wierenga CJ, Walsh MF, Turrigiano GG (2006) Temporal regulation of the expression locus of homeostatic plasticity. J Neurophysiol 96:2127-2133.
Wiesel TN, Hubel DH (1963) Effects Of Visual Deprivation On Morphology And Physiology Of Cells In The Cats Lateral Geniculate Body. J Neurophysiol 26:978-993.
Xia J, Zhang X, Staudinger J, Huganir RL (1999) Clustering of AMPA receptors by the synaptic PDZ domain-containing protein PICK1. Neuron 22:179-187.
Yoshii A, Sheng MH, Constantine-Paton M (2003) Eye opening induces a rapid dendritic localization of PSD-95 in central visual neurons. Proc Natl Acad Sci U S A 100:1334-1339.
Zamanillo D, Sprengel R, Hvalby O, Jensen V, Burnashev N, Rozov A, Kaiser KM, Koster HJ, Borchardt T, Worley P, Lubke J, Frotscher M, Kelly PH, Sommer B, Andersen P, Seeburg PH, Sakmann B (1999) Importance of AMPA

receptors for hippocampal synaptic plasticity but not for spatial learning. Science 284:1805-1811.
Zhu JJ, Esteban JA, Hayashi Y, Malinow R (2000) Postnatal synaptic potentiation: delivery of GluR4-containing AMPA receptors by spontaneous activity. Nat Neurosci 3:1098-1106.
Zuo Y, Yang G, Kwon E, Gan WB (2005) Long-term sensory deprivation prevents dendritic spine loss in primary somatosensory cortex. Nature 436:261-265.